

PAR

EGG-SEMI-5859

April 1982

QUICK LOOK REPORT FOR SEMISCALE INTERMEDIATE  
BREAK TEST S-IB-1

*Pre Research and/or Technical Assistance Report*

A. G. Stephens

C. M. Kullberg

U.S. Department of Energy

Idaho Operations Office • Idaho National Engineering Laboratory



This is an informal report intended for use as a preliminary or working document

Prepared for the U.S. Nuclear  
Regulatory Commission under DOE  
Contract No. DE-AC07-761D01570  
FIN No. A6038



8208040007 820430  
PDR RES  
8208040007 PDR



FORM EG&G 398  
(Rev. 11-79)

## INTERIM REPORT

Accession No. \_\_\_\_\_

Report No. EGG-SEMI-5859

**Contract Program or Project Title:**

Semiscale Program

**Subject of this Document:**

Quick Look Report for Semiscale intermediate Break Test S-IB-1

**Type of Document:**

Quick Look Report

**Author(s):**

A. G. Stephens  
C. M. Kullberg

**Date of Document:**

April 1982

**Responsible NRC Individual and NRC Office or Division:**

W. C. Lyon,  
Reactor Safety Research

This document was prepared primarily for preliminary or internal use. It has not received full review and approval. Since there may be substantive changes, this document should not be considered final.

EG&G Idaho, Inc.  
Idaho Falls, Idaho 83415

Prepared for the  
U.S. Nuclear Regulatory Commission  
Washington, D.C.  
Under DOE Contract No. DE-AC07-76ID01570  
NRC FIN No. A6038

## INTERIM REPORT

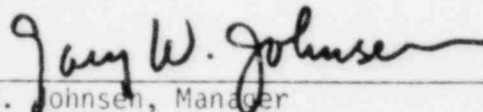
QUICK LOOK REPORT FOR  
SEMISCALE INTERMEDIATE BREAK TEST S-IB-1

by

A. G. Stephens  
C. M. Kullberg

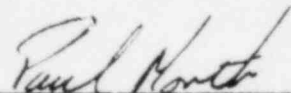
April 1982

Approval:



G. W. Johnson, Manager  
WRRTF Experiment Planning and Analysis Branch

Approval:



P. North, Manager  
Water Reactor Research  
Test Facilities Division

Work supported by: \_\_\_\_\_

## ABSTRACT

Results are presented from a preliminary analysis of Semiscale Mod-2A Test S-1B-1. This test was a 100% communicative cold leg break loss of coolant experiment and was the first of the Intermediate break series. The test was intended to provide reference data for evaluation and assessment of reactor safety code capabilities to predict integral blowdown, refill/reflood experiments for intermediate break sizes, and for providing data to extend the code into the reflood regime. Particular emphasis was placed on providing extensive core fluid and heater rod measurements to facilitate this assessment.

## TABLE OF CONTENTS

ABSTRACT .....	ii
TABLE OF CONTENTS .....	iii
LIST OF FIGURES .....	v
LIST OF TABLES .....	vii
SUMMARY .....	viii
1. INTRODUCTION .....	1
2. SYSTEM CONFIGURATION AND TEST CONDUCT .....	2
2.1 System Configuration .....	2
2.1.1 Fluid System Configuration .....	3
2.1.2 Control System Configuration .....	11
2.1.3 Measurement System Configuration .....	17
2.2 Test Procedures .....	21
2.2.1 Pretest Day Checkouts .....	21
2.2.2 Test Day Warmup Operations .....	21
2.2.3 Initial Conditions and Sequence of Controlled Events .....	22
2.3 Comparison of Specified and Actual Configuration and Operations .....	22
2.3.1 Configuration .....	22
2.3.2 Initial Conditions .....	22
2.3.3 Controlled Parameters .....	28
3. TEST RESULTS .....	30
3.1 Description of the Transient .....	30
3.1.1 General System Response .....	30
3.1.2 Reactor Vessel and Loop Hydraulics .....	30
3.1.3 ECC and Core Thermal Response .....	50
3.2 Comparison with Other Experiments .....	60
3.3 Research Issues .....	67
4. COMPARISON OF SELECTED DATA TO PRETEST CALCULATIONS .....	69
5. CONCLUSIONS .....	79

6. REFERENCES .....	82
7. APPENDIX .....	83

## LIST OF FIGURES

1.	Mod-2A system for IB test series .....	4
2.	Semiscale Mod-2A pressure vessel .....	5
3.	Axial core power profile .....	6
4.	Upper head, upper plenum schematic drawing showing upper head internals modifications .....	7
5.	Cross-section of the Semiscale Mod-2A steam generator .....	9
6.	Break simulator for Tests S-IB-1, S-IB-2 .....	10
7.	Normalized core power decay curve for Test S-IB-1 .....	14
8.	Normalized pump speeds from beginning of coastdown for broken and intact loop pumps .....	15
9.	HPIS and LPIS injection rate .....	16
10.	Core and downcomer measurements .....	19
11.	Heater rod and core fluid thermocouple locations .....	20
12.	Measured core power .....	29
13.	Pressure upstream of the break orifice .....	31
14.	Core bottom liquid level .....	32
15.	Highest measured heater rod temperature (231 cm in rod C3) .....	33
16.	Upper plenum pressure .....	36
17.	Upper core region fluid density (342 cm) .....	37
18.	Lower core region fluid density (13 cm) .....	38
19.	Core fluid density 6 cm below heated length .....	40
20.	Fluid density at top of downcomer .....	41
21.	Fluid density at bottom of downcomer .....	42
22.	Broken loop fluid densities .....	43
23.	Liquid level in broken loop seal .....	44
24.	Fluid density in broken loop seal .....	45
25.	Broken loop hot leg volumetric flow .....	46

26. Break mass flow rate .....	47
27. Guide tube momentum flux and flow direction .....	48
28. Upper head fluid density at top of guide tube .....	49
29. Volumetric flow in the downcomer .....	51
30. Volumetric flow in the intact loop cold leg .....	52
31. Core bypass line differential pressure between upper head and downcomer .....	53
32. Accumulator volumetric flow .....	54
33. Fluid density in the broken loop cold leg between downcomer and break .....	55
34. Core heater rod average temperature .....	57
35. Upper-head-liquid cooling at the top of the core .....	58
36. Upper-head-liquid cooling at core midplane .....	59
37. Accumulator-liquid cooling at bottom of core .....	61
38. Accumulator-liquid cooling 1/3 up from core bottom .....	62
39. Comparison of core midplane temperatures in row 2 .....	63
40. Comparison of core midplane temperatures in column D .....	64
41. Comparison of core axial temperatures in heater rod B3 .....	65
42. Comparison of measured and calculated upper plenum pressures ....	70
43. Comparison of measured and calculated break mass flow rates .....	71
44. Comparison of measured and calculated pressurizer pressures .....	73
45. Comparison of measured and calculated downcomer mass flow rates .....	74
46. Comparison of measured and calculated midplane heater rod temperatures at elevation 183-214 cm .....	76
47. Comparison of measured and calculated core powers .....	77
48. Comparison of measured and calculated guide tube mass flow rates .....	78
49. Comparison of measured and calculated accumulator volumetric flow rates .....	80



LIST OF TABLES

1.	General System Configuration .....	12
2.	Miscellaneous Configuration Items .....	13
3.	Specified Initial Conditions .....	23
4.	Specified Sequence of Controlled Events .....	25
5.	Specified, Measured and Calculated Initial Conditions .....	27
6.	Chronology S-IB-1 .....	34

## SUMMARY

This report presents the results of a preliminary analysis of the data from Semiscale Mod-2A Test S-IB-1. This 100% break test was the first in the three-test Intermediate Break Series. The test series is intended to provide scoping data covering the gap between 200% and 10% break sizes.

Test S-IB-1 was conducted from an initial system pressure of 15.8 MPa, a core inlet temperature of 558 K, core temperature rise of 38.6 K and a steady state initial power of 2.02 MW. Twenty-three of the twenty-five rods were powered and a flat radial profile was used. The peak linear heat generation rate of the cosine axial power profile was 36.8 kW/m. The transient power profile applied to the core was based on the ANS decay heat curve, the stored energy and conduction characteristics of a nuclear rod and of a Semiscale electrical rod, and the core hydraulics for the 100% break.

Ambient temperature ECC was injected into only the intact loop cold leg. The accumulator set pressure was 4.45 MPa and a scaled accumulator water volume was used. The intended HPIS/LPIS flow corresponded to that scaled down from only one train of a PWR plant and the flow initiation was delayed by 25 s after the low pressure trip signal to simulate PWR system start up time requirements. The actual HPIS/LPIS flow did not follow that specified; it started and remained at approximately 1/3 the flow expected of the LPIS rate. This extended the reflooding time significantly, permitted correspondingly high core temperatures, and prevented recording of the quenching of the core due to the limited storage capacity of the data system.

The intact loop pump speed was reduced to 50% of initial condition speed by 6 s and left at that value for the remainder of the test. However the broken loop pump speed was increased to 130% of its initial condition value to simulate an expected overspeed. Both loop generator steam valves were closed upon low pressure trip but feed valves were left open for an additional 20 s to obtain correctly scaled secondary liquid levels.

An evaluation of the results from Test S-1B-1 indicates that the blowdown transient was qualitatively similar to the response observed in earlier large break tests, e.g., Test S-07-6.<sup>3</sup> The transient core power profile, cooling due to upper-head-liquid draining into the core region, the (minor) cooling of the bottom of the core due to accumulator water, and the cooling of the core by the degraded HPIS/LPIS flow were the principal factors affecting the core temperatures. Early heatup initiation (less than 1 s) due to the immediate core voiding occurred and culminated in peak clad temperatures during blowdown of approximately 900 K. These were subsequently exceeded during the extended reflood with the highest recorded cladding temperature reaching 1300 K.

The accumulator water played no essential role in the transient, almost all of it bypassing the downcomer and core. Thus a "normal" reflood driven by a full downcomer liquid level did not occur. Instead the LPIS flow provided the cooling which ultimately turned over the core temperatures. Thus no oscillatory fluid conditions existed in this test and the benign reflood was totally different from that observed in Test S-07-6.<sup>3</sup> The ECC bypass problem in Semiscale, and its modeling, are being recommended for additional review and possible small hardware and computer model modification.

A comparison of the RELAP5 calculated pretest prediction to the measured results for Test S-1B-1 indicates that most major trends of the system thermal-hydraulic response were in good agreement during the blowdown phase of the transient. The "blind" test prediction was performed through most of the blowdown phase of the transient when computational problems were encountered which caused termination of the calculation at 49 s. The calculated system depressurization and break mass flow rate were in good quantitative agreement with the data. Generally, the calculated heater rod temperature responses agreed qualitatively with the data. However, heater rod cooling induced by upper vessel head drainage was not accurately predicted.

## 1. INTRODUCTION

Testing performed in the Semiscale Mod-2A is part of the water reactor safety research effort directed toward assessing and improving the analytical capability of computer codes which are used to predict the behavior of pressurized water reactors (PWR's) during postulated accident scenarios. For this purpose, the Mod-2A system was designed as a small-scale model of the primary system of a four loop PWR nuclear generating plant. The system incorporates the major components of a PWR including steam generators, vessel, pumps, pressurizer, and loop piping. The intact loop is scaled to simulate the three intact loops in a PWR, while the broken loop simulates the single loop in which a break is postulated to occur in a PWR. Geometric similarity has been maintained between a PWR and Mod-2A, most notably in the design of a 25 rod, full length, electrically heated core, full length upper head and upper plenum reactor vessel, and relative elevations of various components. Equipment in the upper head of the Mod-2A vessel has been designed to simulate the fluid flow paths found in a PWR which has the inverted top hat upper head internals package.<sup>a</sup> The scaling philosophy followed in the design of the Mod-2A system (modified volume scaling) preserves most of the important first order effects thought important for LOCA transients.<sup>2</sup>

This report presents a preliminary analysis of data from Semiscale Test S-IB-1 which is the first of the three-test Intermediate Break series. It was conducted on January 14, 1982. This test was a 100%, communicative, cold leg break loss-of-coolant experiment. The primary objective of this test was to provide reference data for evaluation and assessment of reactor safety code capabilities to predict integral blowdown, refill/reflood experiments for intermediate break sizes. Also, another important objective was to expand the break spectrum data base to

---

a. This is a recent modification to the Semiscale Mod-2A reactor vessel upper head. The modification is described in Reference 1.

cover the 10 to 200% range in order to determine if other phenomena are important to core cooling and to evaluate the Mod-2A system response to breaks in this range. A secondary objective was to assess the response of the Westinghouse Reactor Vessel Level Indicating System to a 100% break transient.

The experiment incorporated an (electrical) core power decay profile calculated to best represent a nuclear core subjected to the same hydraulic conditions. The primary coolant pumps were subjected to controlled speed transients expected to be typical of PWR pump responses. Emergency core coolant consisted of accumulator and high and low pressure injection system flows. The test was initiated using a rupture disc assembly and the system effluent was directed to and contained in a partially water filled pressure suppression tank.

The following sections present a preliminary analysis of S-IB-1 test results. Section 2 contains a detailed description of the configuration of the fluid, control and measurement systems, and of the test procedures, initial conditions and sequence of controlled events. Section 3 presents selected test results and analysis. Section 4 contains a comparison of selected test results with pretest prediction calculations and Section 5 presents preliminary conclusions.

## 2. SYSTEM CONFIGURATION AND TEST CONDUCT

### 2.1 System Configuration

The entire test facility consists of the fluid system (pipes, pumps, vessel, heat exchangers, etc.), the control system (power to core, pumps, valves, and instrument air and control signals), and the experimental measurement system (transducers, amplifiers, digital data system). These are described in detail in Reference 1 and will only be summarily described here.

### 2.1.1 Fluid System Configuration

The Semiscale Mod-2A fluid system configured for the IB test series is shown in Figure 1. It is a 2500 psi, 650°F 1-3 in. IPS stainless steel type system. It consists of an Intact loop and a Broken loop, the former representing three of the four loops in a PWR. Thus, flow rates and equipment sizes are in the ratio of 3:1 for the two loops. The pressurizer is connected to the Intact loop hot leg, the pressure suppression header and tank are connected via the rupture disk break assembly to the Broken loop cold leg. Emergency core coolant from an accumulator and high or low pressure injection system pumps are routed to the loop cold legs (Intact loop only in these IB tests). Feedwater is supplied to the two steam generators from a heated tank and the steam routed through control valves to the atmosphere, i.e., an open loop secondary coolant system is used.

In Semiscale, the PWR vessel's annular downcomer is replaced with an external pipe to permit extensive instrumenting of both the core and downcomer regions. These are shown in Figure 2. Most of the fluid system components are full height, including the core which consists of a 5 x 5 array of electrically heated 3.66 m long rods which simulate the fuel rods in a 15 x 15 type PWR core. The number of turns per inch of the electrical heating coil is varied along the rod length to give the staircase approximation of a cosine axial heat flux shape shown in Figure 3. Total core power is 2 MW.

The upper head, upper plenum and core flow bypass arrangement in the Semiscale reactor vessel was modified in November, 1981 to better simulate a Westinghouse inverted top hat, upper head internals package design (the older UHI design no longer exists). The modifications are noted in Figure 4.

The steam generators incorporate the standard PWR 7/8 in. OD Inconel inverted U-tubes, six in the Intact loop generator and two in the Broken loop unit. The tube lengths cover the range found in a PWR generator. The tubes are supplied with small diameter Inconel sheathed thermocouples brazed to the tubes which provide primary and secondary coolant

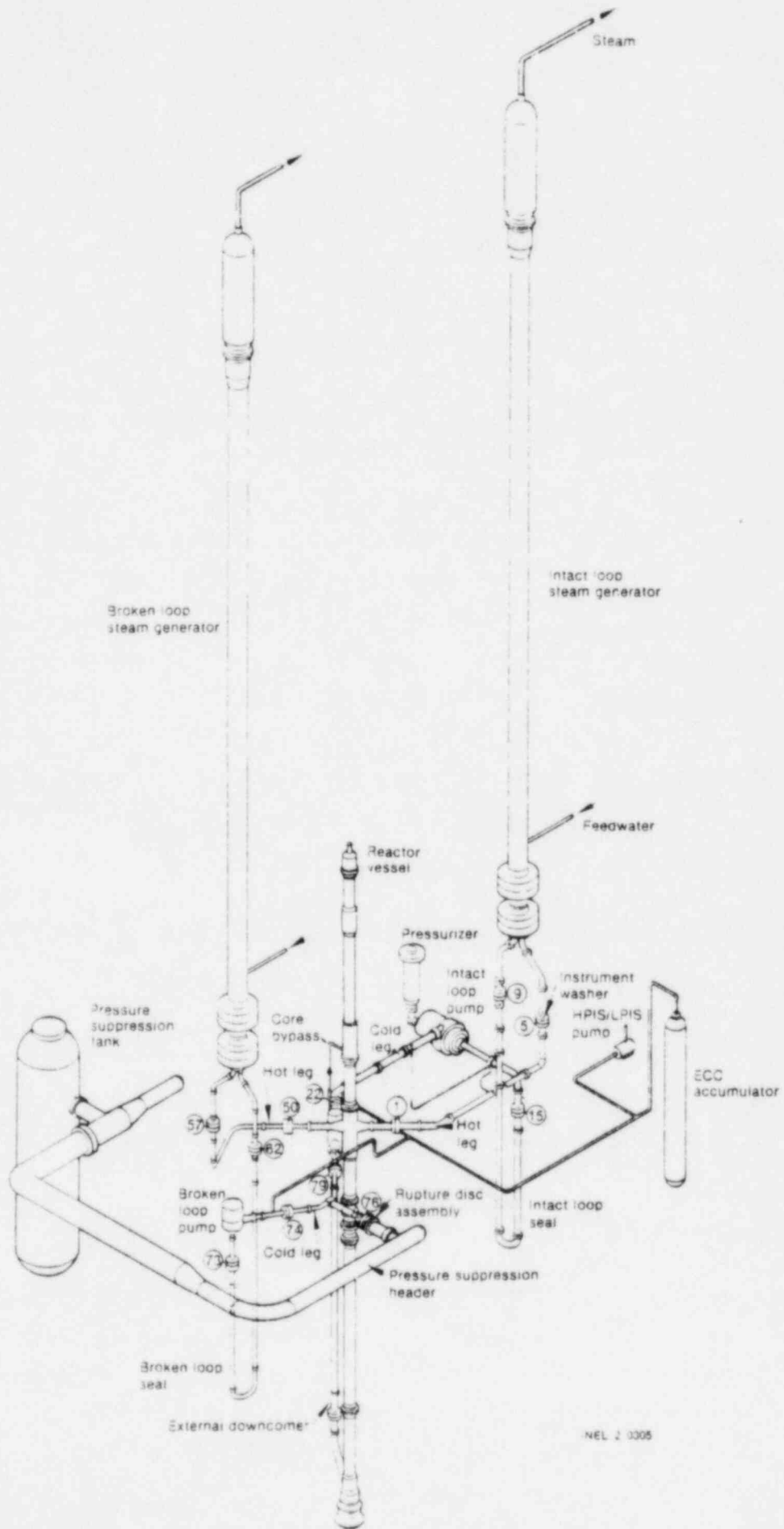


Figure 1. Mod-2A system for IB test series.

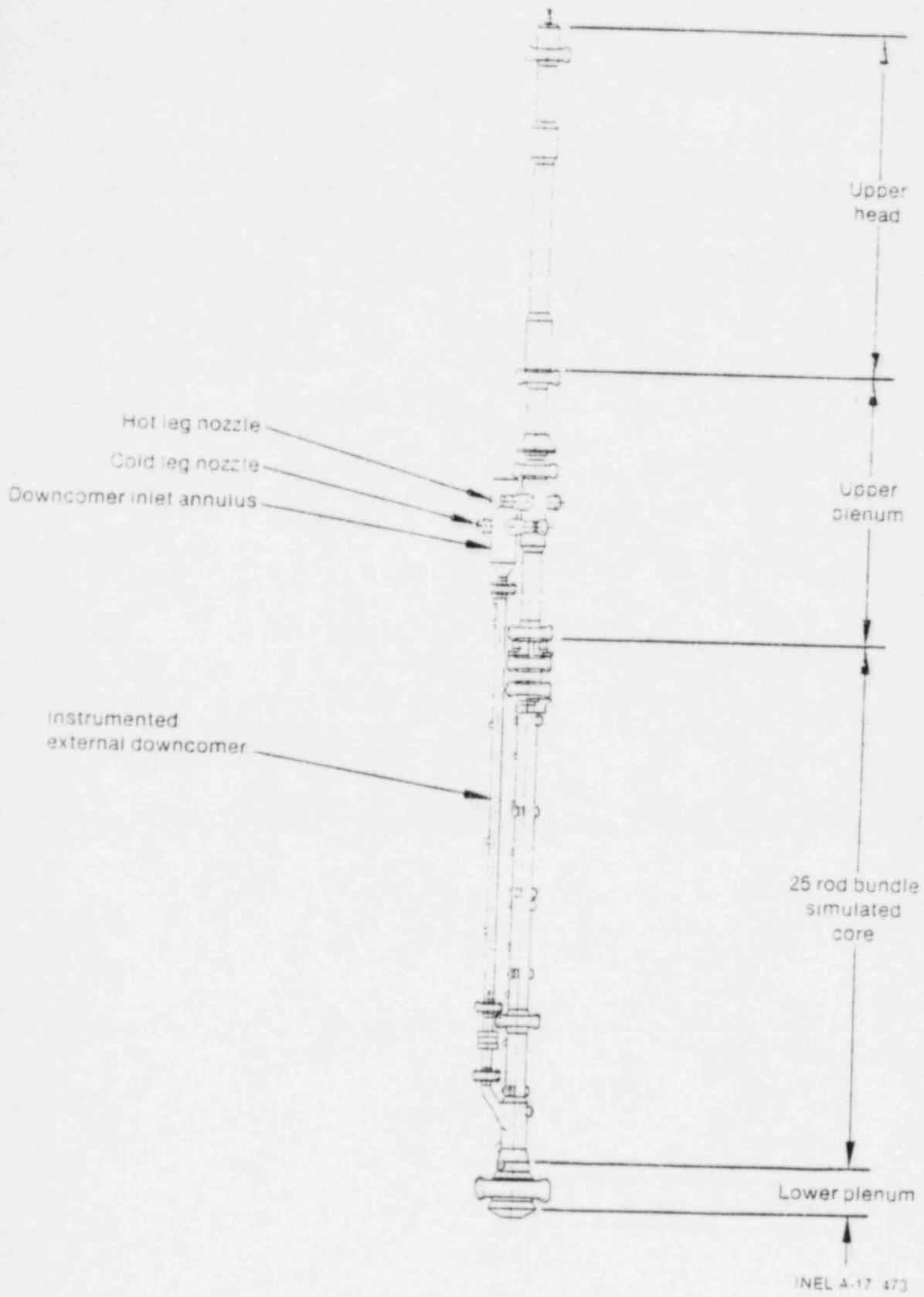


Figure 2. Semiscale Mod-2A pressure vessel.



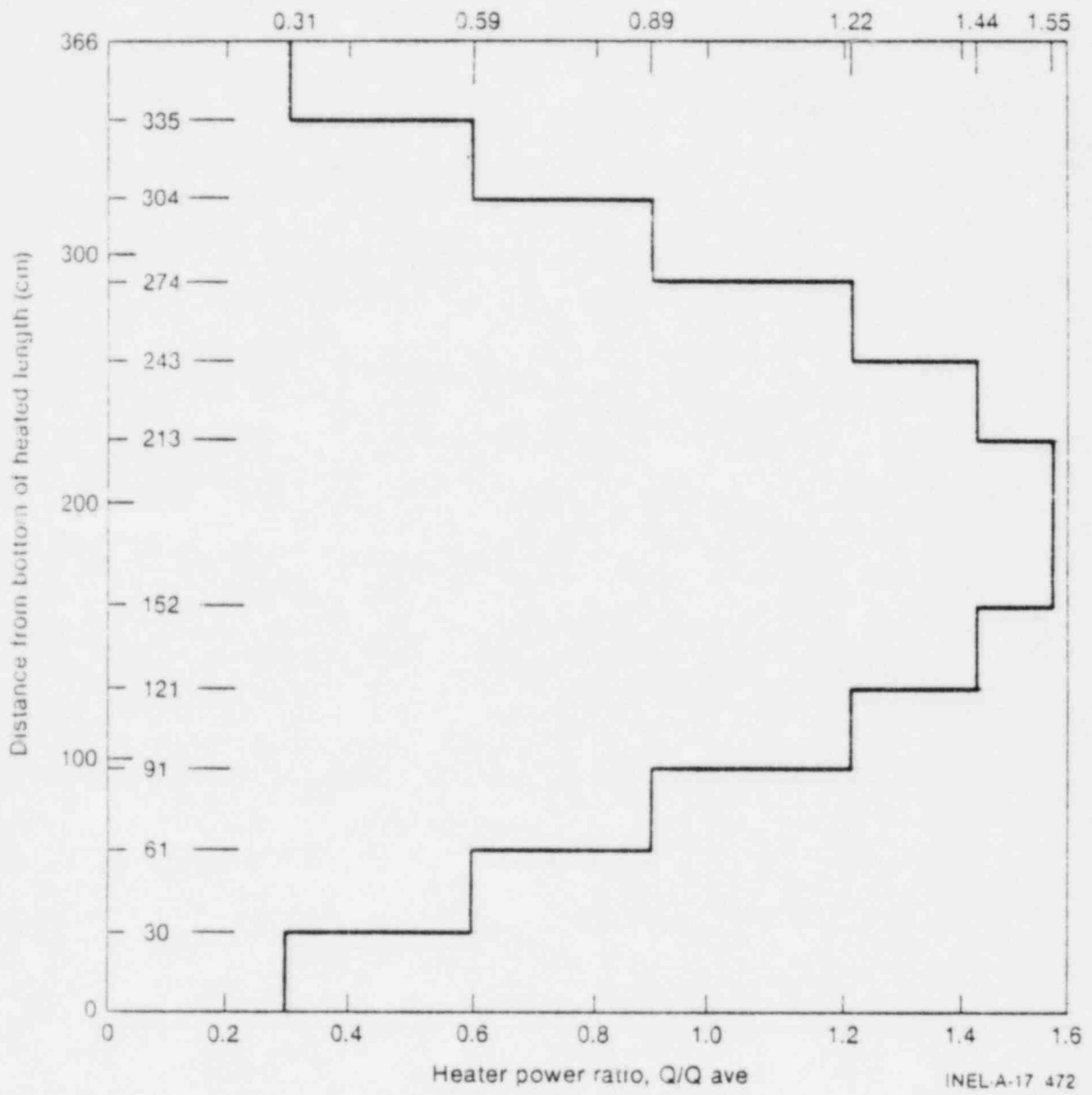


Figure 3. Axial core power profile.

\* MODIFICATIONS MADE TO BETTER SIMULATE WESTINGHOUSE STD PLANT UPPER HEAD/UPPER PLENUM FLOW PATHS AND HYDRAULIC RESISTANCES.

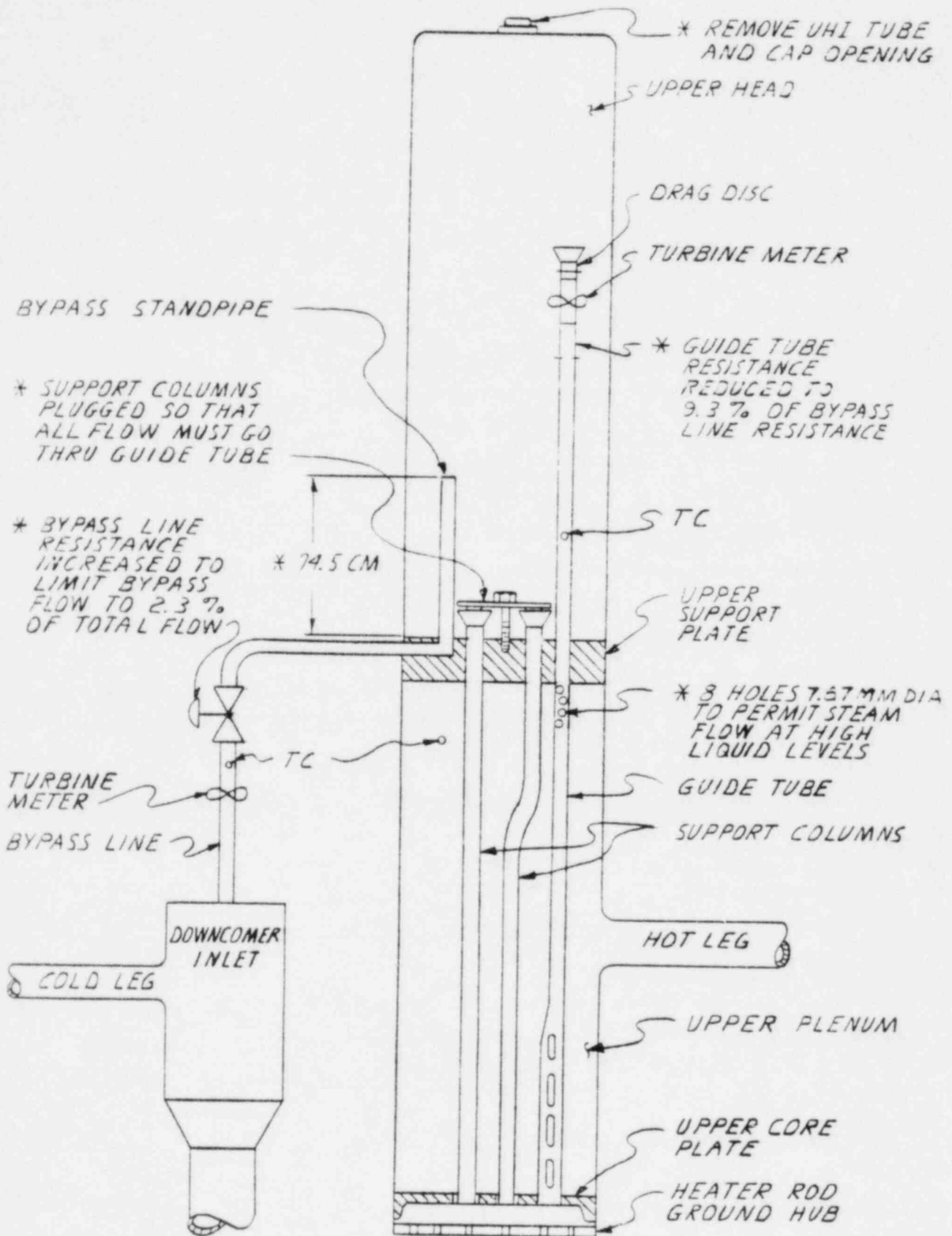


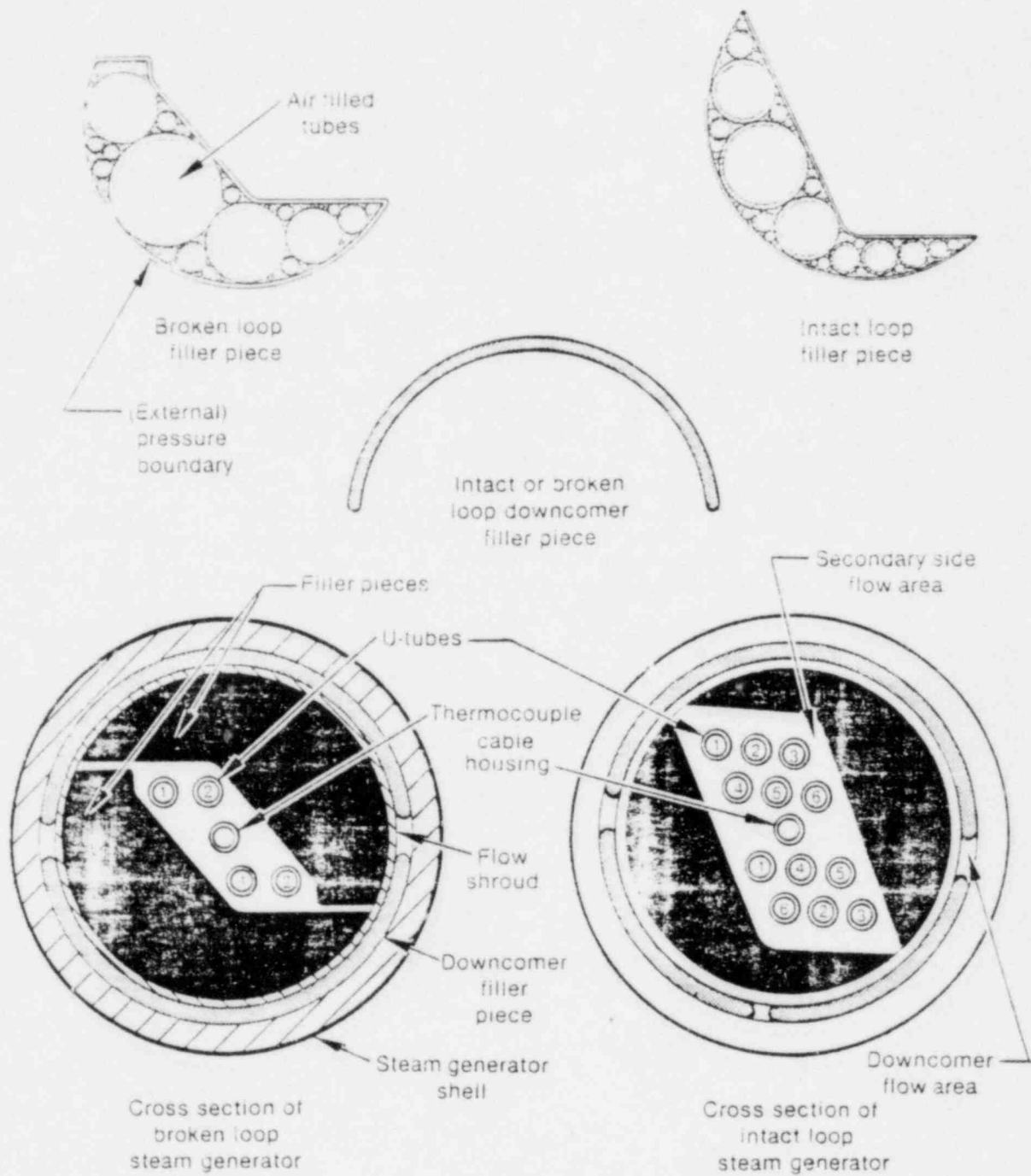
Figure 4. Upper head, upper plenum schematic drawing showing upper head internals modifications.

temperatures and tube wall temperature at various elevations in the upflow and downflow legs. Two tubes are instrumented in each generator for a total of seventy-five thermocouples per generator. A cross section of the generators is shown in Figure 5. Note that the major portion of the secondary flow area/volume is taken up by filler pieces in order to obtain the approximately correct secondary side liquid volume and velocity.

The communicative break orifice assembly is shown in Figure 6. The upstream end of the T-shaped section shown is connected between the Broken loop pump and downcomer inlet. The downstream end is connected via the rupture disc assembly to the pressure suppression (containment simulation) system. As shown in the figure, the break orifice is located at the horizontal midplane of the cold leg pipe and at a position relative to that pipe simulating a break in its wall. Thus, when the disc is ruptured, critical flow is established across the break orifice and the system fluid upstream of the orifice is subjected to reasonably realistic flow direction/length type changes in order to exit the system. The entrance of the orifice is elliptical in shape. Note that the 100% break orifice diameter reflects the PWR/Semiscale (thermal power) scale factor of  $3411/2$  applied to the PWR cold leg ID. This is not, however, the ID of the Semiscale Broken loop cold leg which is somewhat larger than the scaled ID.<sup>2</sup>

The external pipe heaters used in earlier Semiscale long-term-transient test series to make up for system heat losses are not used in the short-term-transient IB test series. An Intact loop HPIS feed tank was installed for the first time for this test. The tank supplies water to the HPIS pump (whose motor speed is computer-controlled to supply flow, per Figure 9, on the basis of the pressurizer pressure). A liquid level measurement on the tank is used to determine the small HPIS flow rate.

Also for this test, the resistance in the Intact loop was increased, and that in the Broken loop decreased in an effort to improve the simulation of PWR loop resistances. Although the Intact loop resistance could not be increased to the scaled value, it was increased significantly, i.e., to the limit established by safe operation of the Intact loop pump



INEL-A-17 490

Figure 5. Cross-section of the Semiscale Mod-2A steam generator.

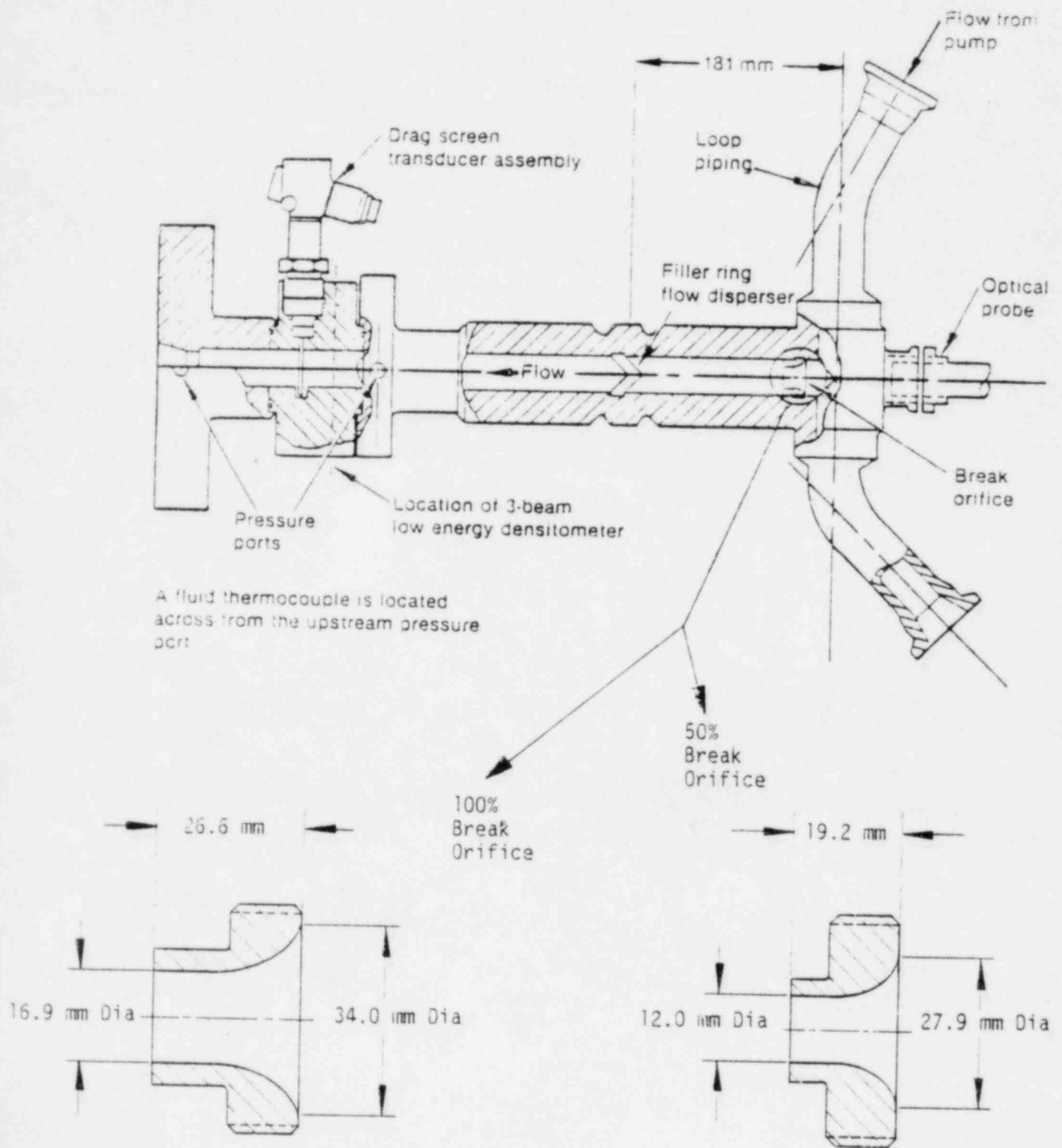


Figure 6. Break simulator for Tests S-IB-1, S-IB-2.

(approximately 3500 rpm). The resistance was incorporated by adding an orifice plate in the vertical downflow pipe from the steam generator outlet to the bottom of the Intact loop seal. It is reflected in the DPI\*9\*14 measurement.

The resistance was decreased in the Broken loop by replacing the orifice plate at the pump discharge with one having essentially the same diameter as the cold leg ID. This resistance is reflected in the DPB\*74\*73 pump head measurement. Table 1 summarizes the general fluid system configuration and Table 2 lists miscellaneous configuration information of interest.

### 2.1.2 Control System Configuration

The functions of the control system of particular significance to these tests are the control of the core power, primary coolant pump speed, HPIS/LPIS pump speed and isolation of the steam generators. The normal control functions involved in obtaining and maintaining steady-state initial conditions and then in the break initiation itself are not discussed here.

The 2 MW of core power is provided via seven DC power supplies, three units supplying the nine center rods and the other four units supplying the fourteen heated peripheral rods. Control signals to the power supplies come from a mini-computer, operating in an open loop mode, which has been programmed to provide a specified power decay profile. The profile, Figure 7, is based on the stored energy and the conduction characteristics of a nuclear fuel rod. The ANS decay heat curve was used as one input, the other being the core hydraulics for a 100% break. The profile reflects an attempt to simulate the response of a nuclear core (rods having a clad/fuel gap) with an electrical core (rods which have no interior gaps).

Figure 8 shows the specified Intact and Broken loop pump speeds and Figure 9 the HPIS/LPIS flow rate versus pressurizer pressure. The Broken loop pump speed was increased to reflect the expected effect of a break at it's discharge (to the extent that such speed increase could be safely

TABLE 1. GENERAL SYSTEM CONFIGURATION

Basic fluid system configuration	Mod 2A with unpowered external heaters
Major fluid systems used	Intact and Broken Loop Primary Coolant; Secondary Coolant; Coolant Injection; Pressure Suppression.
Reactor Vessel	Inverted top hat upper head internals.
Core	23 powered rods (A1, E5 not powered); flat radial profile; open loop control of heater rod power.
Steam Generators	Secondaries operational to establish primary coolant initial conditions, but then isolated during transient; feedwater injected at bottom of downcomers; no auxiliary feedwater used.
Primary Coolant Pumps	Open loop controlled speed reduction.
ECC	Accumulator and HPIS/LPIS into Intact loop only.
HPIS/LPIS	Delayed start; closed loop flow control on basis of primary system pressure.
Accumulator	Inject both water and then nitrogen
Break	
Location	Cold leg
Configuration	Communicative, rupture disc assembly connected to pressure suppression system
Size	100%

TABLE 2. MISCELLANEOUS CONFIGURATION ITEMS

Item	Drawing Number or other Reference ID	Status
Broken Loop Pump Discharge Resistance	410748, Rev. A	Installed orifice plate, part number -2 (orifice hole diameter = 3.25 cm)
Break flow spool bleed flow		Tubing connected from tap located between instrumented spool 76 and rupture disc assembly to suction of Broken loop pump (Spool 73). Flow restricted by use of small diameter tubing; Remotely controlled (on/off) valve in tubing line was closed before break initiation.
Accumulator CI-T-3 and diptube (ECC to Intact loop only)		Use 1.13 m diptube for water-followed- by nitrogen injection
ECC injection line valve CI-V-4	404726, Rev.N	Adjust to achieve injection line $R'$ of $8.1 \pm 0.8 \times 10^8 \text{ m}^{-4}$ (specified)
Pressurizer surge line orifice		Provide orifice to achieve surge line $R'$ of $1.1 \pm 0.1 \times 10^9 \text{ m}^{-4}$ (specified)
Downcomer/Upper Head Bypass Line Valve		Adjust to achieve 9.3% pressure drop ratio and record bypass/core flow ratio (Pressure drop ratio: upper head to upper plenum $\Delta P$ /downcomer to upper head $\Delta P$ )
Intact Loop Steam Generator Outlet Resistance	405207, Rev. H	Install orifice plate, part number -1 to give maximum Intact loop resistance. (orifice hole diameter = 2.16 cm)



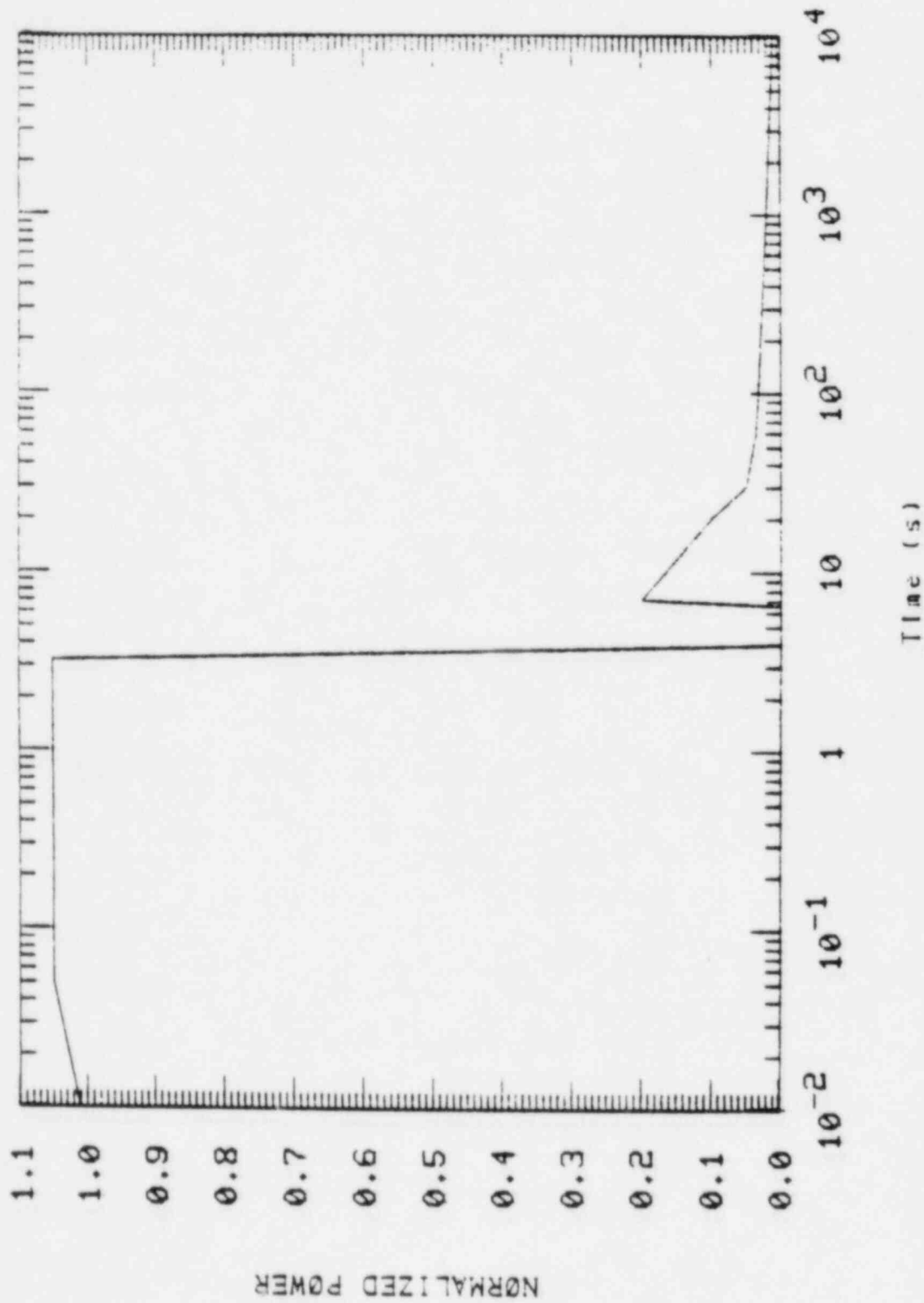


Figure 7. Normalized core power decay curve for Test S-IB-1.

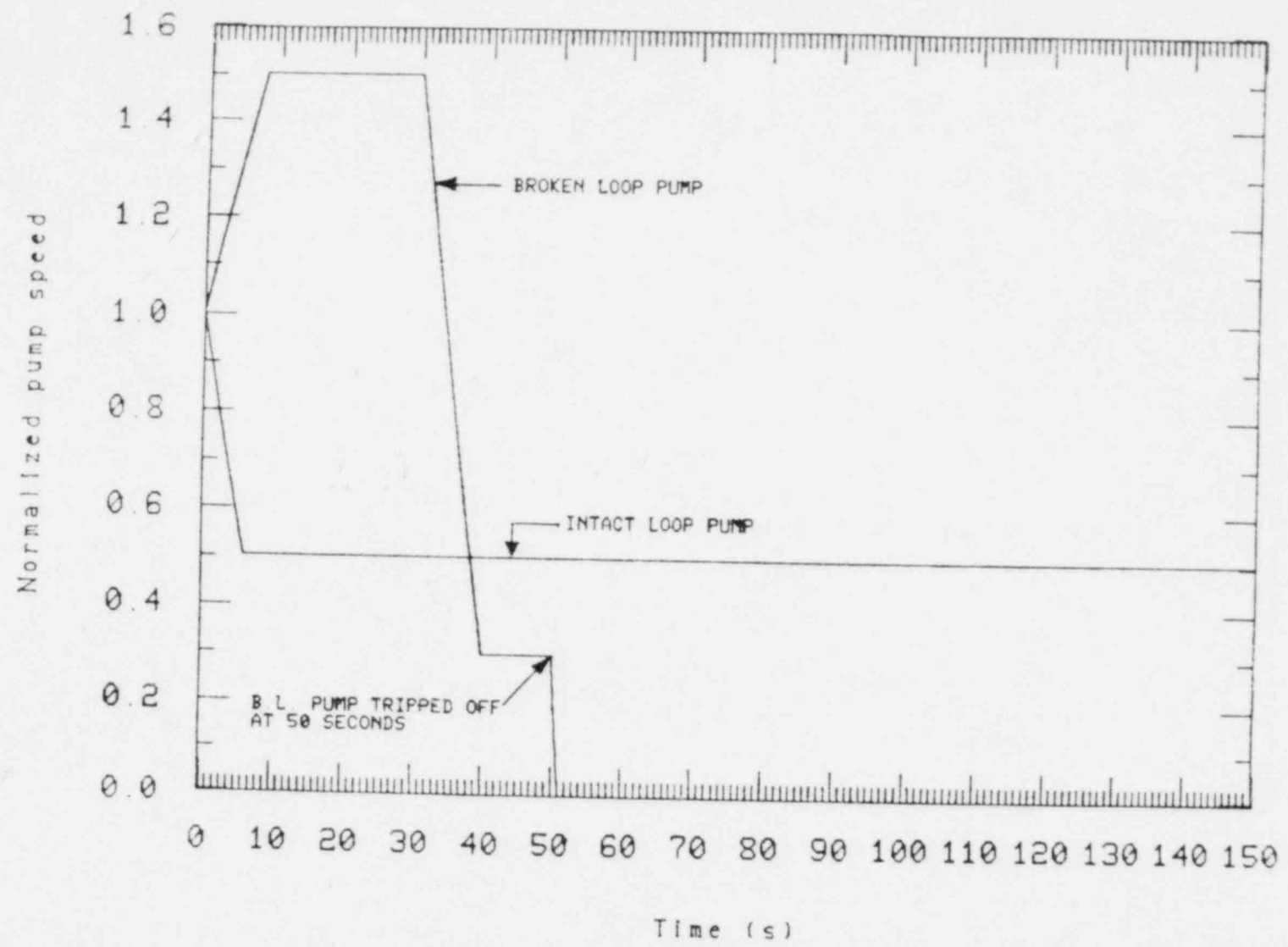


Figure 8. Normalized pump speeds from beginning of coastdown for broken and intact loop pumps.

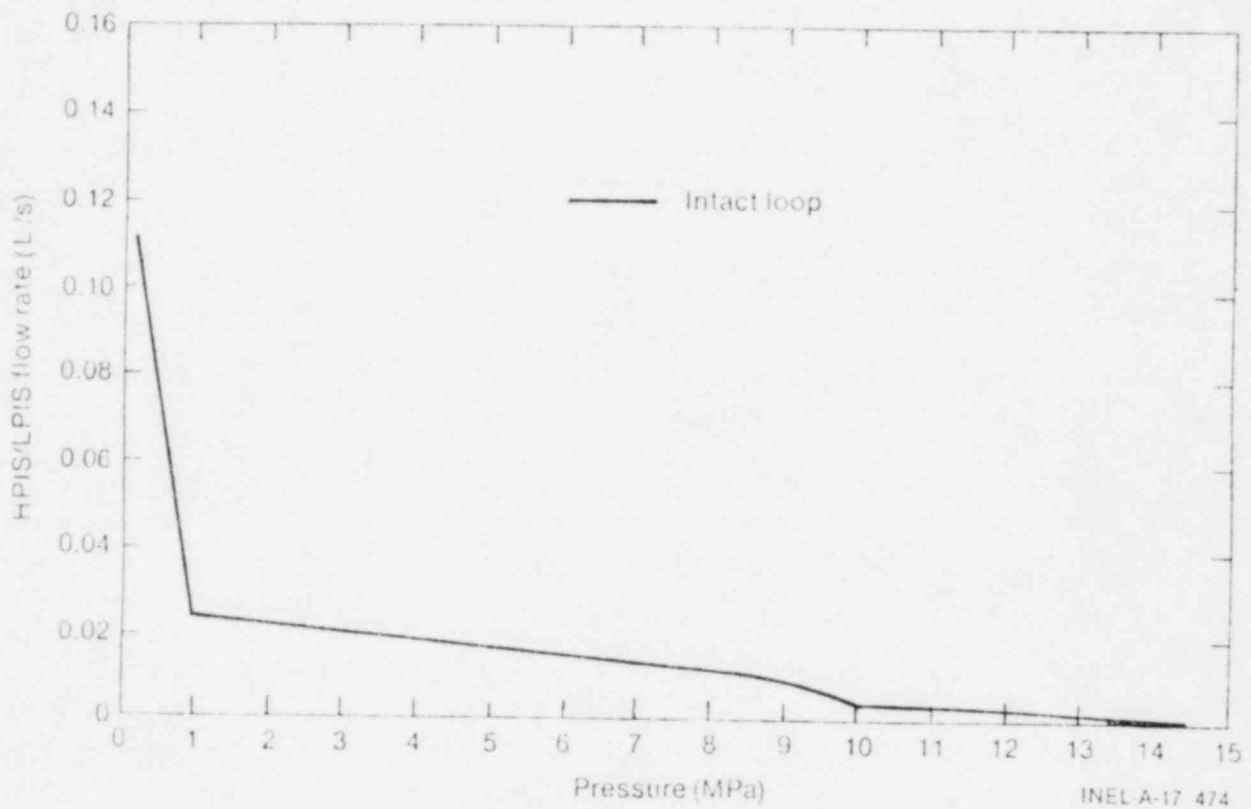


Figure 9. HPIS and LPIS injection rate.

accomplished in Semiscale). The pumped injection flows are combined into a single trace since it is convenient, in Semiscale, to have a single, computer-controlled pump provide the total flow. The specified rate reflects the assumption that one of the two ECC and charging pump PWR trains fail, resulting in only 78% of the flow from two train operation. The steam generator steam valves are closed at the normal 12.6 MPa pressurizer pressure trip, but the feed valves are left open for an additional 20 s as a means to obtain correct secondary side liquid level.

### 2.1.3 Measurement System Configuration

The 313 experimental measurements specified for this test are listed in the Appendix along with the initial condition values for each. These are preliminary data. Not necessarily have all obvious errors been found. The measurement identifier code is explained in detail in Reference 3. In general the code is intended to identify the measured parameter (TF - fluid temperatures) and the measurement location (I - Intact loop; 1 - spool piece No. 1). Thus, TFI\*1 is as explained. Figure 1 identifies the locations of the instrumented spool pieces in the Intact and Broken loops. The system elevation reference is the cold leg centerline, above which elevations are positive. Generally, elevations in a vessel are listed in cm measured from a reference point on that vessel, e.g., the top of the steam generator tube sheet. The elevations of these vessel reference points, relative to the cold leg centerline, are listed in Reference 3.

Figure 10 shows the measurements made in the core and downcomer regions of the reactor vessel, as well as the location of the grid spacers and of the cosine staircase steps. Figure 11 shows the azimuthal orientations of the heater rod thermocouples in the core, as well as a cross section of a typical rod showing the radial location of the measuring element, and finally, the x-y locations of the in-core fluid temperature measurements. These thermocouples are attached to the core grid spacers and measure the fluid temperature about 1.2 cm above the tops of the spacers.

Densities	Levels	Grid Spacer <sup>a,b</sup> Fluid T/C's	Fluid T/C's	Flows	Pressures
RV*AB-6	LV-13M-105	TFV*D1+122	TFV*UPM-13	QV*UP+1	PV*UP-13
RV*23-13	LV-105-195	TFV*D1+162	TFV*UP-63	FV*UP-9	PV*LP-57E
RV*23+113	LV-195-278	TFV*D1+323	TFV*LP-552		
RV*AB+173	LV-278-360	TFV*B3+45			
RV*23-183	LV-360-442	TFV*B3+122	TFV*DC-84	QV*DC-423	PV*DC-29
RV*23+253	LV-442-501	TFV*B3+162	TFV*DC-270	FV*DC-441	PV*DC-435
RV*23+342	LV-501-578	TFV*B3+242	TFV*DC-436		
RV*UP-11	LV-13M-578	TFV*B3+323			
		TFV*A4+79			
RV*DC-72	LVD+29-170	TFV*A4+162			
RV*DC-260	LVD-170-435	TFV*A4+242			
RV*DC-456	LVD-435-578	TFV*A4+283			
	LVD+29-578	TFV*A4+323			
		TFV*A4+361			

HEATER ROD T/C GROUPS<sup>a</sup>  
(TH-1 thru TH-10)

Group 1	Group 2	Group 3	Group 4	Group 5
(Elev. -12 to 20)	(Elev. 106 to 115)	(Elev. 131 to 141)	(Elev. 168 to 172)	(Elev. 178 to 187)
THV*B1+11	THV*A1+115	THV*A3+137	THV*B4+170	THV*A2+182
THV*B4-12	THV*A2+112	THV*B4+140	THV*C2+168	THV*A4+185
THV*C2+16	THV*A4+115	THV*B5+133	THV*E1+172	THV*A5+185
THV*C4+20	THV*B2+107	THV*C1+140		THV*B1+183
THV*D2+16	THV*B3+114	THV*C2+137		THV*B2+180
THV*D5+13	THV*D3+109	THV*C3+140		THV*B3+184
	THV*D4+106	THV*C4+142		THV*B5+180
	THV*E2+109	THV*C5+133		THV*C4+187
	THV*E4+112	THV*D1+131		THV*D1+178
		THV*D2+138		THV*D2+185
		THV*D5+139		THV*D4+179
		THV*E3+141		THV*D5+184
				THV*E2+181
				THV*E4+183
				THV*E5+181
Group 6	Group 7	Group 8	Group 9	Group 10
(Elev. 207 to 211)	(Elev. 227 to 232)	(Elev. 251 to 257)	(Elev. 290 to 292)	(Elev. 352 to 355)
THV*A3+208	THV*A3+228	THV*B1+253	THV*A3+291	THV*A2+353
THV*C1+211	THV*B2+227	THV*B4+256	THV*C1+292	THV*A4+355
THV*C5+207	THV*B3+229	THV*B5+252	THV*C3+292	THV*B2+353
THV*E3+211	THV*C1+232	THV*C2+254	THV*C5+290	THV*B3+354
	THV*C3+231	THV*C4+257	THV*E3+292	THV*D3+354
	THV*C5+228	THV*D1+251		THV*D4+352
	THV*D3+227	THV*D2+254		THV*E2+354
	THV*D4+228			THV*E4+354
	THV*E3+231			

- a. All thermal-hydraulic measurements in the region of the core have elevations referenced to the bottom of the heated length (496 cm below cold leg centerline).
- b. TF's shown in core are grid spacer locations; fluid T/C's are approximately one-half inch above or below the grid spacers.

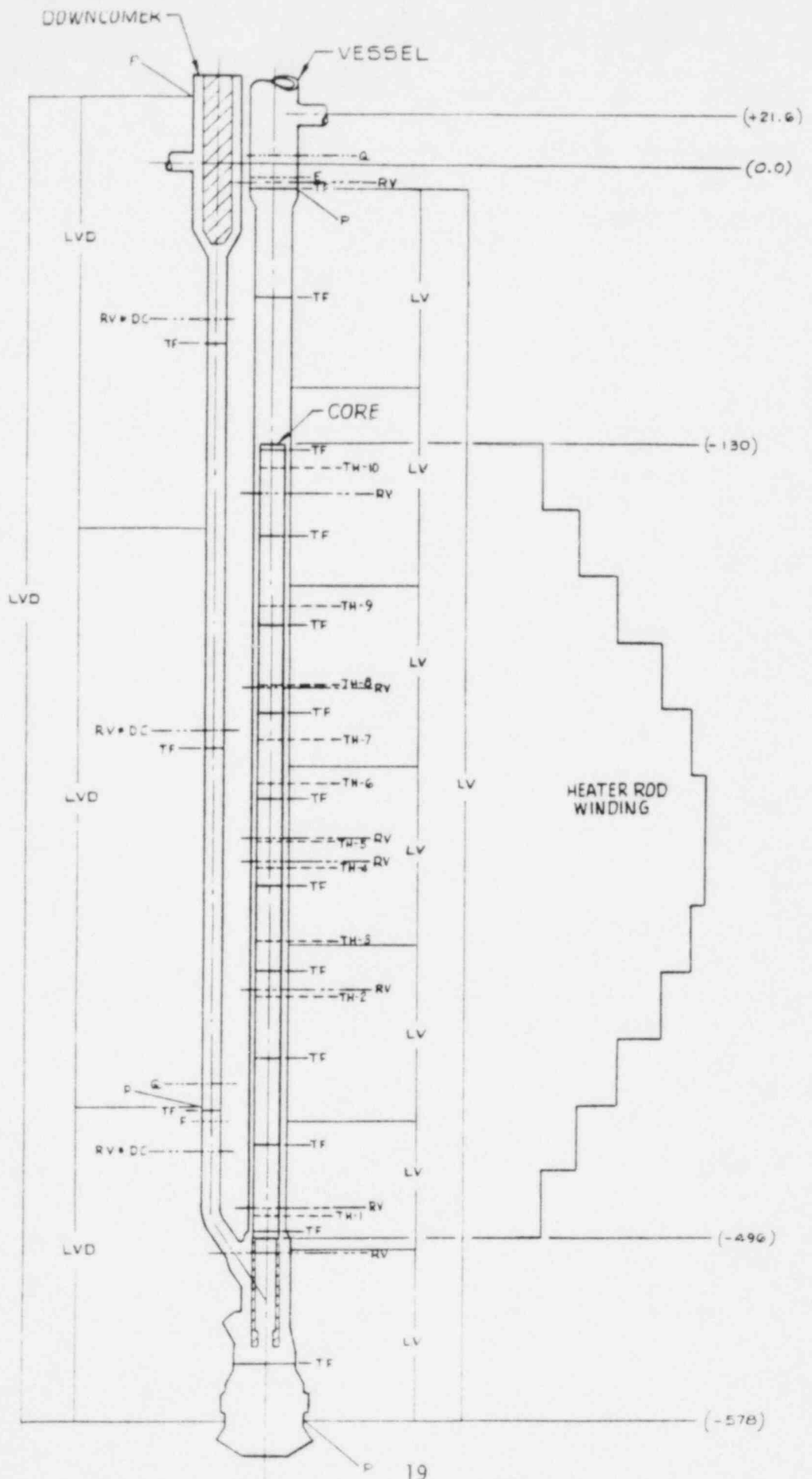
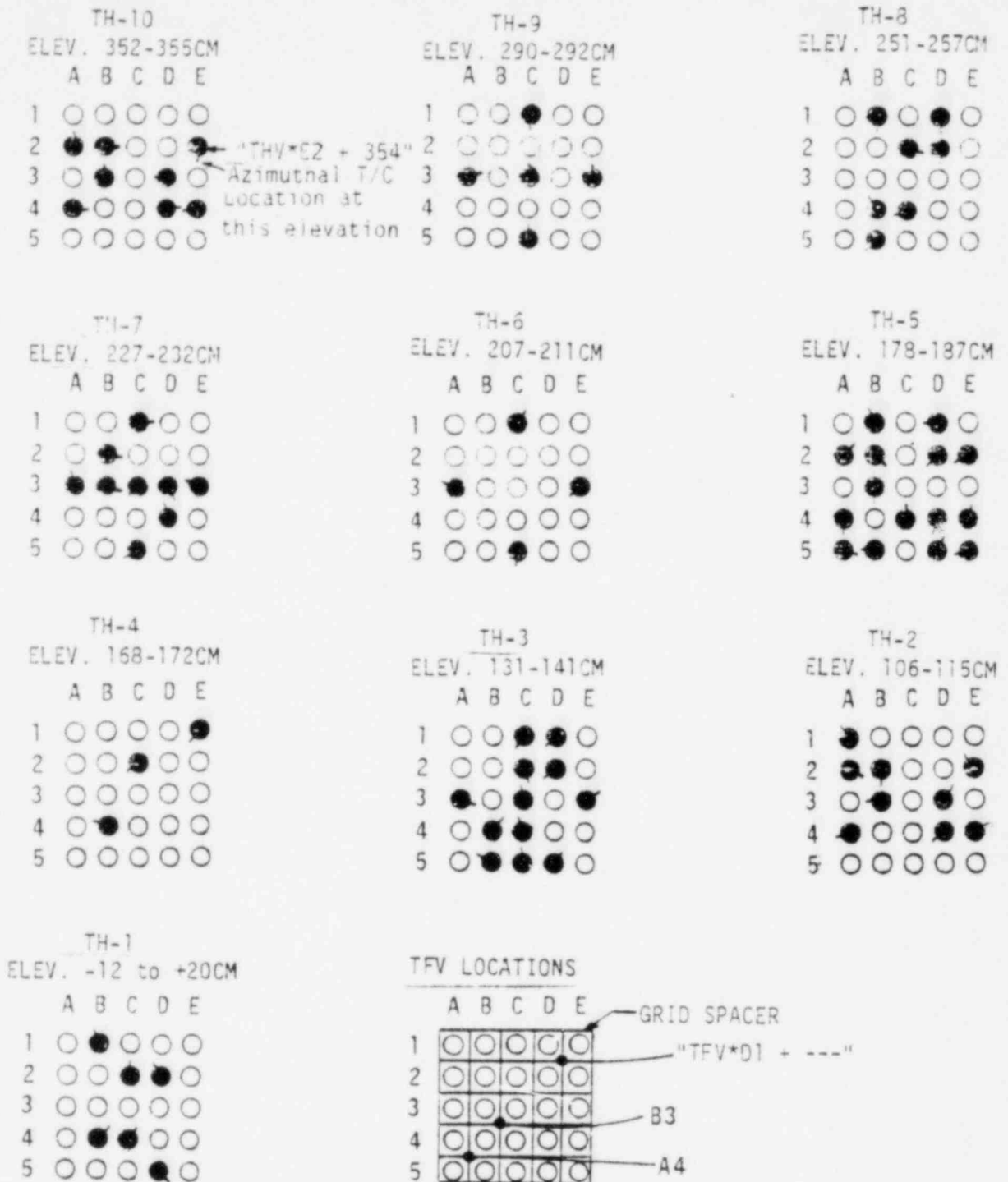


Figure 10. Core and downcomer measurements.



TFV LOCATIONS

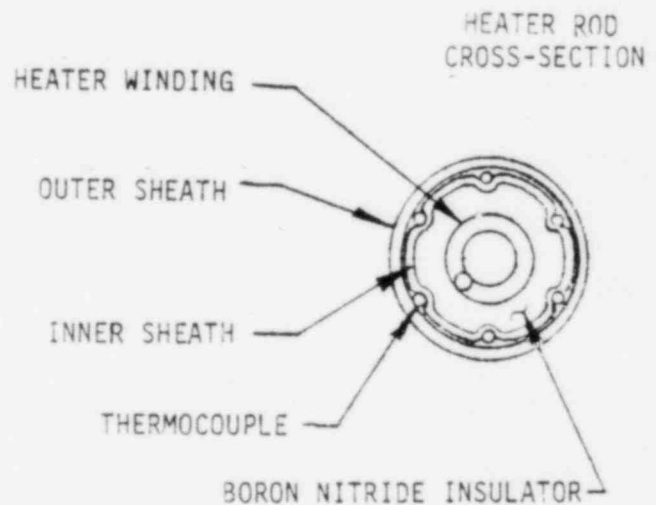
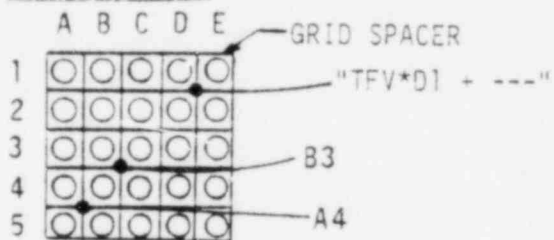


Figure 11. Heater rod and core fluid thermocouple locations.

Voltages were digitized by the data systems at the rate of 40 times per second for those measurements on System I and 80 times per second on System II. System I/II information is included with each measurement listed in the Appendix. The instrument amplifier filter 3 db frequency was set at 3 Hz for all channels except the absolute pressures, for which the setting was 50 Hz. These channels are also identified in the Appendix list. All measured-data plots in this report reflect the results of the Semiscale data compression process. Thus, for the compression rate of three on a typical -10 to +60 s plot, each plotted point is the arithmetic average of the three succeeding values initially recorded on the data system during the test. The present data reduction technique forms this average value prior to conversion to engineering units, and some conversion relations are non-linear. Software modifications in progress will reverse this averaging/conversion processing of data for tests in later series.

## 2.2 Test Procedures

### 2.2.1 Pretest Day Checkouts

Reference 1 lists the various measurement checks, controlled parameter checks, injection line resistance checks, etc. which were specified and accomplished in the two days before test day. These included such checks as liquid level "drain condition" differential pressures, densitometer empty/full ratios, turbine and drag screen flow checks, pressure checks, etc.

### 2.2.2 Test Day Warmup Operations

On test day, the fluid system is warmed to initial fluid temperatures and pressures over a few hour period and during this warmup, various additional measurement checks are performed. These include flow/no-flow comparisons, power pulse (to identify a sensitivity of any measurement to time varying core electrical power), leak rates, etc. These checks are done to establish and verify the operational readiness of the facility and measurement and control systems to perform the specified test.



### 2.2.3 Initial Conditions and Sequence of Controlled Events

The specified initial conditions are given in Table 3, abstracted from Reference 1, and the specified sequence of controlled events is given in Table 4.

### 2.3 Comparison of Specified and Actual Configuration and Operations

None of the differences enumerated below, either taken singly or in concert, were considered to be sufficient to prevent general achievement of the test objectives. However, it is considered useful to note these differences in order to provide a better understanding of the test results, and document the actual conditions vis-a-vis those given in Reference 1.

#### 2.3.1 Configuration

The configuration was as specified in Tables 1 and 2 except as follows. The pressurizer surge line R' (resistance) was  $5.4 \times 10^8 \text{ m}^{-4}$  compared to the specified  $1.1 \times 10^9 \text{ m}^{-4}$ . A component in the pressurizer pressure signal path to the computer controlling the HPIS pump flow was incorrectly adjusted, resulting in a low HPIS/LPIS flow as noted below. Minor differences were found in the core bypass/upper head internals pressure drop and flow rate.

#### 2.3.2 Initial Conditions

Table 5 is a comparison of specified, measured and calculated (RELAP5) initial conditions. Although the average of the measured cold leg temperatures falls within the specified range, both of the individual values were outside that range, the Intact cold leg temperature being 554 K and the Broken loop being 562 K. This is also reflected in the different steam generator pressures. Also, a primary coolant system leak which appeared after several minutes at initial conditions caused a decreasing pressurizer level just prior to blowdown.

TABLE 3. SPECIFIED INITIAL CONDITIONS<sup>e</sup>

1. <u>Primary Coolant System</u>	
Intact/Broken loop flow rate ratio (QI*1, QB*50)	3:1 <sup>a</sup>
Pressurizer pressure	15.5 ± 0.2 MPa
Core temperature rise	37 ± 2 K <sup>b</sup>
Cold leg fluid temperature (average of both loops at downcomer inlet)	557 ± 2 K
Total core electrical power	1.95 ± 0.05 MW
Core flow rate	9-10 kg/s <sup>c</sup>
Pressurizer liquid mass	10.4 ± 0.1 kg
2. <u>Secondary Coolant System</u>	
Steam generator steam dome pressure (average)	5.8 ± 0.2 MPa
Steam generator feedwater temperature (average)	495 ± 2 K
Steam generator steam and feed flows and secondary levels	See Note d
3. <u>Coolant Injection System</u>	
Intact loop accumulator	
Accumulator pressure	4.24 ± 0.1 MPa
Water volume	0.048 ± 0.001 m <sup>3</sup>
Nitrogen volume	0.025 ± 0.001 m <sup>3</sup>
Water temperature	300 ± 10 K
4. <u>Pressure Suppression System</u>	
Suppression tank pressure	0.24 ± 0.01 MPa
Suppression tank liquid level	0.25 ± 0.02 m downcomer submergence

a. Intact loop pump speed will need to be increased above past normal settings to achieve the required flow rate and still accommodate the greater loop resistance due to the new orifice plates (see Table 2). The Broken loop pump speed could be lower than past normal settings because of the reduced resistance at its discharge but this effect may be offset by the need for extra flow through the pump involved with the bleed flow from spool piece 76 to 73 (also see Table 2).

b. Core temperature rise may be temporarily determined by Intact loop hot leg/cold leg temperature difference while arrangements are being made to obtain actual core inlet/outlet measurements.

c. Approximate value; flow should be adjusted to achieve required core  $\Delta T$ .

TABLE 3. (continued)

---

d. Maximum stable secondary liquid levels should be used. Steam and feed flow rates should be adjusted to obtain required primary side temperature and  $\Delta T$ .

e. Initial conditions should be maintained for approximately ten (10) minutes (feedwater availability permitting) to establish and verify their steadiness and reproducibility. At least three (3) sets of time-average data should be obtained during this time.

---

TABLE 4. SPECIFIED SEQUENCE OF CONTROLLED EVENTS

Preblowdown

Final initial condition data set has been taken and steadiness of initial conditions (Table 3) has been verified.

- |    |               |   |
|----|---------------|---|
| 1. | T-60 seconds  | Start sequencer   |
| 2. | T-30 seconds  | Start countdown   |
| 3. | T-28 seconds  | Start continuous experimental data acquisition  |
| 4. | T-15 seconds  | Verify operational data system  |
| 5. | T-2.5 seconds | <ul style="list-style-type: none"> <li>A. Valve out the primary coolant ion exchanger if not done previously</li> <li>B. Close isolation valve in the circulation line from spool piece 76 to 73.</li> <li>C. Turn off makeup pump system</li> <li>D. Turn off pressurizer heaters</li> </ul> |
| 6. | T-0.2 s       | Pressurize rupture disk assembly to start blowdown transient  |

Blowdown

- |    |                 |   |
|----|-----------------|---|
| 1. | T = 0.0 seconds | <ul style="list-style-type: none"> <li>A. Core power computer begins controlling electrical power to heater rods. (See Figure 7.)</li> <li>B. Primary coolant pump speeds begin controlled transients. (See Figure 8.)</li> </ul> |
|----|-----------------|---|

Postblowdown

- |    |   |   |
|----|---|---|
| 1. | T + 0.01 seconds  | Isolate rupture disk pressurization system  |
| 2. | T + 1 second  | Valve off N <sub>2</sub> supply to ECC accumulator and enable accumulator liquid flow to start (when accumulator pressure exceeds system pressure). |
| 3. | Pressurizer pressure reaches 12.6 MPa (t = 0.0 seconds) | Close Intact and Broken loop steam valves   |

TABLE 4. (continued)

---

4. $t = 20$ seconds	Close Intact and Broken loop steam generator feed valves.
5. $t = 25$ seconds	HPIS/LPIS pump starts injection into the Intact loop (only) with flow rate corresponding to pressurizer pressure at that time per Figure 9.
6. $T = 50.0$ seconds	Trip power to Broken loop pump
7. Terminate test	Trip core power; trip HPIS/LPIS pump power; trip Intact loop pump power; secure system.

---

TABLE 5. SPECIFIED, MEASURED AND CALCULATED INITIAL CONDITIONS

	<u>Specified</u>	<u>Measured</u>	<u>RELAP5 Calculated</u>
<u>1. Primary Coolant System</u>			
Intact/Broken loop flow rate (hot legs)	3:1	3.00	3.00
Pressurizer pressure, MPa	15.5 + 0.2	15.78	15.5
Core temperature rise, K	37 + 2	38.6	35
Cold leg fluid temperature (average of both), K	557 + 2	558	558
Total core electrical power, MW	1.95 + 0.05	2.02	1.90
Core flow rate, kg/s	9-10	9.86	9.35
Pressurizer liquid mass, kg	10.4 + 0.1	10	13.6
<u>2. Secondary Coolant System</u>			
Steam generator steam dome pressures, MPa	5.8 + 0.2	I - 5.53 B - 6.15	5.84 5.87
Steam generator feedwater temperatures, K	495 + 2	I - 497 B - 492	495 495
<u>3. Coolant Injection System</u>			
Intact loop accumulator			
Pressure, MPa	4.24 + 0.1	4.45	4.24
Water volume, m <sup>3</sup> (including injection line)	0.048 + 0.001	0.040	0.045
Nitrogen volume, m <sup>3</sup>	0.025 + 0.001	0.033	0.026
Water temperature, K	300 + 10	296	300
<u>4. Pressure Suppression System</u>			
Suppression tank pressure, MPa	0.24 + 0.01	0.25	0.24
Suppression tank water level, m	0.25 + 0.02	0.78	--

The accumulator pressure at initial conditions was high (4.45 MPa versus 4.24 MPa specified), however the pressure fell to approximately 3.85 MPa when the N<sub>2</sub> supply to the accumulator was valved off 2 s after blowdown. Thus, when flow actually started from the accumulator, the driving force was lower than specified (3.85 versus 4.24 MPa). The actual accumulator water volume injected into the primary system for the test was approximately 8 liters less than specified (40 versus 48) as determined by integration of liquid level and turbine readings. Presumably, the N<sub>2</sub> volume was thus similarly high by the same 8 liters.

### 2.3.3 Controlled Parameters

As noted above, the pressurizer pressure signal controlling the HPIS pump speed was in error. As a result, the pumped injection flow started at 0.042  $\epsilon$ /s, and remained constant at that value throughout the test. At the time it started (correctly at 30 s), the pressurizer pressure was 3.0 MPa and the HPIS flow should have been approximately 0.021  $\epsilon$ /s, per Figure 9. At 60 s the pressure was approximately 0.3 MPa and the total pumped injection flow should have been about 0.110  $\epsilon$ /s, but was still 0.042  $\epsilon$ /s.

The actual core power is shown in Figure 12 and is shown with the specified power profile in Figure 47. The decrease in actual power that was to have started at 3.2 s started at 3.7 s and lasted until 4.7 s (should have been over at 4 s). The actual power did not subsequently increase to 20% until 8.4 s as opposed to the specified 7.0 s, but followed the specified behavior thereafter.

The Intact loop pump speed followed the specified profile, but the Broken loop pump overspeed went only to 135% instead of the specified 150%. The steam generator feed and steam valves were closed as specified.

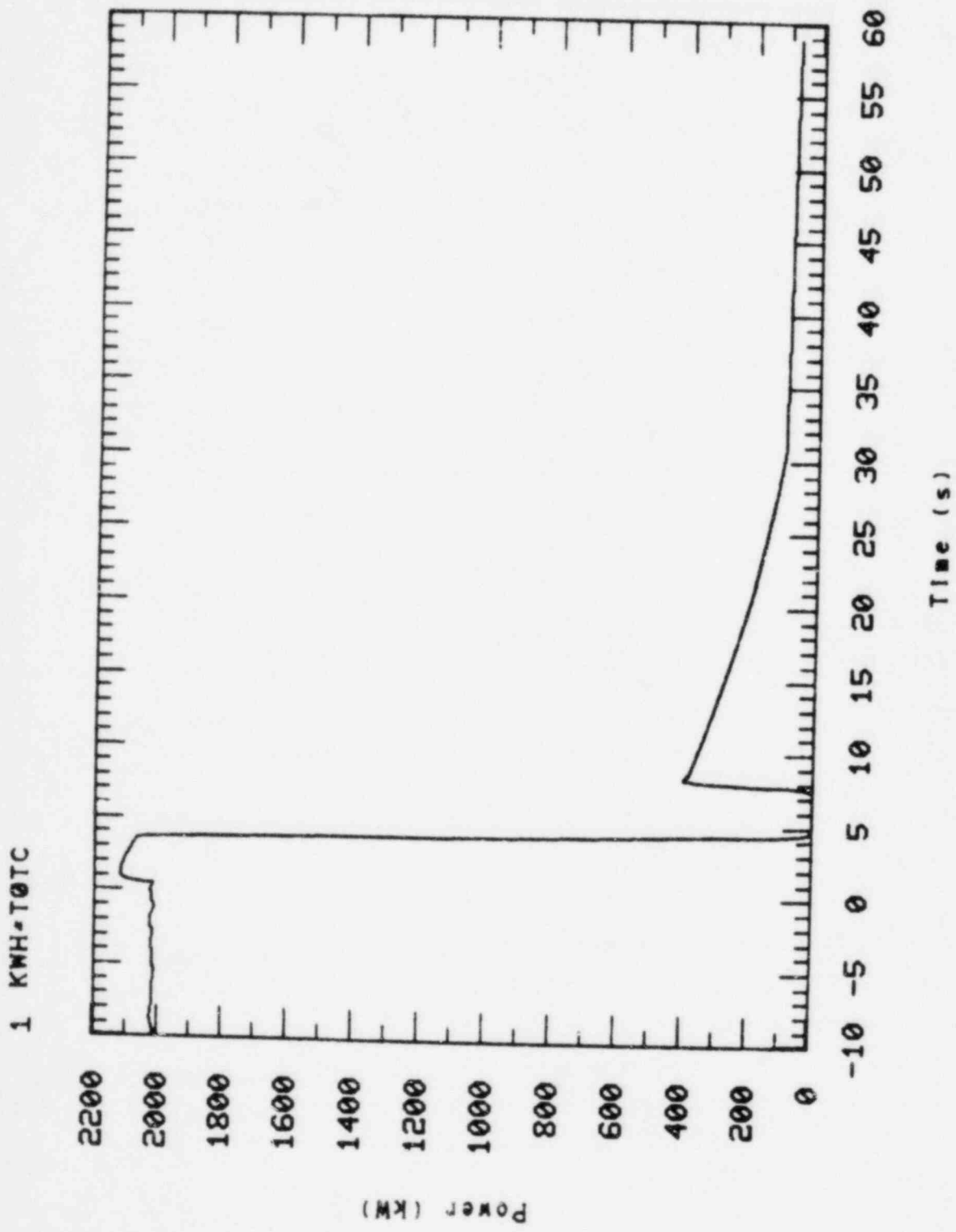


Figure 12. Measured core power.



### 3. TEST RESULTS

#### 3.1 Description of the Transient

##### 3.1.1 General System Response

Data were obtained to approximately 500 seconds after system rupture was initiated. Of this time, the first 55 seconds was consumed in the blowdown (Figure 13); refilling of the lower plenum was completed at about 140 seconds (Figure 14); and the remainder of the time was spent in reflood. The highest parts of the core were not quenched until about 750 sec although one recorded heater rod thermocouple at 355 cm (above bottom of heated length) had reached its peak temperature at 360 seconds. The long refill and reflood times were due to the low pumped-ECC injection flow rate noted earlier and the fact that the scaled accumulator liquid volume was exhausted only 3 seconds after blowdown was over. Thus the downcomer never filled with accumulator liquid, and while the (inadvertently) degraded pumped-ECC flow did quench the core, the reflood time was long and the core temperatures correspondingly high. The highest measured heater temperature occurred in the center rod, C3, at the 231 cm elevation (Figure 15) at 370 seconds and was 1295 K; the thermocouple at core midplane (183 cm) in that rod was not operational for this test. Table 6 lists events of interest, most of which occurred during the blowdown.

##### 3.1.2 Reactor Vessel and Loop Hydraulics

Figure 16 shows the upper plenum pressure and several of the events listed in Table 6. Within the first second after rupture, the flows in the downcomer, core bypass and guide tube reversed direction and the liquid in the core and upper plenum regions started to flash. By 2 seconds, the fluid in the hot leg pipes had reached saturation and started vaporizing, and the core fluid void fraction varied from 82 to 98% (Figures 17, 18) with a pressure at that time of 9.0 MPa. This short-duration, large

1 PB•76U

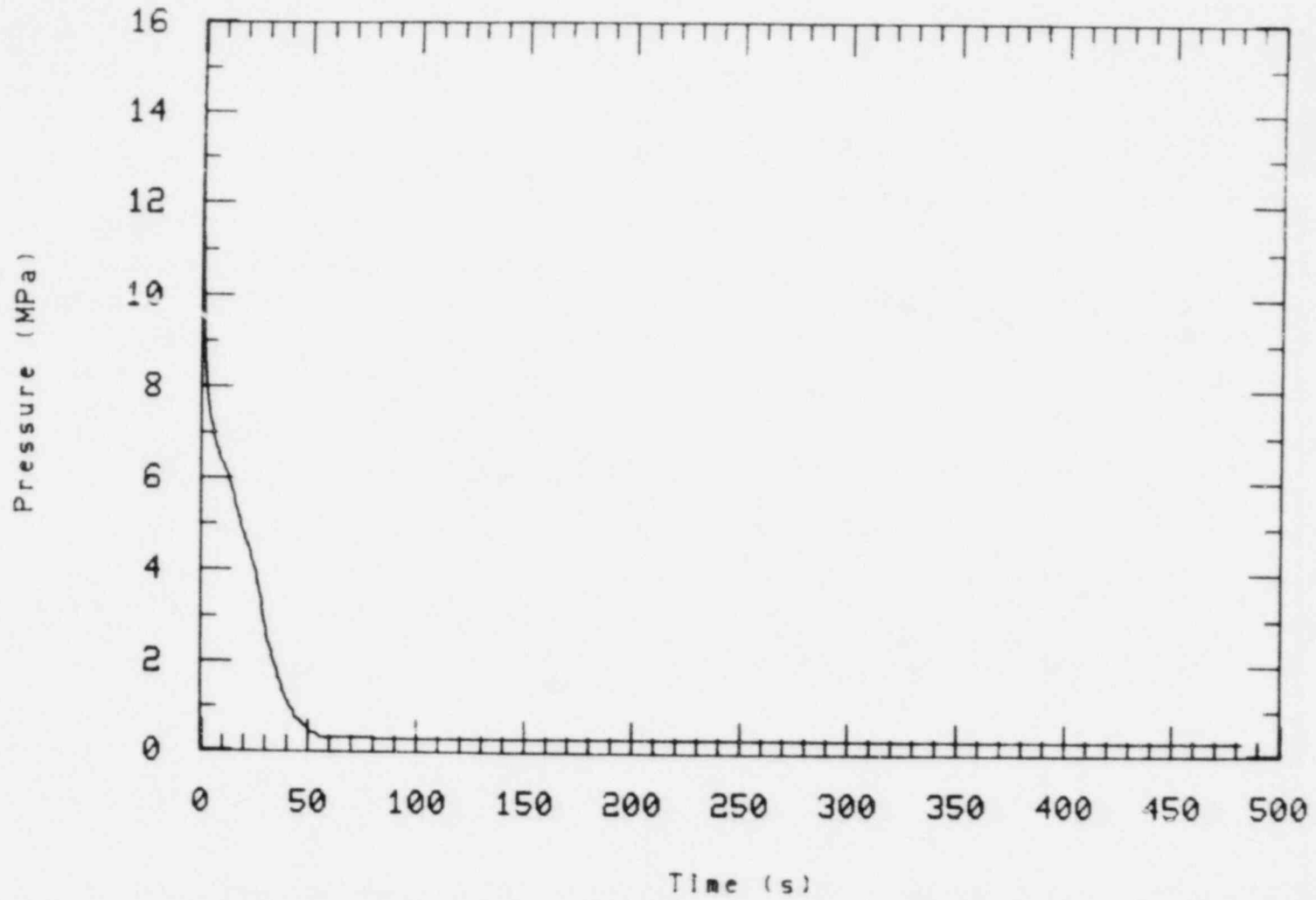


Figure 13. Pressure upstream of the break orifice.

1 VLBET-442-501

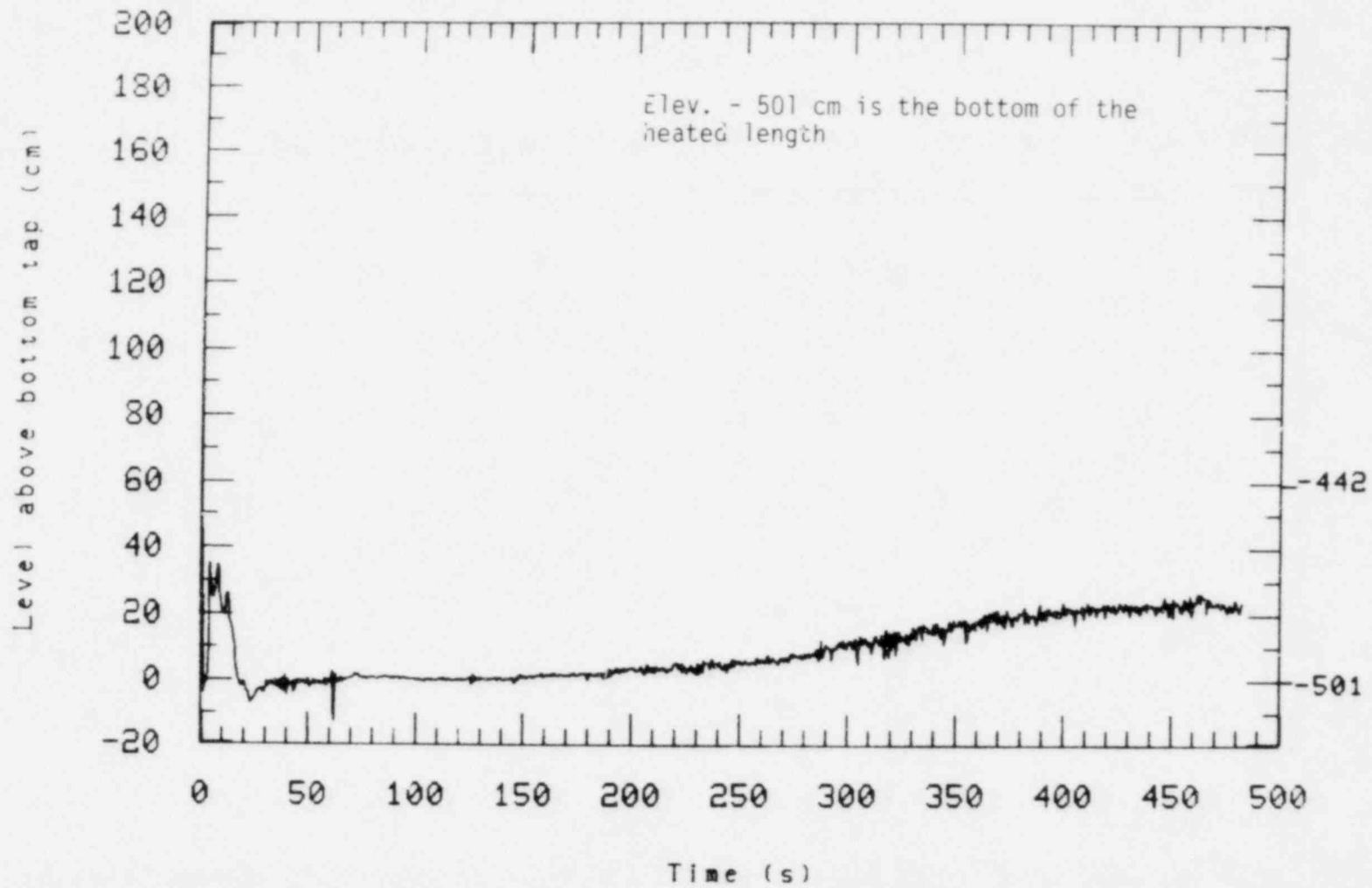


Figure 14. Core bottom liquid level.

1 THV•C3+231

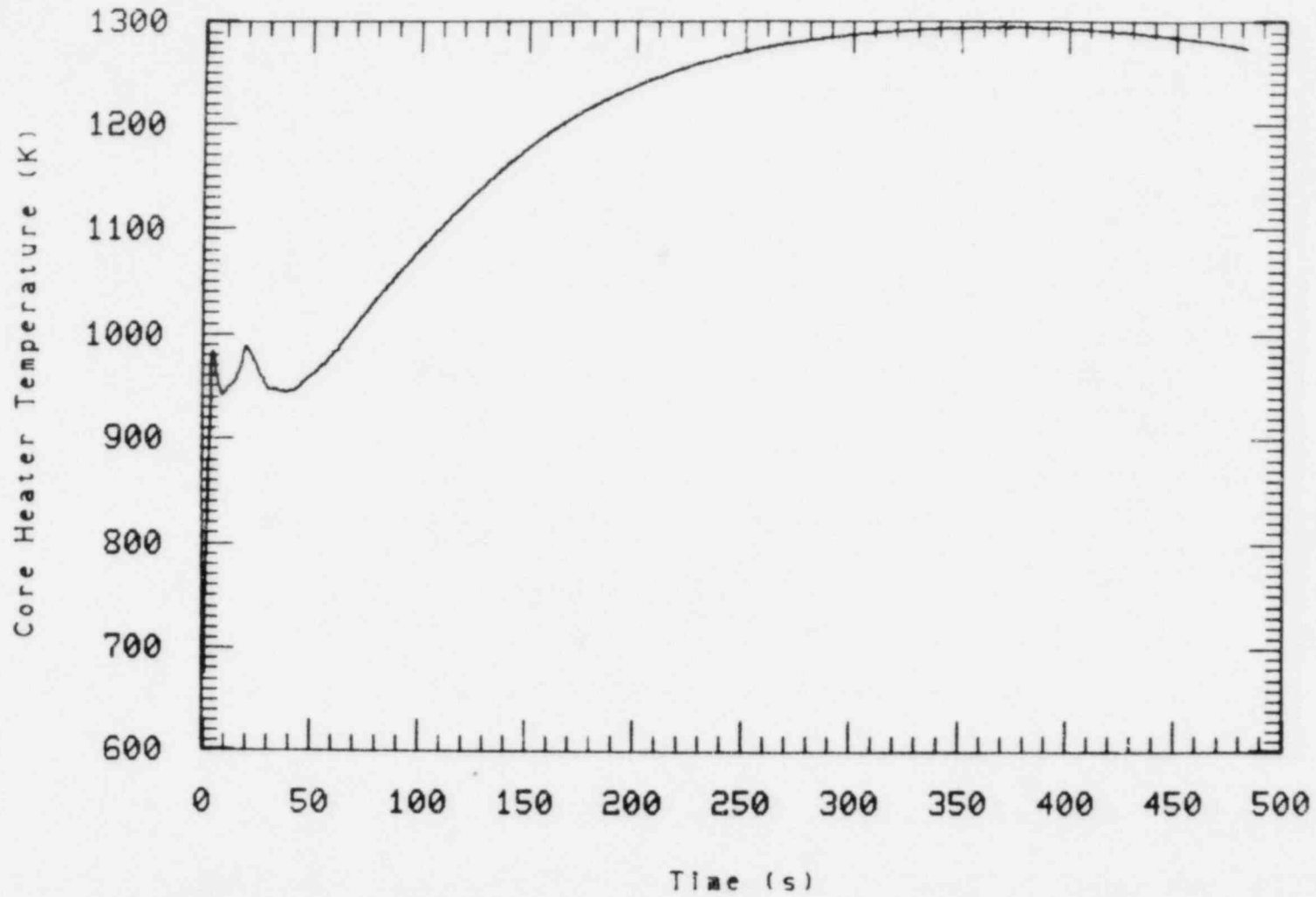


Figure 15. Highest measured heater rod temperature (231 cm in rod C3).

TABLE 6. CHRONOLOGY S-IB-1

Event	Time, seconds
Rupture initiated; core power, pump speed transients started	0
Upper plenum fluid saturates	<1
Broken loop cold leg, core bypass, guide tube and downcomer flows reverse	<1
Fluid in intact and broken loop hot legs saturates	1-2
Fluid in lower 2/3 of core: $\alpha > 98\%$	2
Fluid in upper 1/3 of core: $\alpha > 82\%$	2
Pressurizer empties	4.5
Up-flow leg of broken loop seal blows out	5
Broken loop pump head fully degraded	5
Fluid in broken loop cold leg (downcomer to break) saturates	8
Intact, broken loop steam valves closed	8
Fluid in intact loop cold leg saturates	10
Intact loop pump head fully degraded	10
Broken loop pump reaches maximum overspeed; intact loop pump reaches steady half speed	10
Break orifice uncovers	13
Upper head liquid starts flowing down guide tube	13
Broken loop steam generator secondary becomes energy source	17
Top of guide tube uncovers	19
Intact loop steam generator secondary becomes energy source	24
Intact, broken loop generator feed valves closed	25
Accumulator liquid flow starts	27
Top of core bypass line uncovers	30
HPIS flow starts	30
Broken loop pump speed reduction starts	31

TABLE 6. (continued)

Event	Time, seconds
Broken loop pump tripped	50
Blowdown is over	55
Accumulator empties of liquid (N <sub>2</sub> gas flow follows)	58
Upper head liquid level falls below 173 cm	60
Lower plenum refilled, reflood starts	140
Data acquisition system shutdown	487

1 PV-UP-13

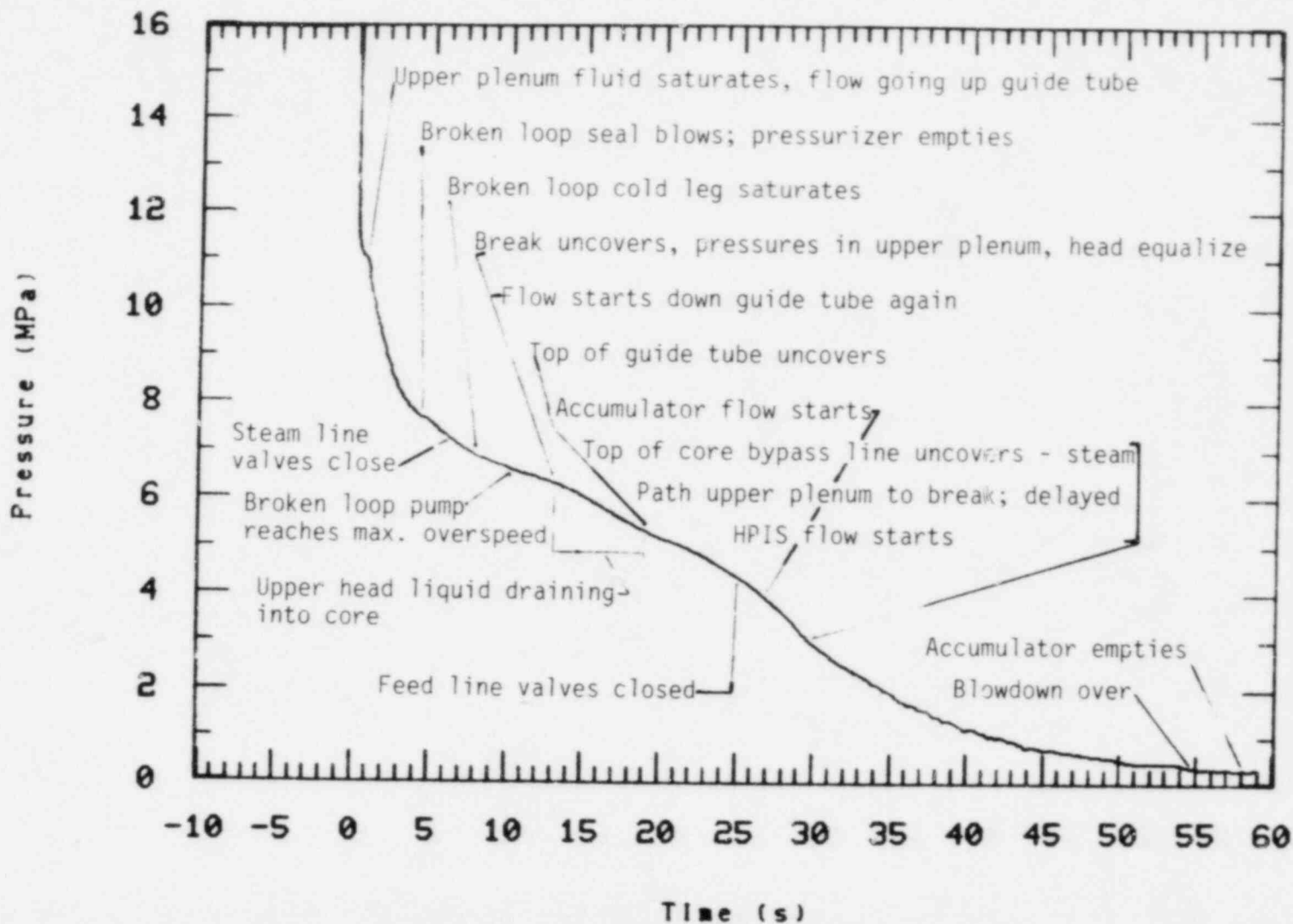


Figure 16. Upper plenum pressure.

1 RV•23•342

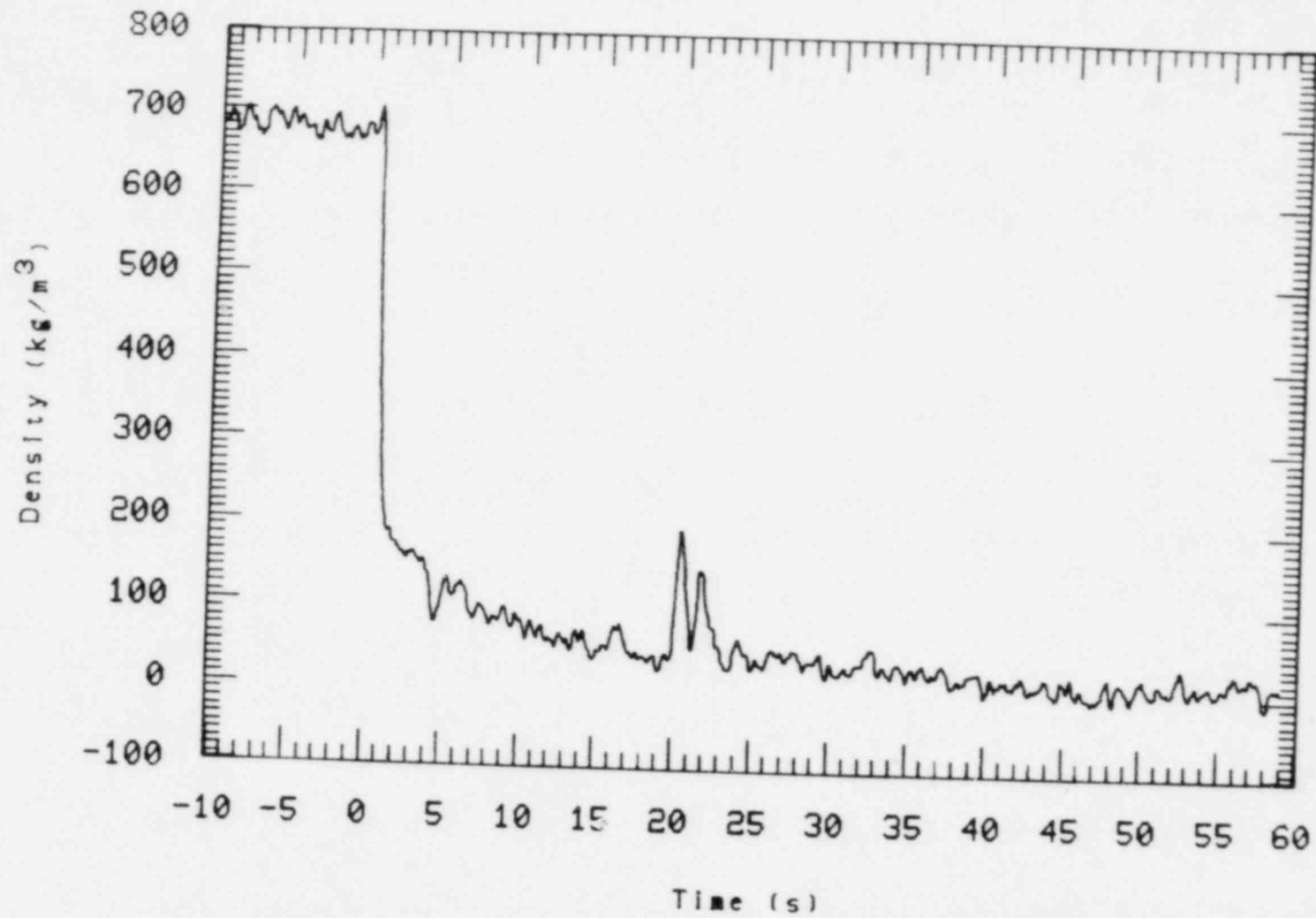


Figure 17. Upper core region fluid density (342 cm)



1 RV-23+13

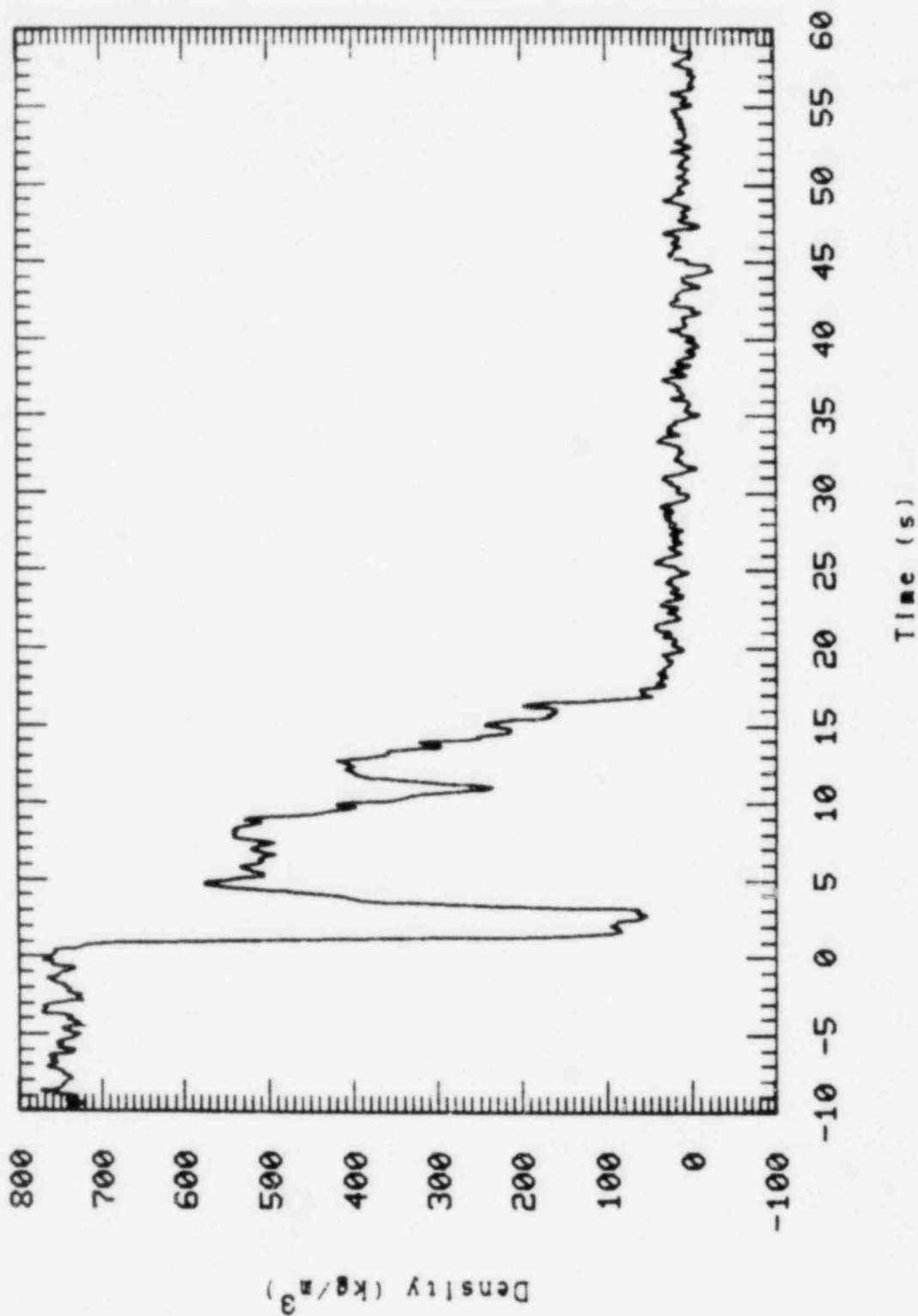


Figure 18. Lower core region fluid density (13 cm).

volume-change condition pushed fluid up the guide tube to the upper head, out the broken loop hot leg, and down into the lower plenum and then back up the downcomer.

In a two cycle, density wave oscillation liquid reappeared in the lowest part of the core twice, before leaving the vessel empty (Figures 18, 19). The initial downward, flashing flow in the vessel was apparently condensed in the lower plenum, since no vapor appeared at the bottom downcomer densitometer. The second vapor surge did appear there (at about 10 seconds) and initiated the subsequent decrease in fluid density seen throughout the downcomer in the following 10 seconds (Figures 20 and 21).

As can be seen in Figures 22 through 24, the broken loop piping and loop seal voided by 5-6 seconds, and the large increases in volumetric flow rates in that loop (typified in Figure 25) subsequent to that time reflect the clearing of this path to the break. The liquid in the other path to the break (downcomer inlet annulus to break via part of broken loop cold leg) saturated at 8 seconds, but the break did not uncover until 13 seconds. The decrease in break mass flow rate with the flashing in the broken loop at 5-6 seconds as well as the uncovering of the break orifice at 13 seconds is shown in Figure 26. This break mass flow rate (also shown in Figure 43) is calculated from two phase mass flow measurements (densitometers, full flow drag screens and full flow turbine meters) located in the two sections of the broken loop cold leg leading to the break orifice.<sup>a</sup>

Also at 13 seconds, pressures in the upper head and upper plenum interchanged and upper head liquid again flowed down the guide tube into the upper plenum (Figure 27), albeit only for the 6 seconds until the liquid level fell below the top of the tube (Figure 28). This upper head

---

a. The backup turbine meter had to be used for the flow in the cold leg section between the downcomer and the break. The calibration relation of such a device under horizontal pipe, stratified flow conditions is unknown and the resulting calculated mass flow during accumulator injection is in error to some greater extent during that time span.

1 RV\*AB-6

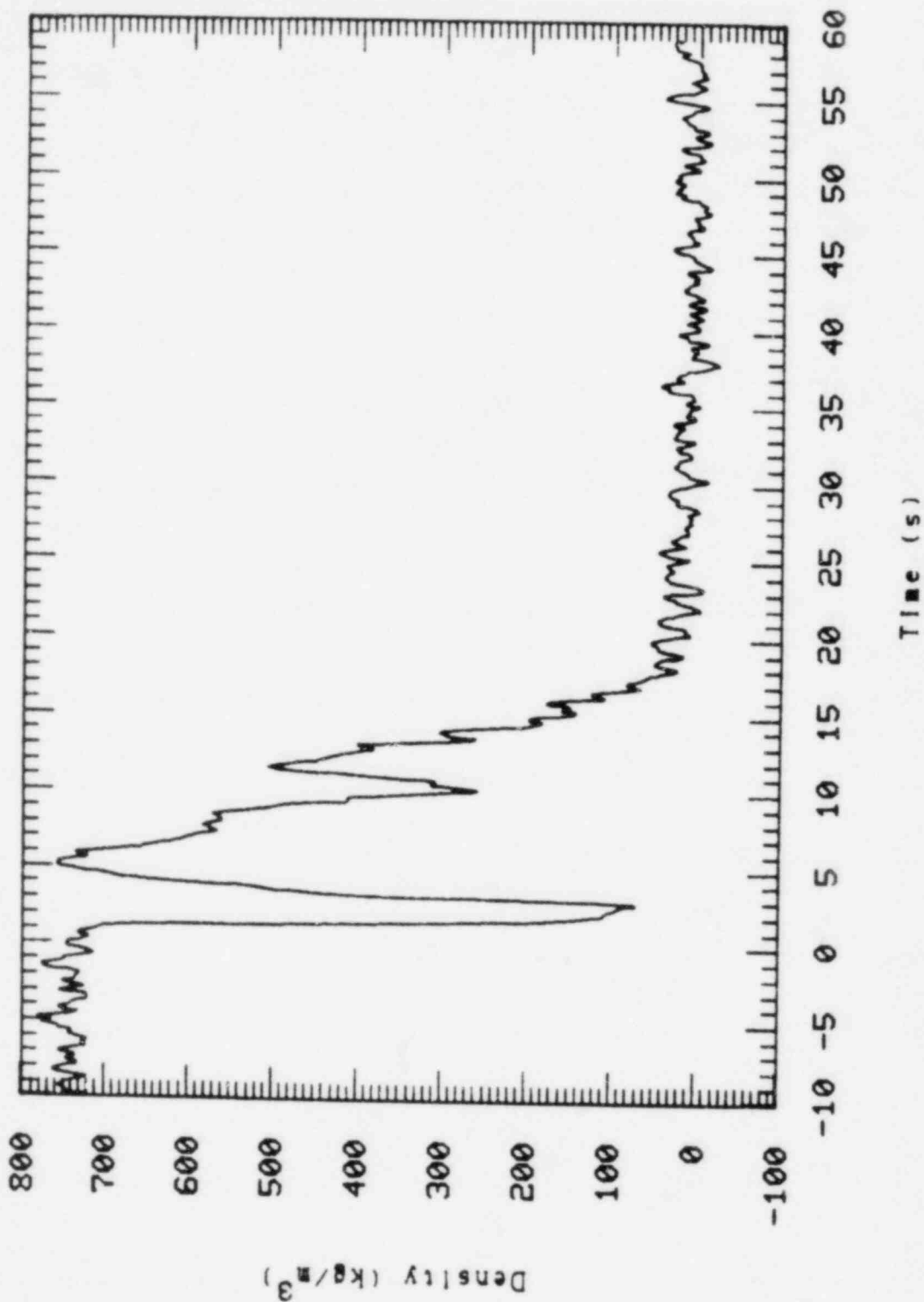


Figure 19. Core fluid density 6 cm below heated length.

1 RV-DC-72

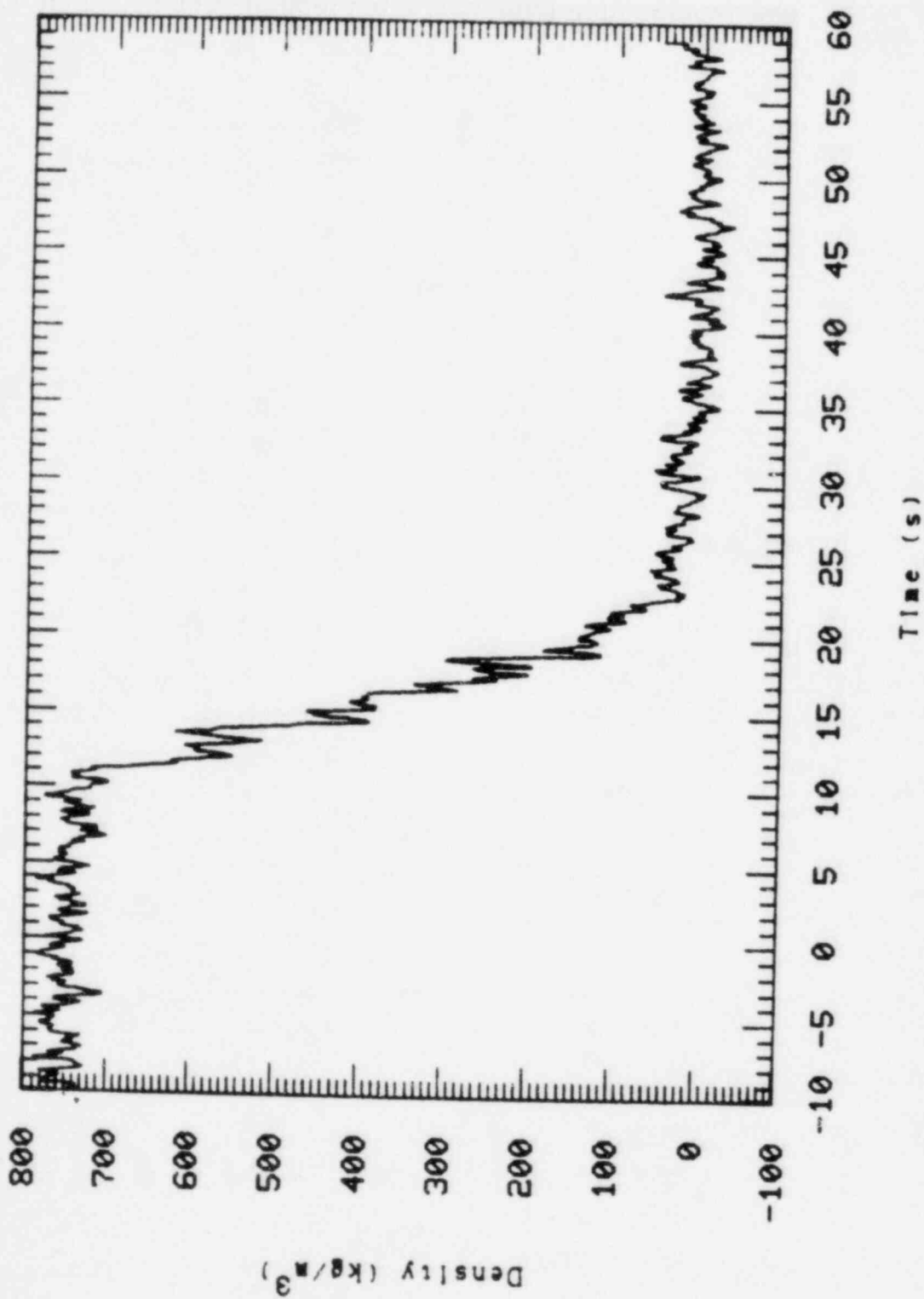


Figure 20. Fluid density at top of downcomer.

1 RV=DC-456

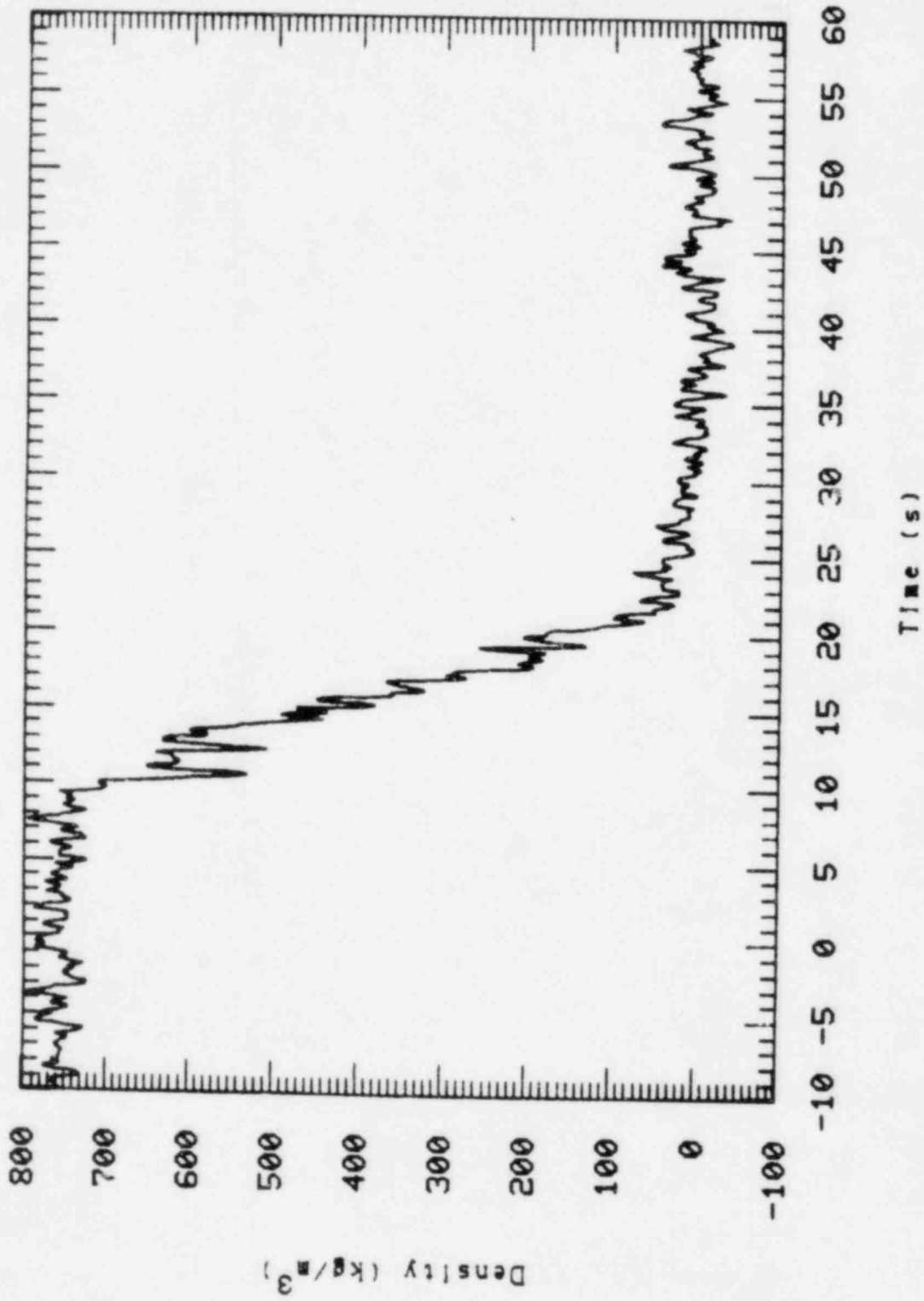


Figure 21. Fluid density at bottom of downcomer.

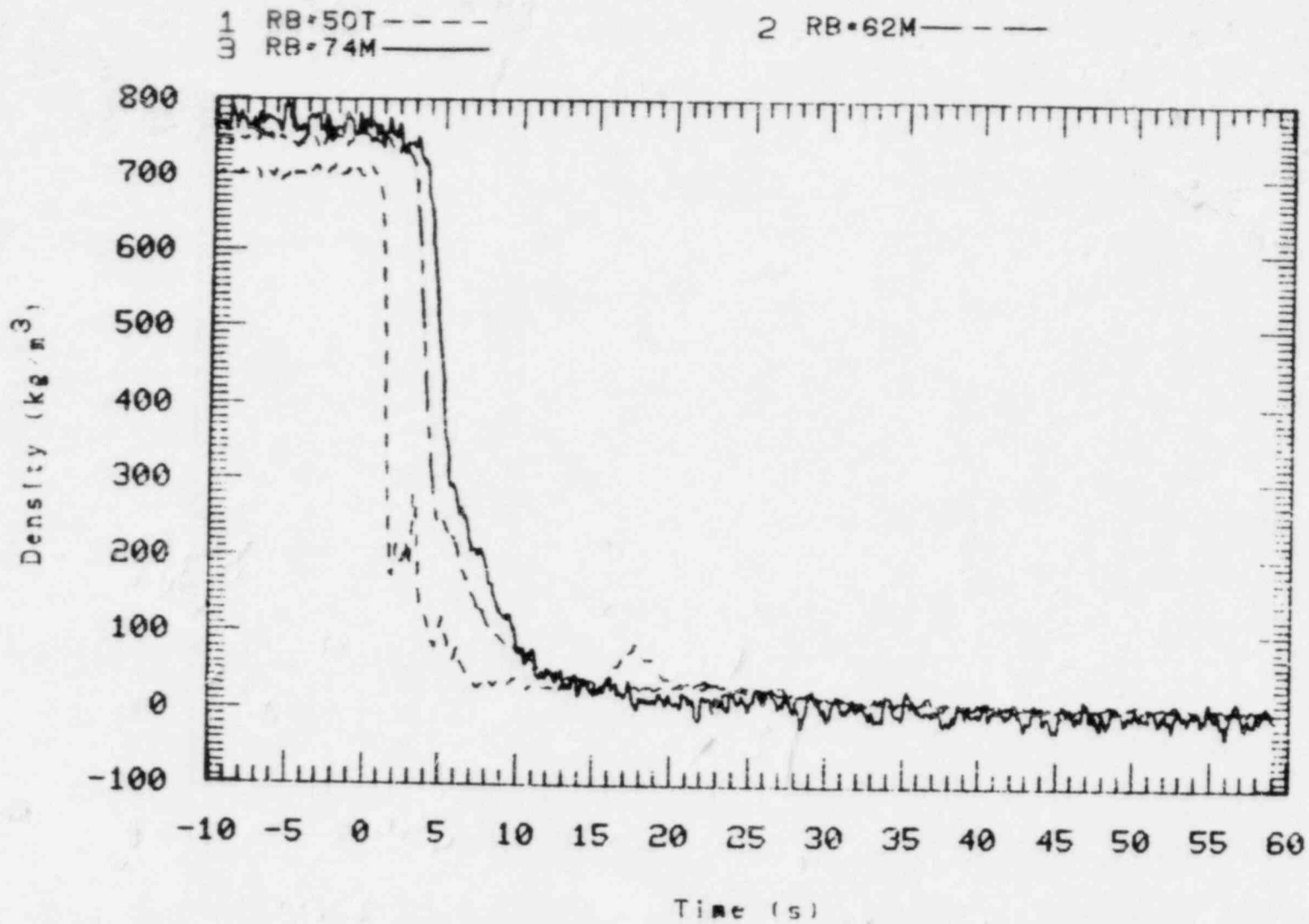


Figure 22. Broken loop fluid densities.

1 DPB•65•73

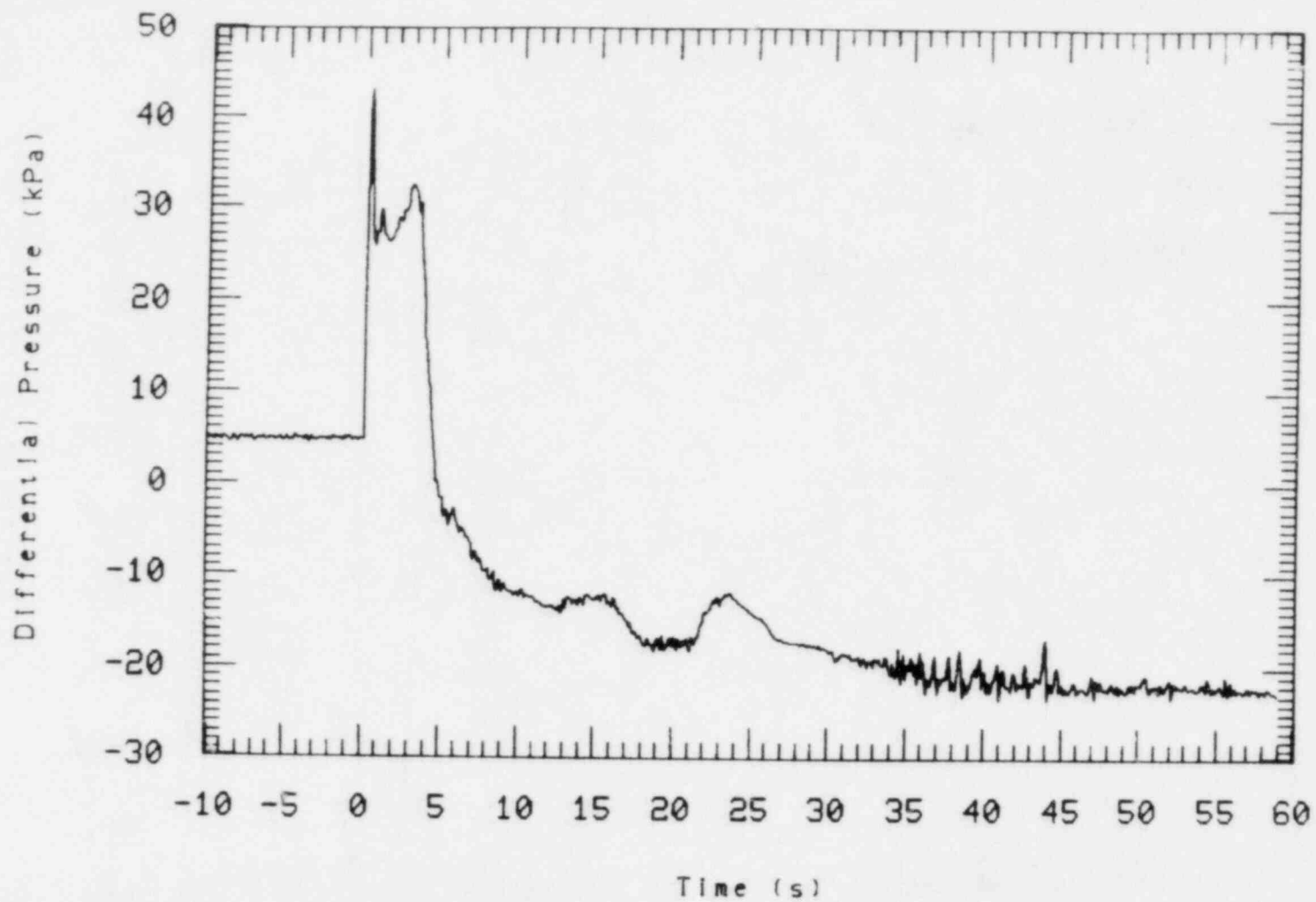


Figure 23. Liquid level in broken loop seal.

1 RB-73

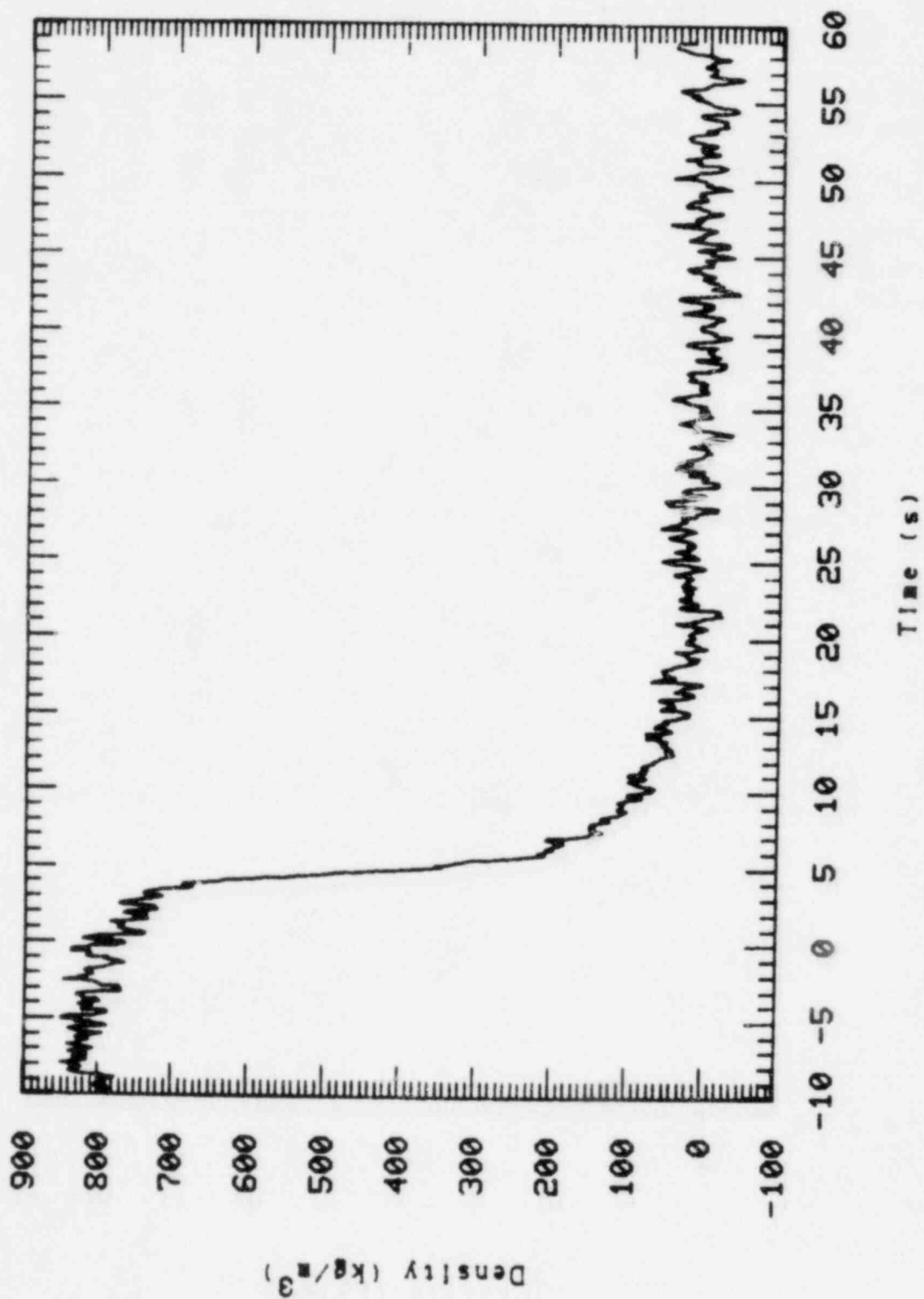


Figure 24. Fluid density in broken loop seal.



1 QB-50

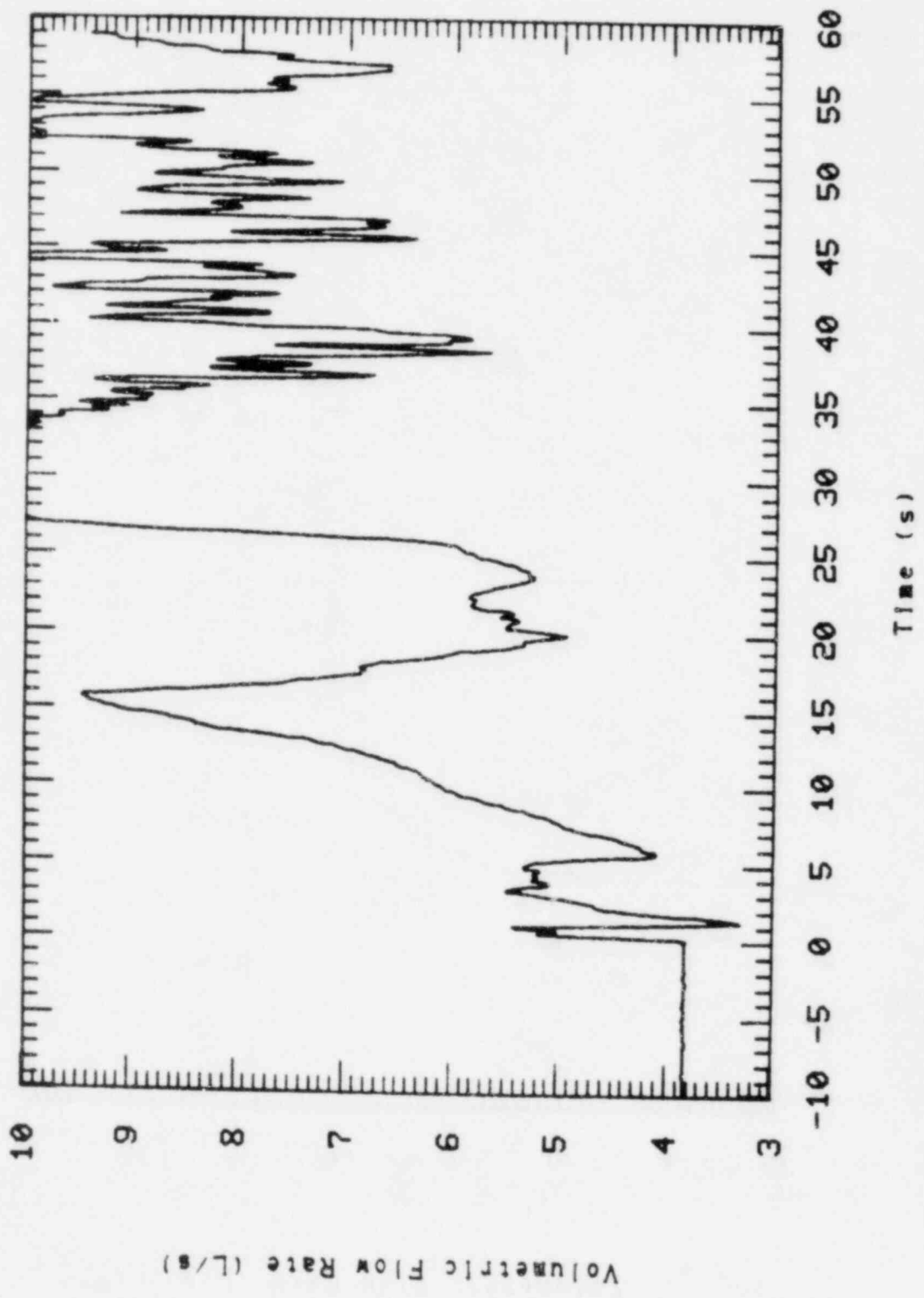


Figure 25. Broken loop hot leg volumetric flow.

1 BREAK-FLOW

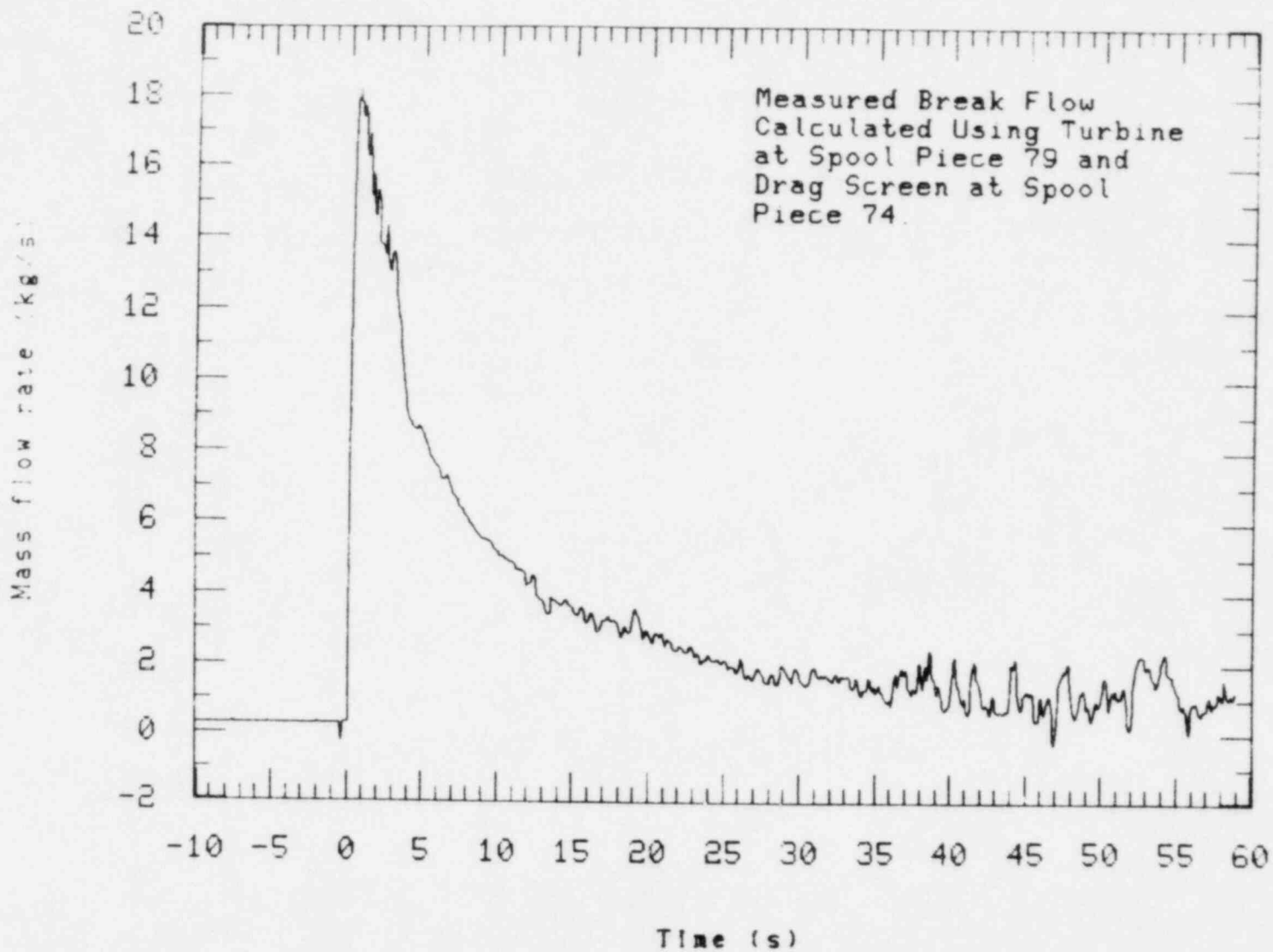


Figure 26. Break mass flow rate.

1 FV\*GT+330

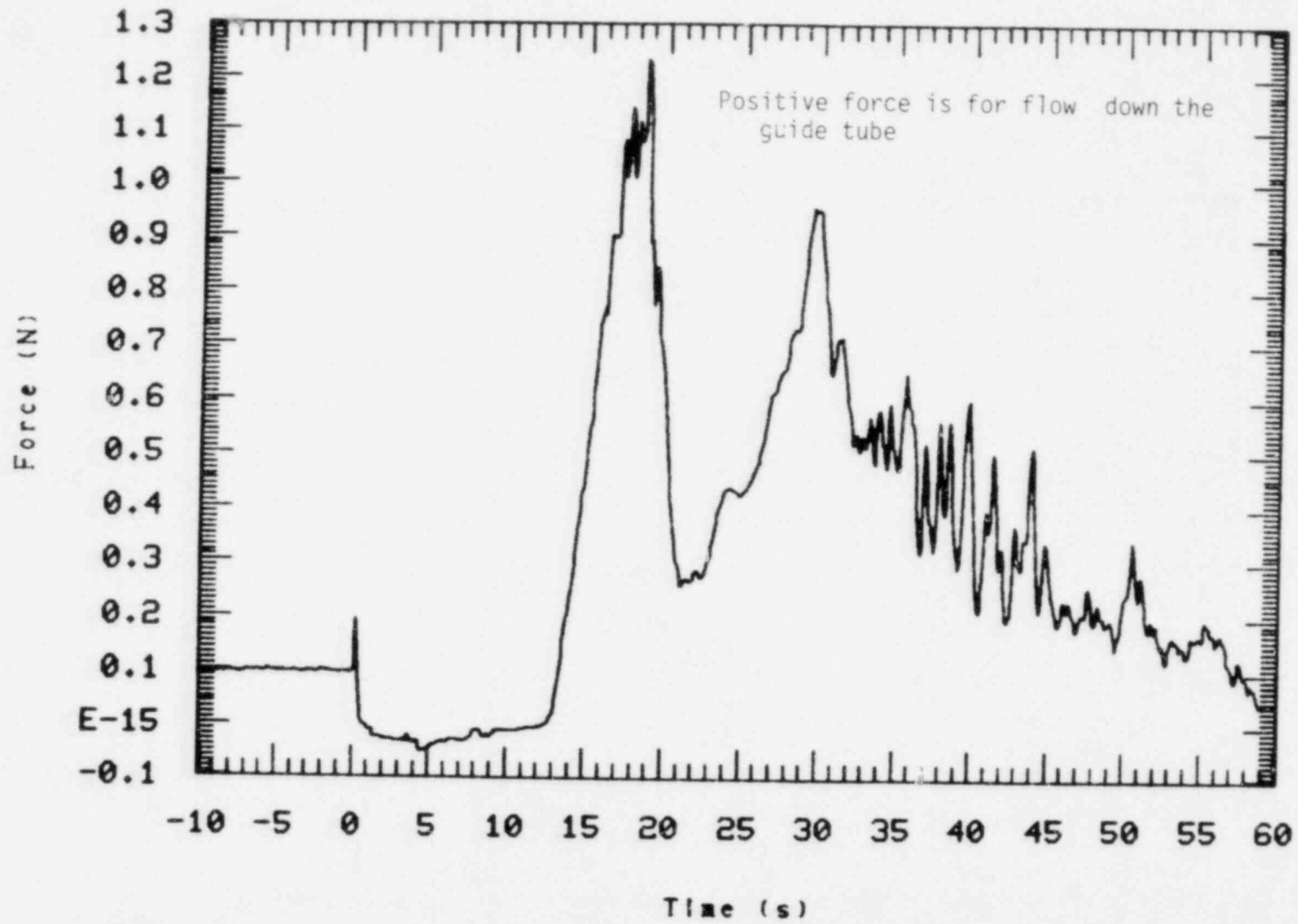


Figure 27. Guide tube momentum flux and flow direction.

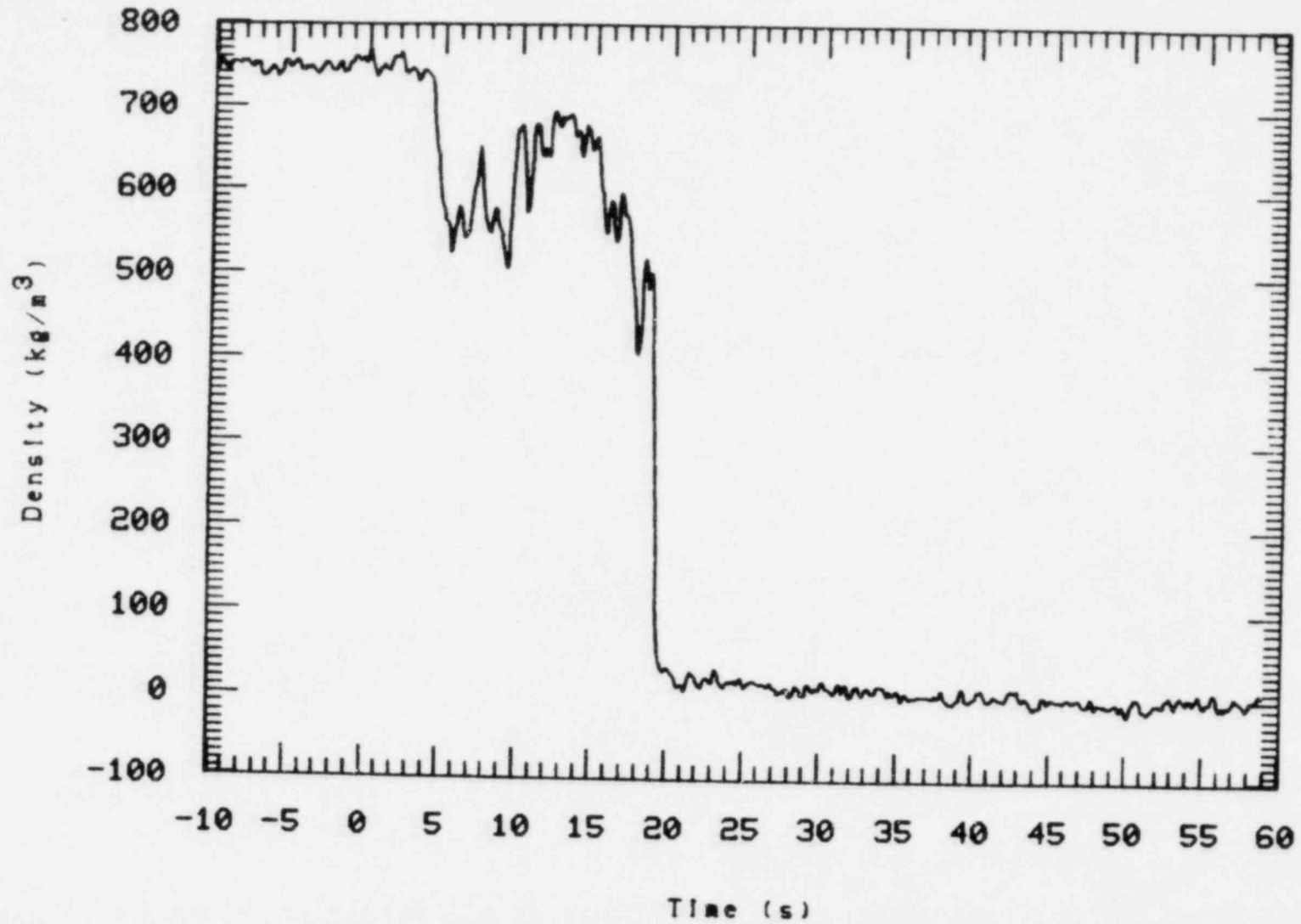


Figure 28. Upper head fluid density at top of guide tube.

liquid flow can be seen passing the upper plenum densitometer at about 15 sec and providing about a  $150 \text{ kg/m}^3$ , 3-second-wide density pulse at 20 seconds, at core top, in Figure 17. The effect of this flow on core temperatures is discussed in Section 3.1.3.

With break uncover at 13 seconds, volumetric flows moving to the downcomer inlet annulus (and then the break) increased. These are shown in Figures 29-31 and include flow up the downcomer, down the core bypass line from the upper head, and out the intact loop cold leg (where the fluid had just become saturated at 10 seconds). Flow direction reversals occurred in the intact loop hot leg at 19 seconds and the upper plenum at 24 seconds, reflecting the less resistive path to the break. In general, the volumetric flows in both loops continued to increase as the system pressure fell toward the accumulator set pressure.

### 3.1.3 ECC and Core Thermal Response

As noted in Figure 16, accumulator liquid started flowing into the intact loop cold leg at 27 seconds (Figure 32). However, because of the high steam flow up the external, single-pipe downcomer, (Figure 29), the ECC flowed around the downcomer inlet annulus to the break (Figures 20, 26, 33), bypassing the core during this time. (Normally, when the blowdown ends, the large driving force for flow up the downcomer disappears and the ECC is able to penetrate the downcomer.) As noted in Section 3.1.1, in this test a correctly scaled amount of accumulator water was used. However, because the bypass period is characteristically long in Semiscale, accumulator ECC liquid flow continued for only 3 seconds beyond the end of blowdown. At the end of liquid flow, the  $\text{N}_2$  accumulator pressurizing gas normally forms a plug of already injected ECC which is then pushed through the intact loop cold leg, part going to the break and part through the downcomer to the core. Because of the coincidental proximity, in time, of the end of blowdown and the end of accumulator liquid injection in this test, the otherwise-separated effects appear as nearly a single event in the data (Figures 20, 29, 33). This accumulator water, the upper head liquid flow into the core mentioned earlier, and the core power are the major factors affecting the core thermal response during blowdown.

1 QV=DC-423

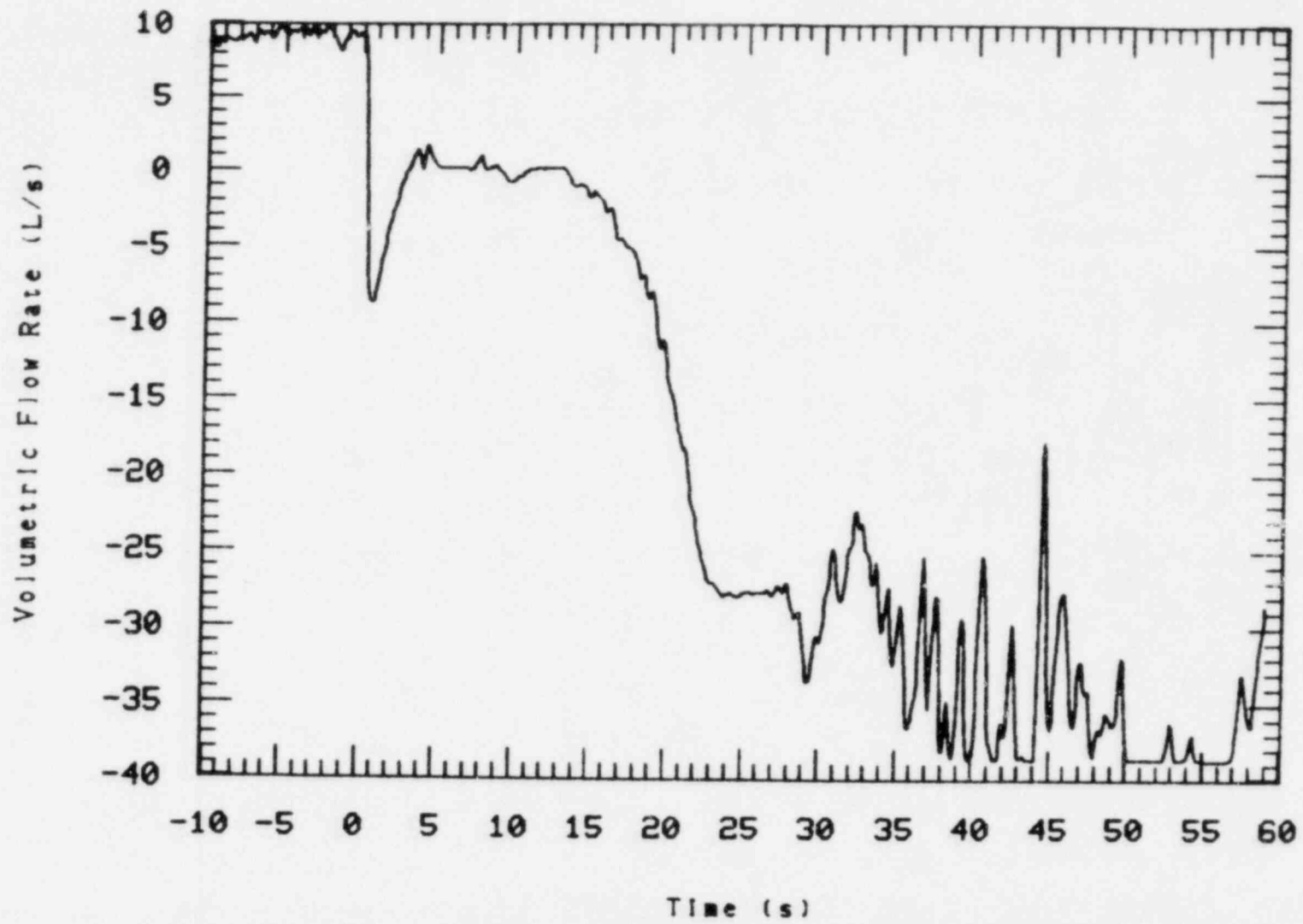


Figure 29. Volumetric flow in the downcomer.

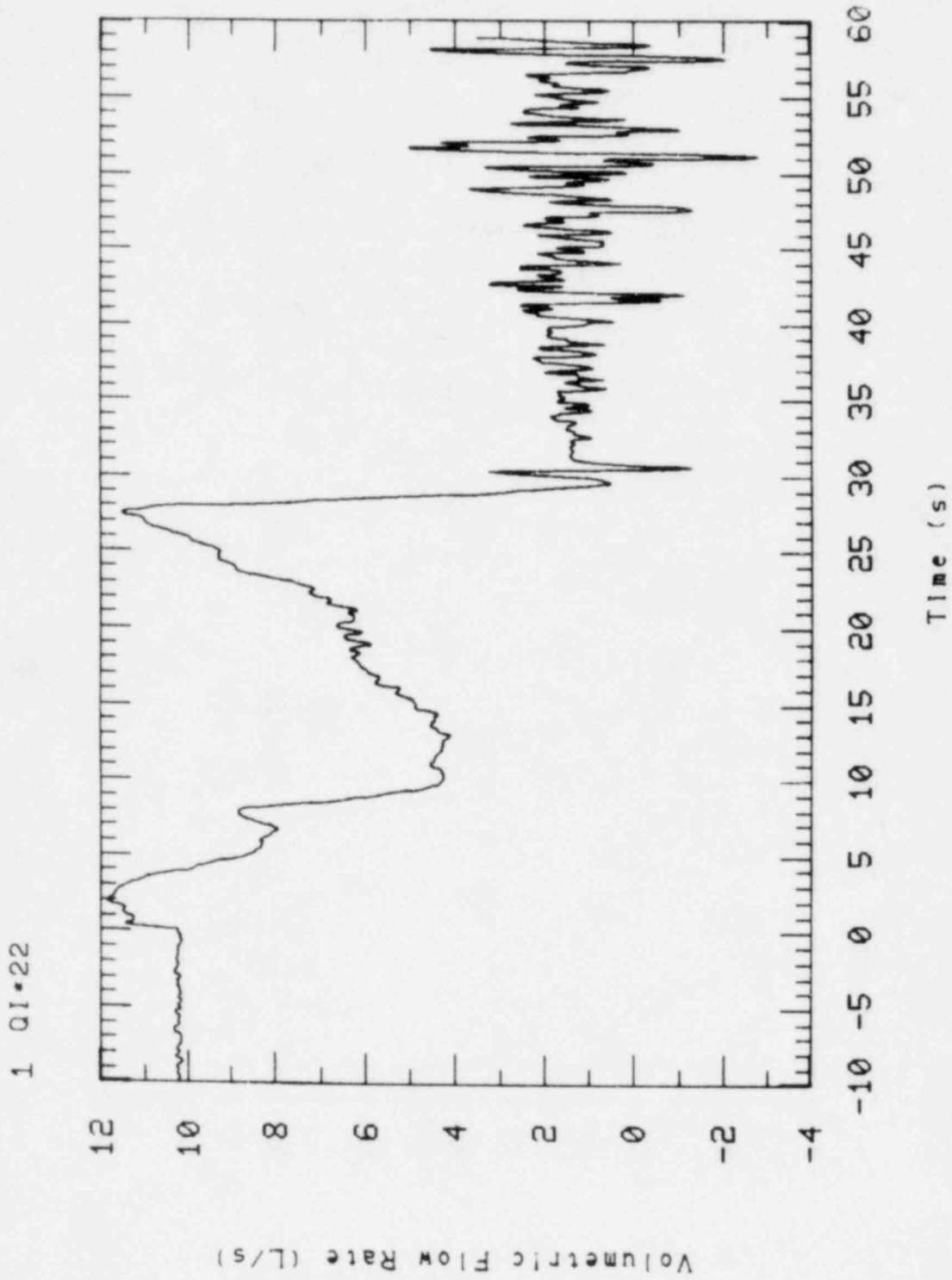


Figure 30. Volumetric flow in the intact loop cold leg.

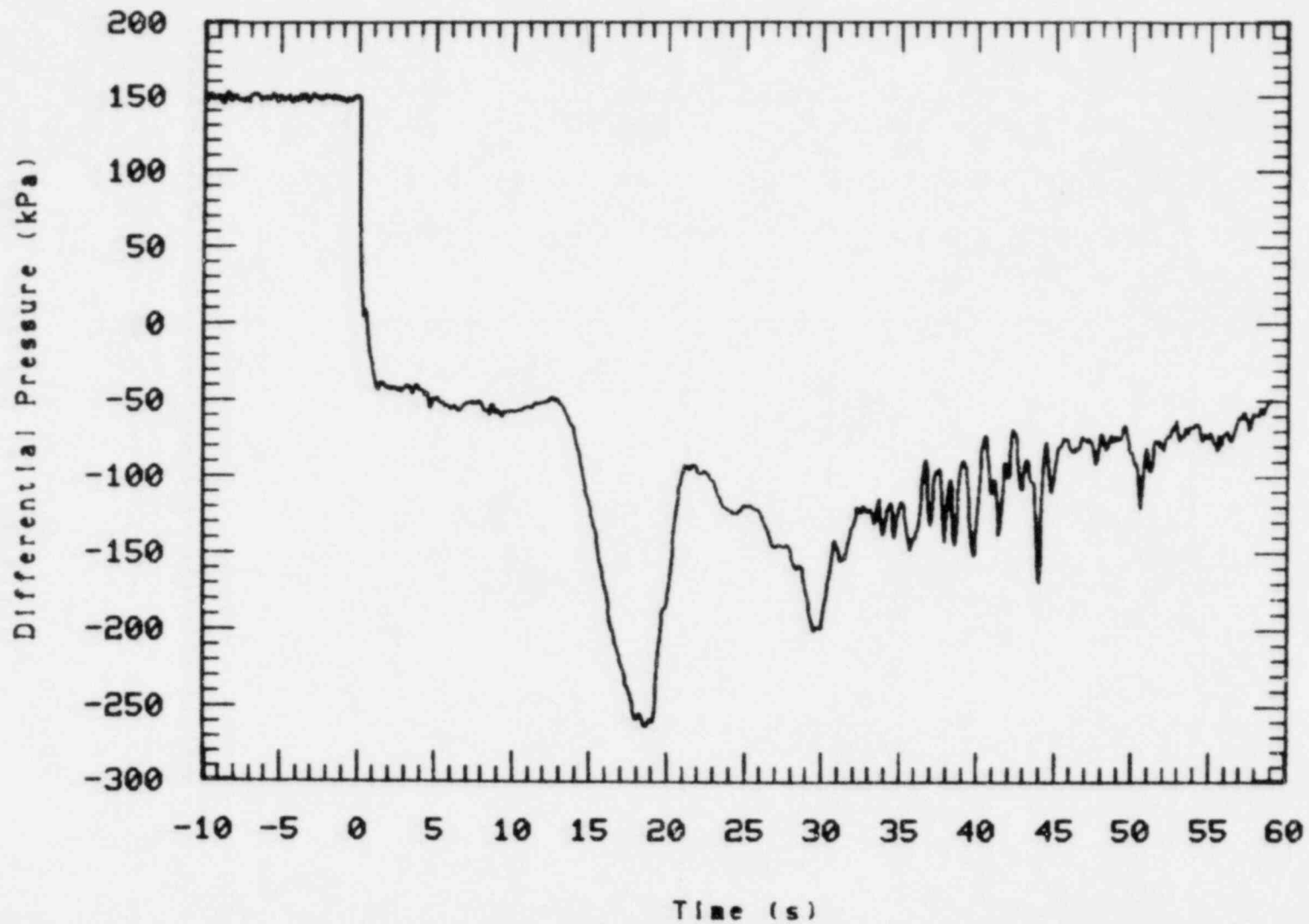
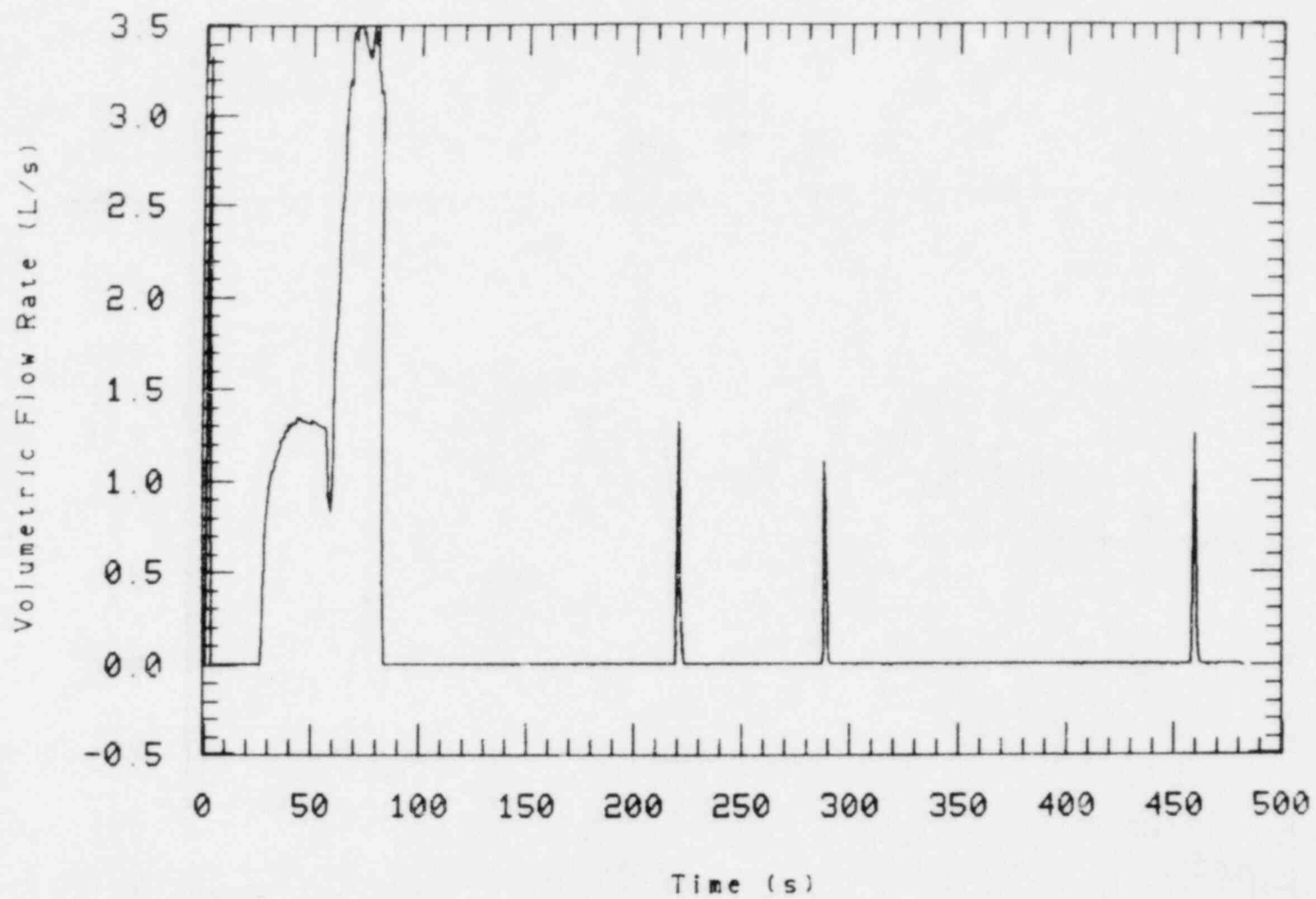


Figure 31. Core bypass line differential pressure between upper head and downcomer.



1 QCI-A3



54

Figure 32. Accumulator volumetric flow.

1 RB-79M

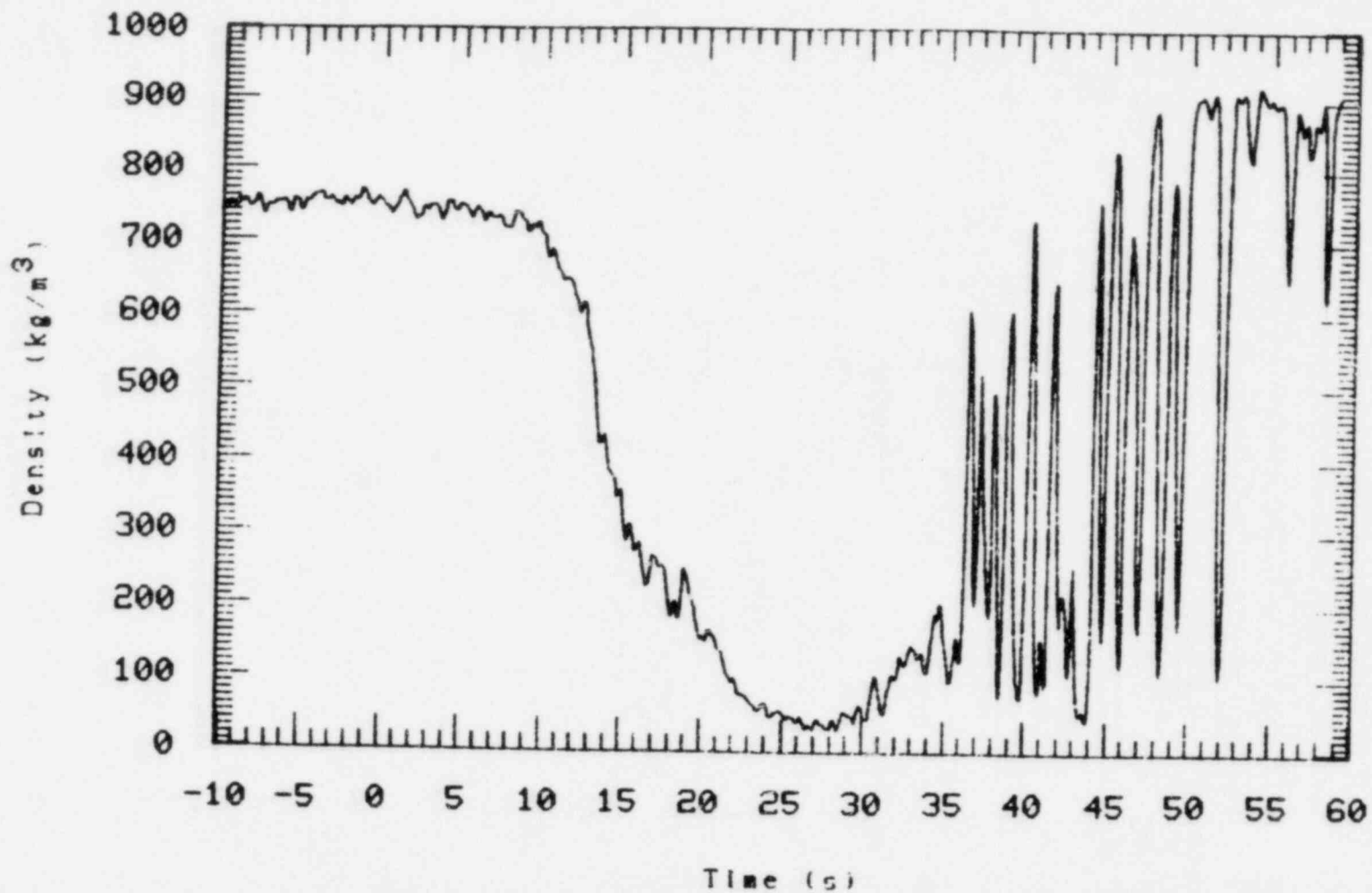


Figure 33. Fluid density in the broken loop cold leg between downcomer and break.

Simply described, a composite core temperature trace (Figure 34) for this test consisted of a sharp rise in temperature to a peak value in the range of 900 K at just about 4 seconds, followed by a decline of 1/4 or less of this rise, and then followed by another, slower, increase recovering to about the initial peak before again declining. This second peak occurs at 20 seconds. After the decline from the 20 second peak, the temperature continues its climb with a long gradual increase over several hundred seconds of slow reflood, culminating in a maximum value approximately 400 K higher than the initial peak temperature. A significant fourth peak and decline exists at 60 seconds for rod positions low in the core. In fact, the absence or presence and magnitude of all the various peaks depends significantly on the axial core location except for the initial peak.

The initial temperature rise is due to the voided-condition, low heat transfer coefficient.<sup>a</sup> The decline from this peak is due to the core power reduction at 4 seconds (Figure 12) and the associated heat capacity and cooling of the heater rods. The core power is increased somewhat at 8 seconds and the heater temperature correspondingly slowly increases to the 20 second peak. The decline from this peak, where it is observed in the core, is due to the cooling afforded by the upper head liquid draining down the guide tube and moving downward in the core. Figures 35 and 36 illustrate this effect and the distribution of this coolant over space and time.

---

a. Before this initial rise, a 10-15 K drop in temperature is commonly seen in the data during the first second after rupture. This is due to the enhanced heat transfer associated with the flashing (nucleation and acceleration) of the primary coolant. At the bottom of the core this 10-15 K drop is not observed; rather an immediate temperature rise occurs during the first second and is associated with the effect of core flow reversal and separation (in this low power, high subcooling region the effect is due to single phase velocity dependence of the heat transfer coefficient, not DNB).

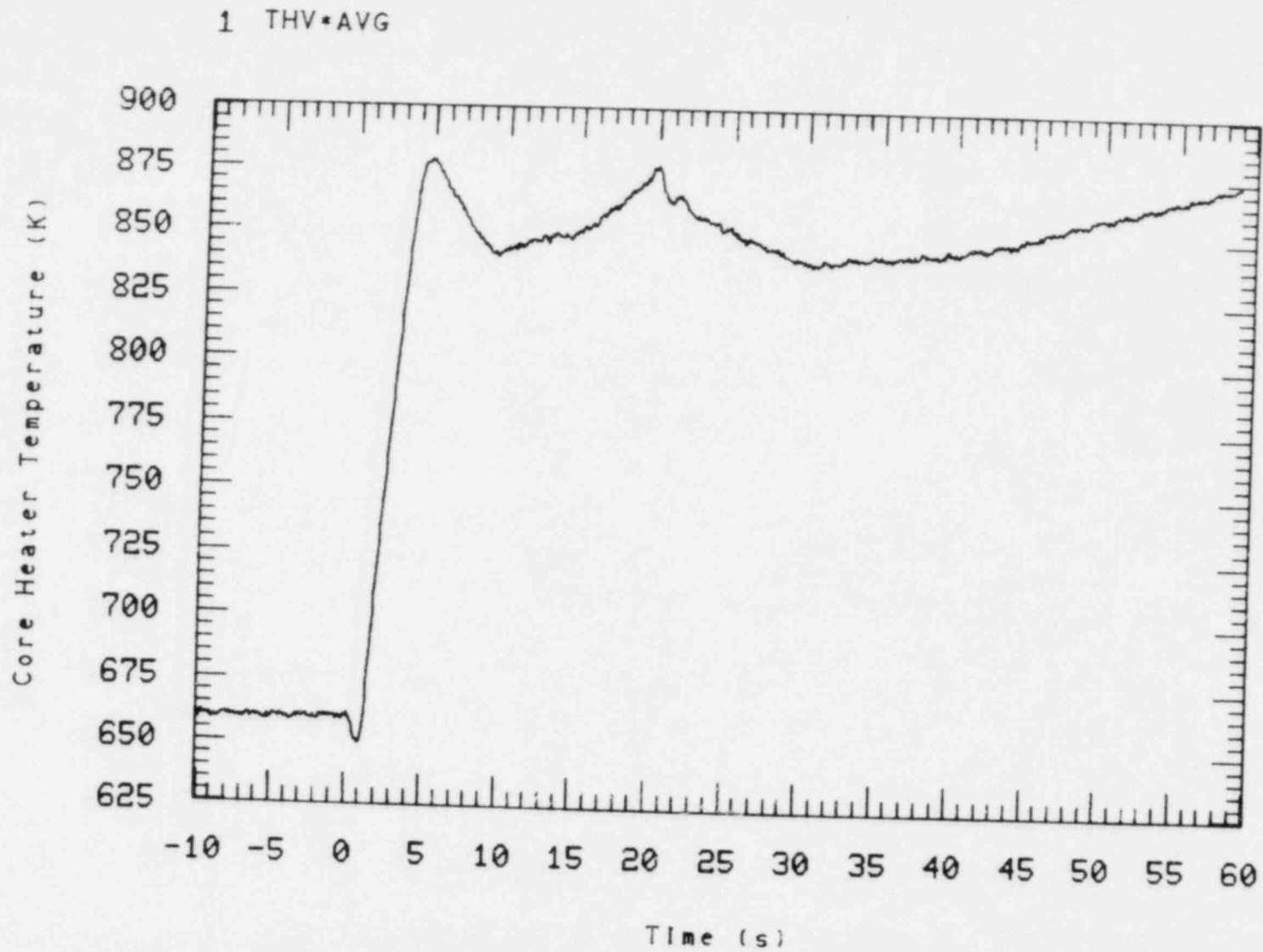


Figure 34. Core heater rod average temperature.

1 THV-B3+354

88

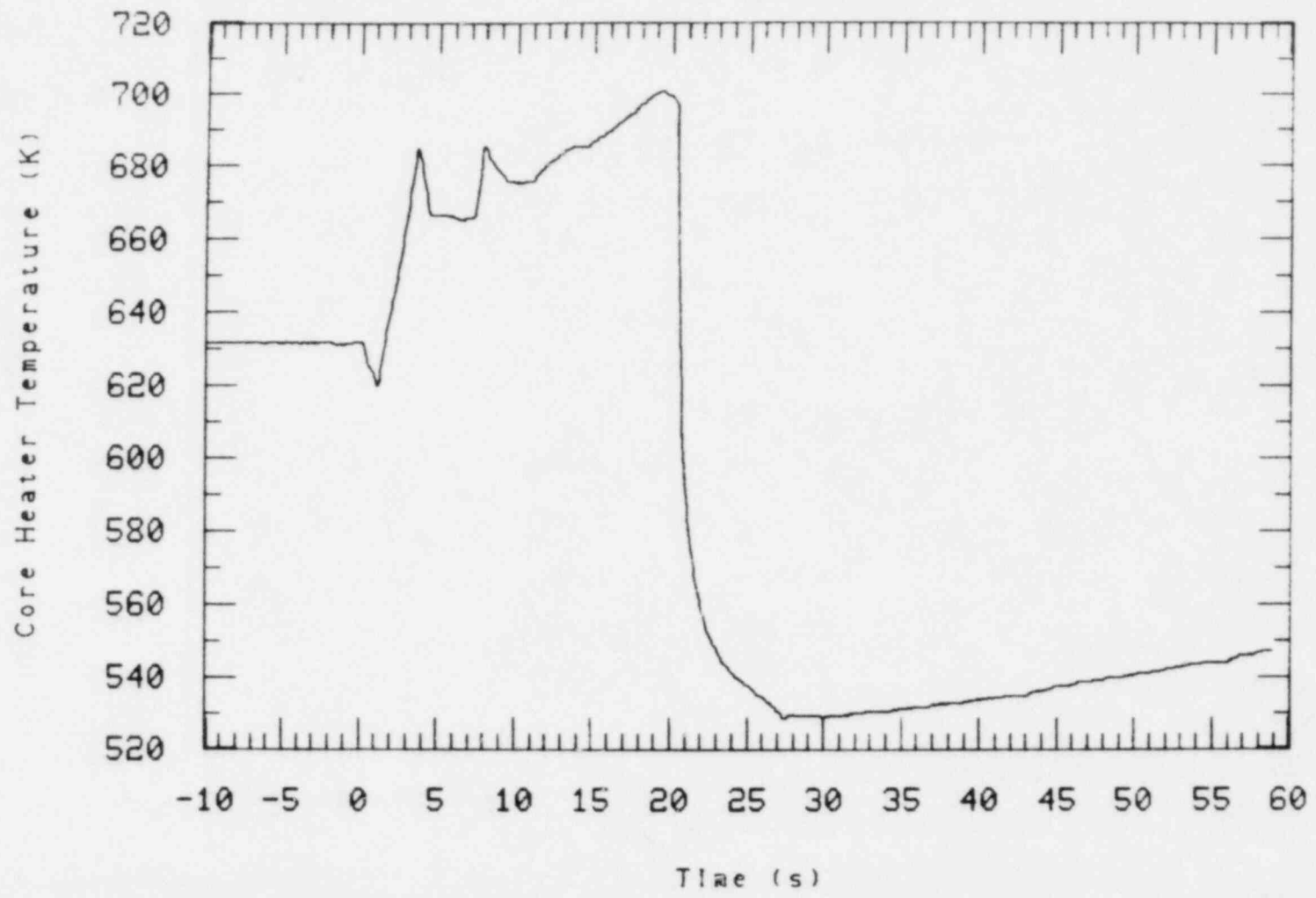
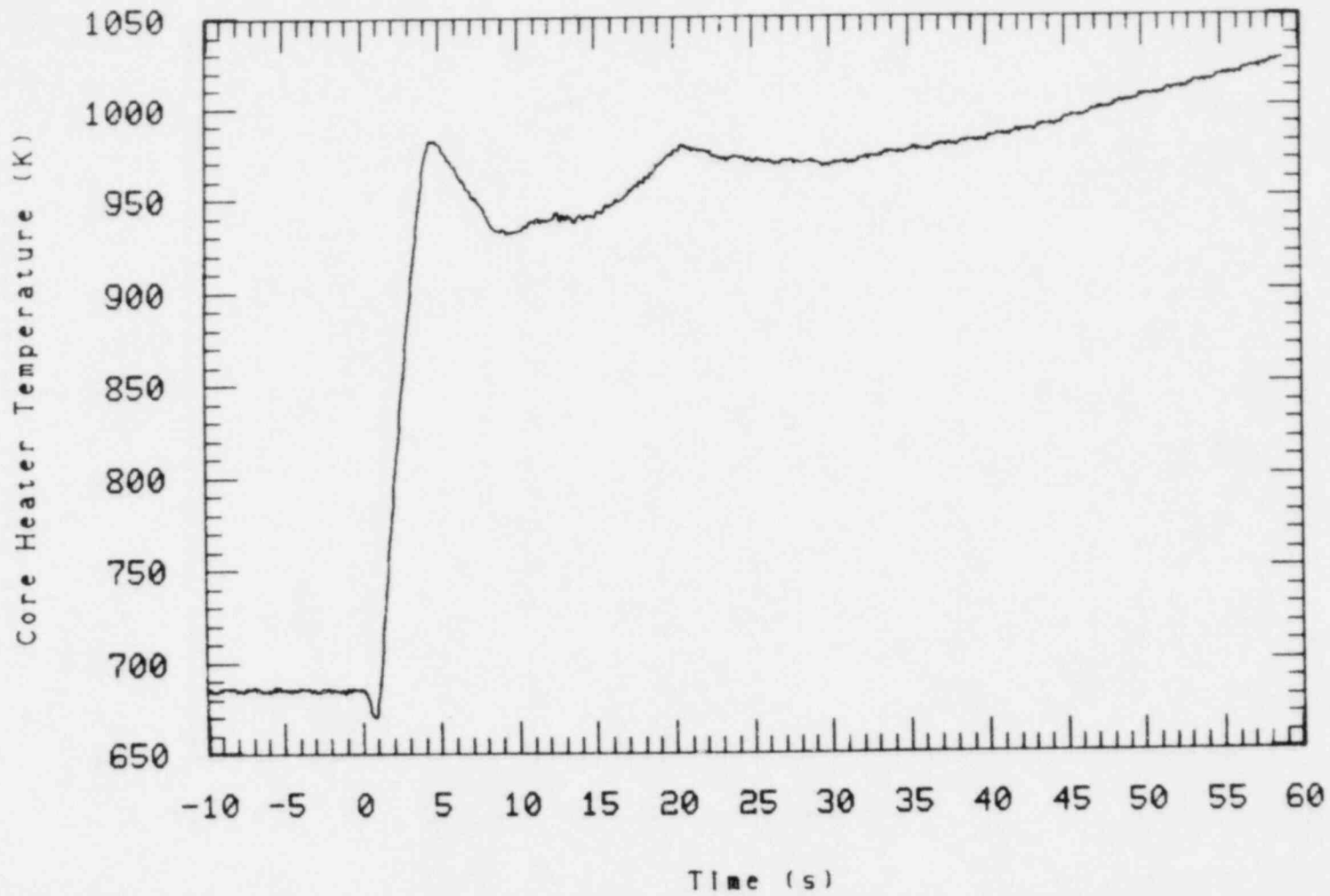


Figure 35. Upper-head-liquid cooling at the top of the core.

1 THV•D2+185



59

Figure 36. Upper-head-liquid cooling at core midplane.

At 60 seconds, accumulator liquid quenches the bottom ends of the heater rods (Figure 37) but is hardly noticeable one third of the way up the core (Figure 38).

After the end of the accumulator injection, only the pumped ECC is available to cool the core, and with only about 1/3 of the specified flow, the core temperatures rise over several hundred seconds, but do ultimately turnover. Figures 39-41 show typical temperature variations along two traverses at the core midplane (radial variations) and axial temperature variations in a central rod. As noted earlier, the reflooding extended beyond the (preprogrammed) data system recording capability.<sup>a</sup>

### 3.2 Comparison with Other Experiments

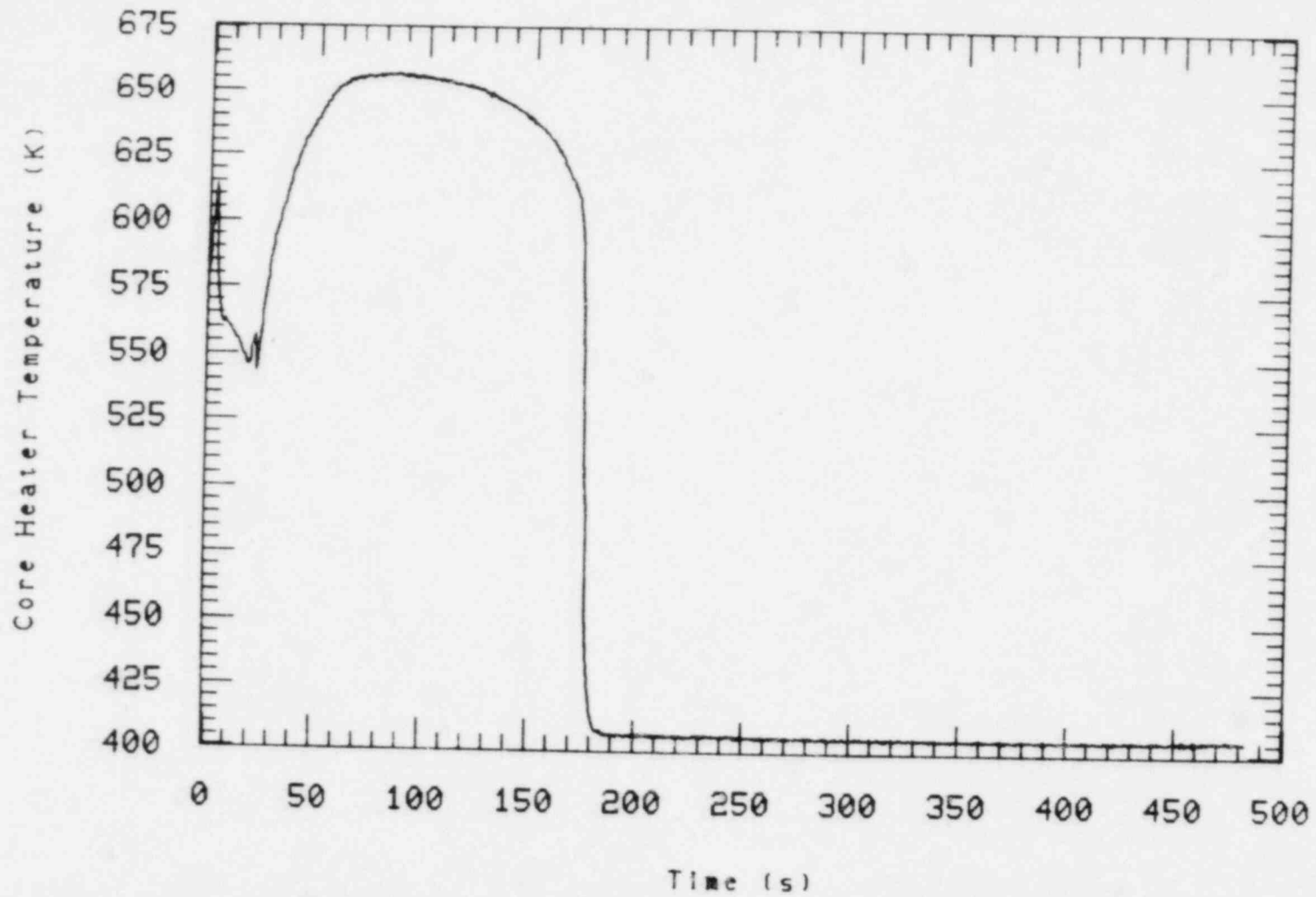
Comparisons are limited due to the fact that a 100%, communicative cold leg break experiment has not been performed in any of the earlier configurations of the Semiscale test facility. Comparison of the present data with that from the 50% break test, S-1B-2, will be contained in the Quick Look Report for that test and comparison of results across the 200% to 10% break spectrum is planned for inclusion in the Intermediate Break Series Test Results Report. For the present, some comparisons with results from the Semiscale MOD-3 200% non-communicative baseline test for integral blowdown and refill/reflood, S-07-6, are given below along with some system-operational-checkout testing done with that same break configuration, but the newer Mod-2A system configuration.

Several features of the S-1B-1 transient are qualitatively similar to those observed in S-07-6. The fluid in the core region was basically expelled within 2 seconds in both tests, void fractions ranging from 80 to

---

a. Lower sampling rates which facilitate longer recording times for fixed data storage capacity cannot be reduced indefinitely because of aliasing problems, and inadequate rates for fast blowdown transients.

1 THV•C2+15



19

Figure 37. Accumulator-liquid cooling at bottom of core.



1 THV-B3-114

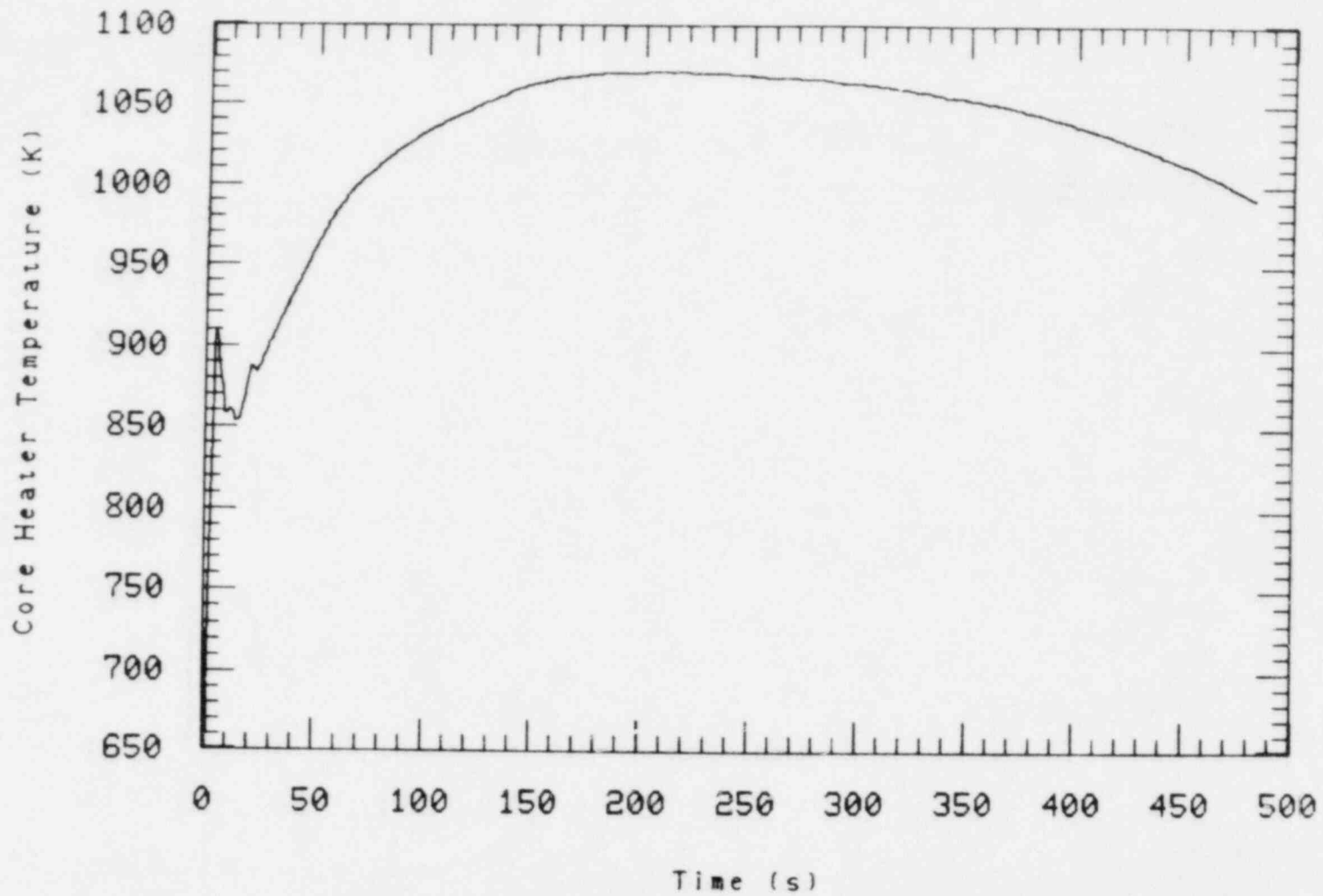


Figure 38. Accumulator-liquid cooling 1/3' up from core bottom.

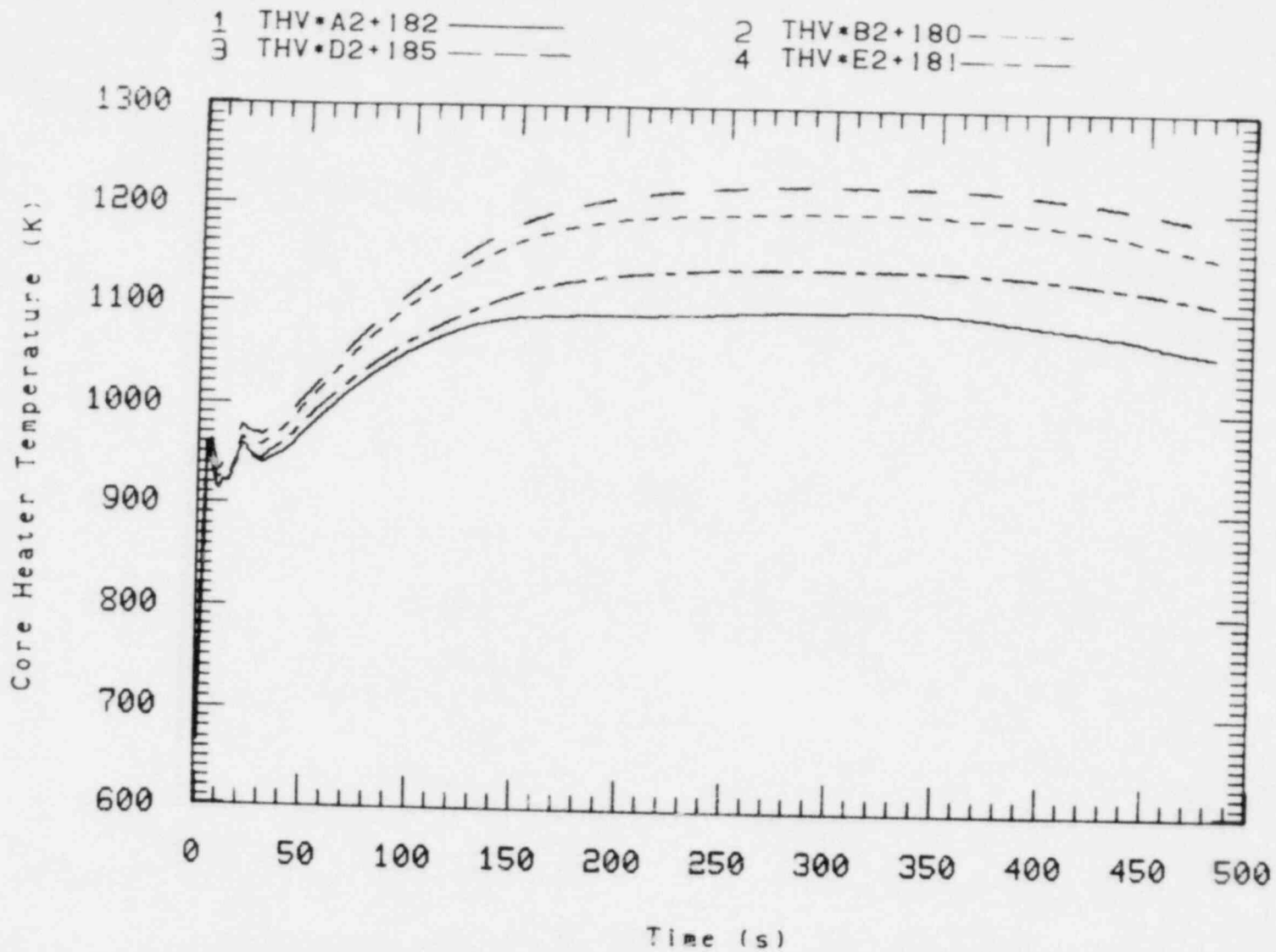


Figure 39. Comparison of core midplane temperatures in row 2.

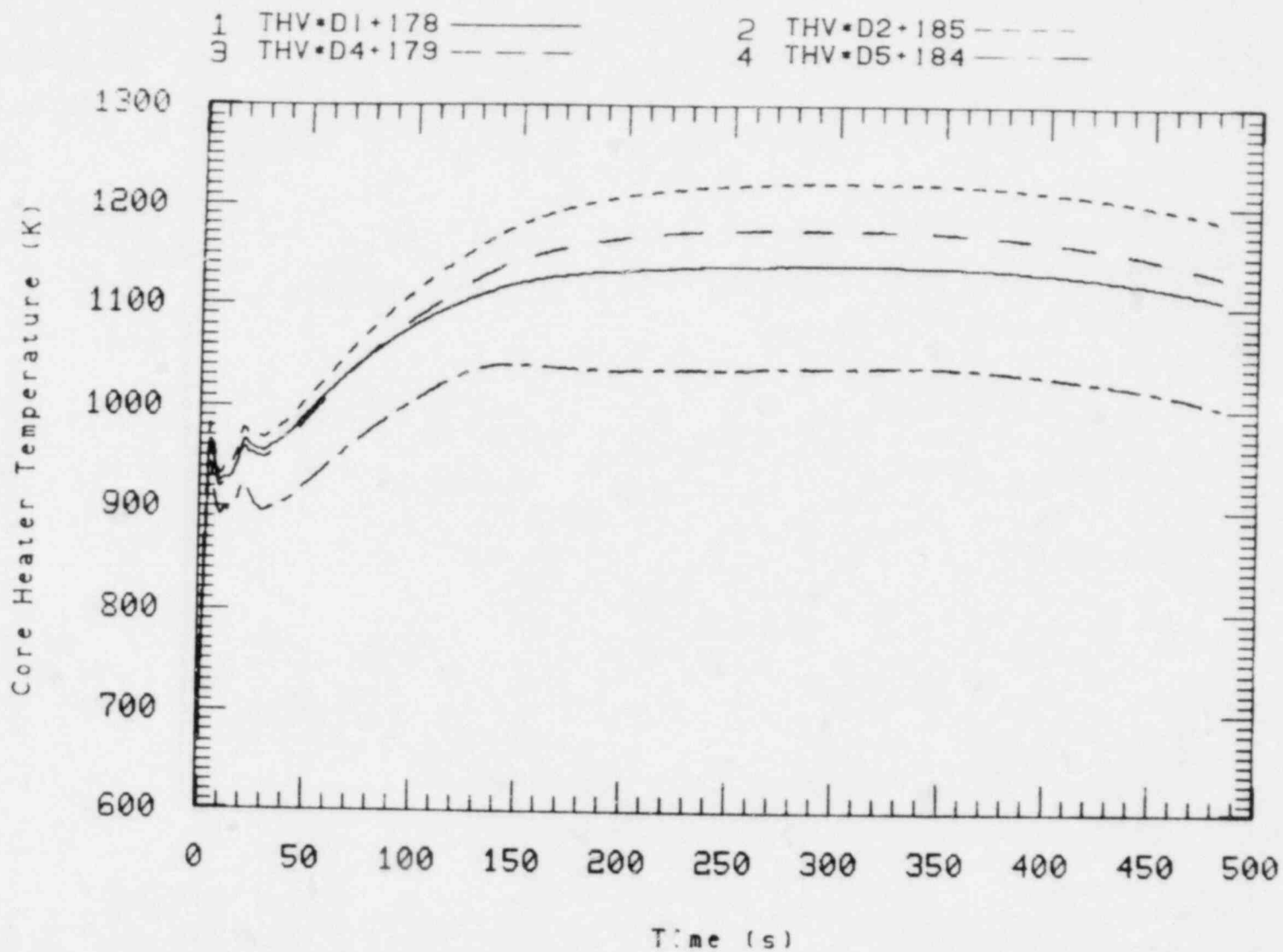


Figure 40. Comparison of core midplane temperatures in column D.

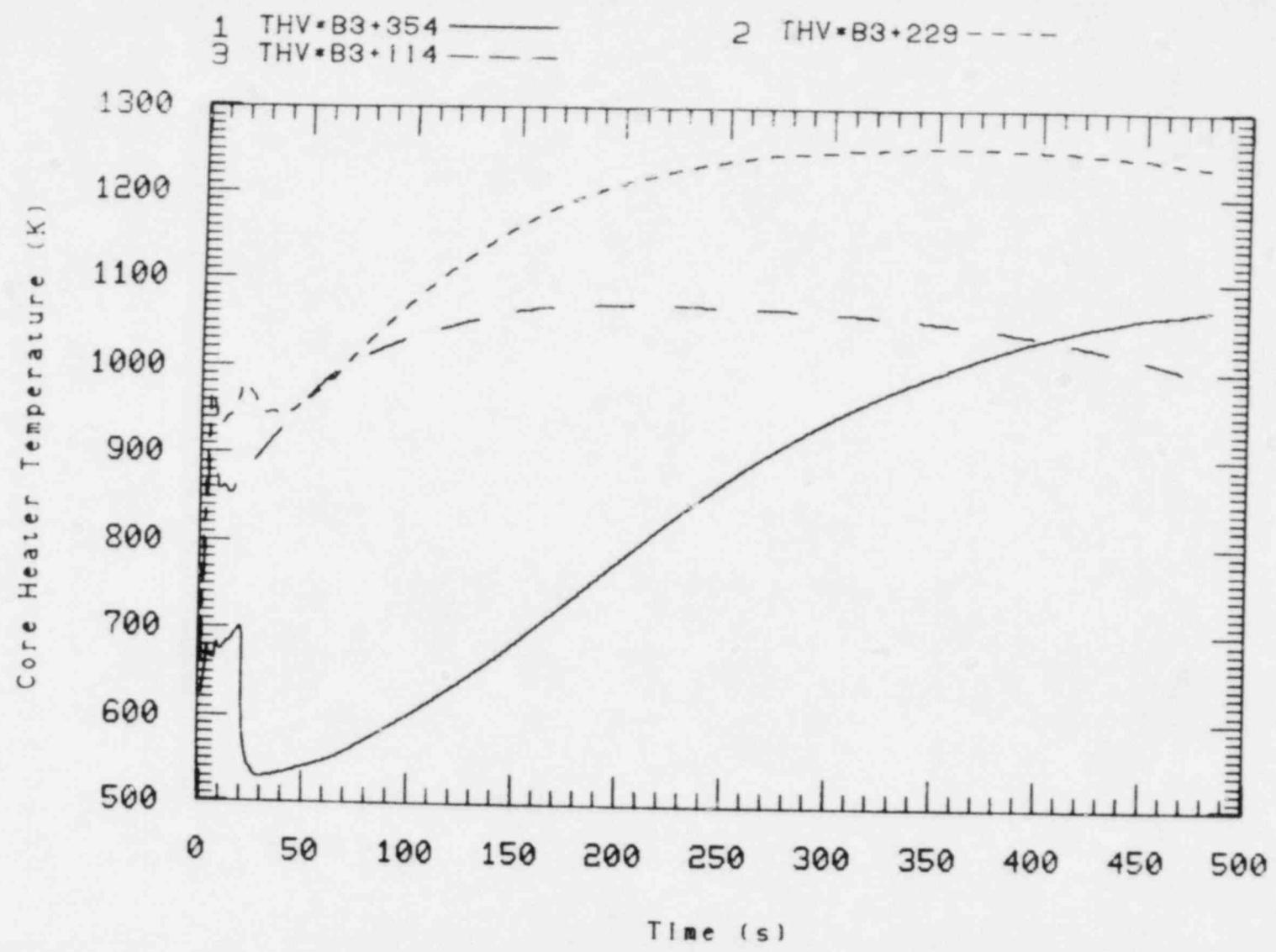


Figure 41. Comparison of core axial temperatures in heater rod B3.

95% over the core height in both. In S-07-6 the liquid continued to stay out of the vessel, but in S-IB-1, the lower plenum and lowest fourth of the core partly refilled by about 4 seconds and then gradually boiled/emptied out over the next 16 seconds. The initial cooling during the first second, noted above for S-IB-1, also existed for S-07-6 and in both experiments the heater rod temperatures then rose rapidly due to the lack of coolant. In S-IB-1 the core power was dropped to zero at 4 sec and then increased again at 8 sec, whereas in S-07-6, the power was reduced uniformly over a 10 second period. As a consequence of the power profile, the first peak in the heater rod temperature in S-IB-1 reached only about 900 K (4 seconds) while the correspondingly induced peak in S-07-6 reached about 1100 K at 10 seconds. In both experiments, upper-head-liquid coming down into the core produced significant cooling. In S-IB-1, this cooling effect, down to midplane height, was more easily discerned than in S-07-6. This is because in the S-IB-1 test this cooling effect and the temperature decrease due to core power were separated in time by about 15 seconds, whereas in S-07-6 the two effects occurred at about the same time (10-11 seconds) and it was therefore difficult to distinguish between them. A second significant cooling event (75-150 K in one second) occurred in S-07-6 at the bottom of the core in the time span from 15-22 seconds. The timing is such that this liquid (confirmed by associated densitometer and core fluid temperature variations) might have been upper-head-liquid. However, for this to be the case, that liquid would have had to travel over most of the core length in channels (e.g., liquid level probe and unheated rod) not monitored by heater rod thermocouples. In the main part of the bundle, heater rod temperatures in S-07-6 did not indicate this flow to go this low in the core. In S-IB-1 there were two unheated rods (no liquid level probe) and thermocouples in both rods showed some cooling (20-40 K) at the proper time. The cooling at the bottom of the core was also observed in S-IB-1 but to a much smaller extent (15-20 K) than in S-07-6, leading to the supposition that the liquid level probe (in Mod-3) may have facilitated this bypass flow.

In both experiments, after these initial variations, heater rod temperatures increased until the effect of accumulator liquid was seen. In S-07-6 the accumulator liquid flow started at 19 seconds, continued until

about 63 seconds, with containment pressure being reached at about 43 seconds (so accumulator liquid started down the downcomer at that time). In S-IB-1, accumulator liquid flow (properly) started later (27 seconds), ended earlier (58 seconds) due to a smaller liquid volume and containment pressure was (properly) reached later (55 seconds). The net result of these differences was that the downcomer and lower plenum were promptly filled in S-07-6 and reflood initiated at about 58 seconds, whereas they never completely filled in S-IB-1 and reflood didn't start until about 140 seconds.

Subsequent to refill, oscillatory level behavior and loss of fluid out the break ("mass depletion" or "geysering") was observed in S-07-6, and relatively low ( $\sim 950$  K) heater rod temperatures resulted. No similar long term (100 second period) oscillation was observed in density, fluid nor heater rod temperature, downcomer nor vessel differential pressure level measurements in S-IB-1. In fact, none of these parameters showed oscillatory behavior of any frequency above the amplitude of the small noise background. Presumably this lack of oscillatory behavior was in part due to the lack of liquid in the vessel and downcomer at early times and resultant low steam generation and concomitant liquid displacement. As a result, however, heater rod and indicated core fluid temperatures rose substantially above those existing during the blowdown in S-IB-1; the peak clad temperature recorded being 1295 K at 370 seconds. Thus the reflood portions of the two experiments were totally different, while the blowdown portions were qualitatively similar.

### 3.3 Research Issues

Issues of interest in this test included:

1. were any new phenomena observed in the blowdown and reflood?
2. did oscillatory fluid conditions occur during reflood (as in Test S-07-6)?
3. was the system response more typical of a large or small break?

No new phenomena were observed in this test. As noted above, the blowdown portion of the test was qualitatively similar to an earlier 200% break test. The oscillatory fluid conditions observed in Test S-07-6 were not observed in Test S-1B-1. However, this is considered to be due to the fact that the downcomer was not refilled at accumulator injection time and the reflood therefore progressed slowly and solely on a degraded HPIS/LPIS flow. Viewed from a different point, this test result is fundamental in the sense that, at least in the Semiscale facility, the absence of accumulator ECC in a 100% break test did not result in an unacceptable heatup.

The system response was clearly typical of a large break. For example, the immediate voiding of the entire core and consequent heatup characteristic of large break tests was observed in this test. Similarly, the core level depression occurring prior to loop seal blowout which is characteristic of, and important to core cooling in small breaks but non-significant in large breaks was not significant in this test.

#### 4. COMPARISON OF SELECTED DATA TO PRETEST CALCULATIONS

This section presents a comparison of selected data from Test S-IB-1 with results of the blind pretest prediction calculation. A detailed description of the calculated results is given in Reference 5. The pretest prediction was performed using the RELAP5/MOD1 (Cycle 15) computer code. The calculation was performed through 49 s of the blowdown portion of the transient until computational problems terminated the calculation. Comparisons presented in this section provide a basis for evaluating the capability of the present analytical model to predict the system response resulting from a 100% communicative cold leg break in the Semiscale Mod-2A facility. Table 5 compares the significant initial conditions specified, measured, and calculated for Test S-IB-1, and Table 6 presents a chronology of significant events for Test S-IB-1.

A comparison of measured and predicted upper-plenum pressures is presented in Figure 42. Both the measured and predicted upper-plenum pressures were characterized by rapid decreases from 15.5 to 7.5 MPa during the first 6 s of the transient. During, approximately the first 0.5 s of the transient the calculated system depressurization rate was somewhat higher than the measured. At approximately 8 s in the test and 6 s in the calculation the liquid upstream of the break reached the saturation temperature and flashed. The subsequent flashing caused the depressurization rate to decrease in both the test and the prediction.<sup>a</sup> After the Broken loop cold leg fluid flashed, the measured and calculated depressurization rates were in good agreement. This initial disparity between the measured and calculated depressurization is due to differences in the break mass flow rates.

Presented in Figure 43 are the measured and calculated mass flow rates. During the initial 0.5 s of the transient, the measured break mass

---

a. The Intact and Broken loop cold legs were calculated to flash simultaneously. However, the Intact loop was measured to flash 2 s after the Broken loop flashed. This difference was caused by the initial Intact loop cold leg temperature being 8 K below the Broken loop temperature.



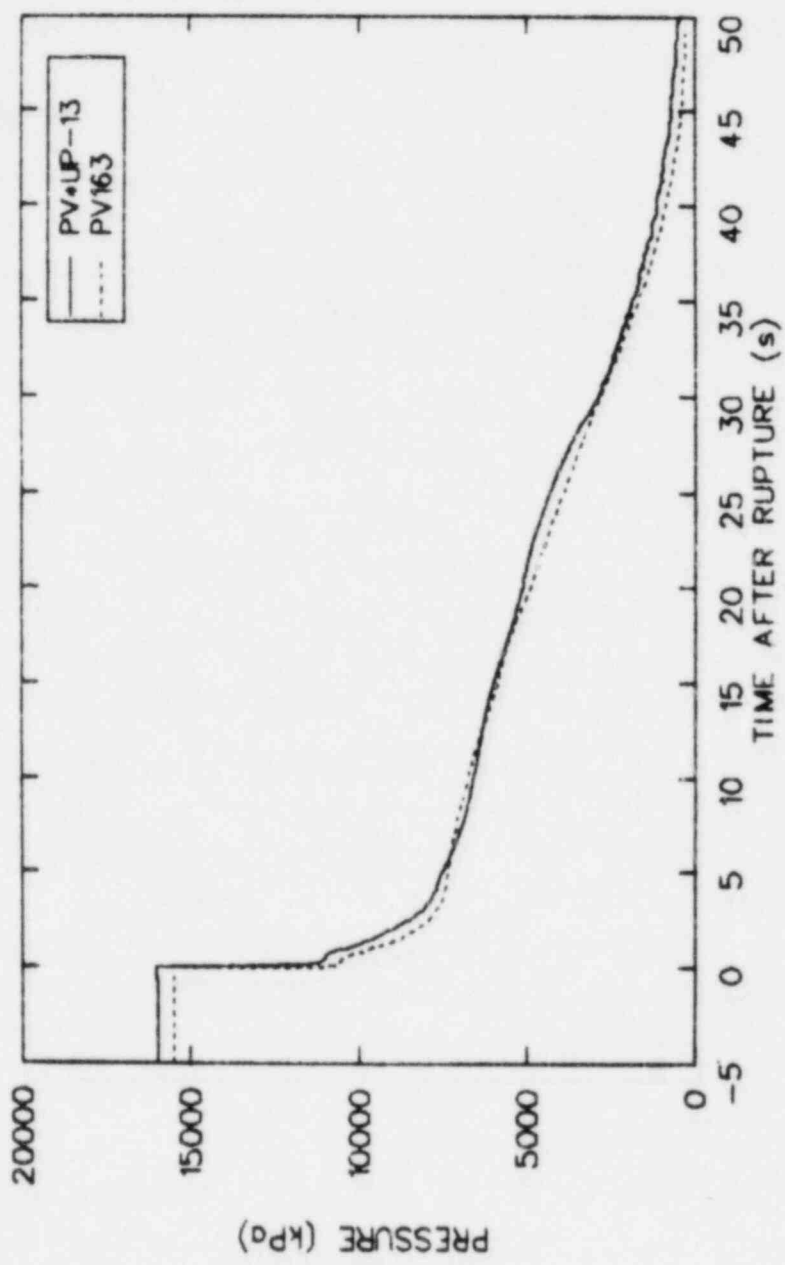


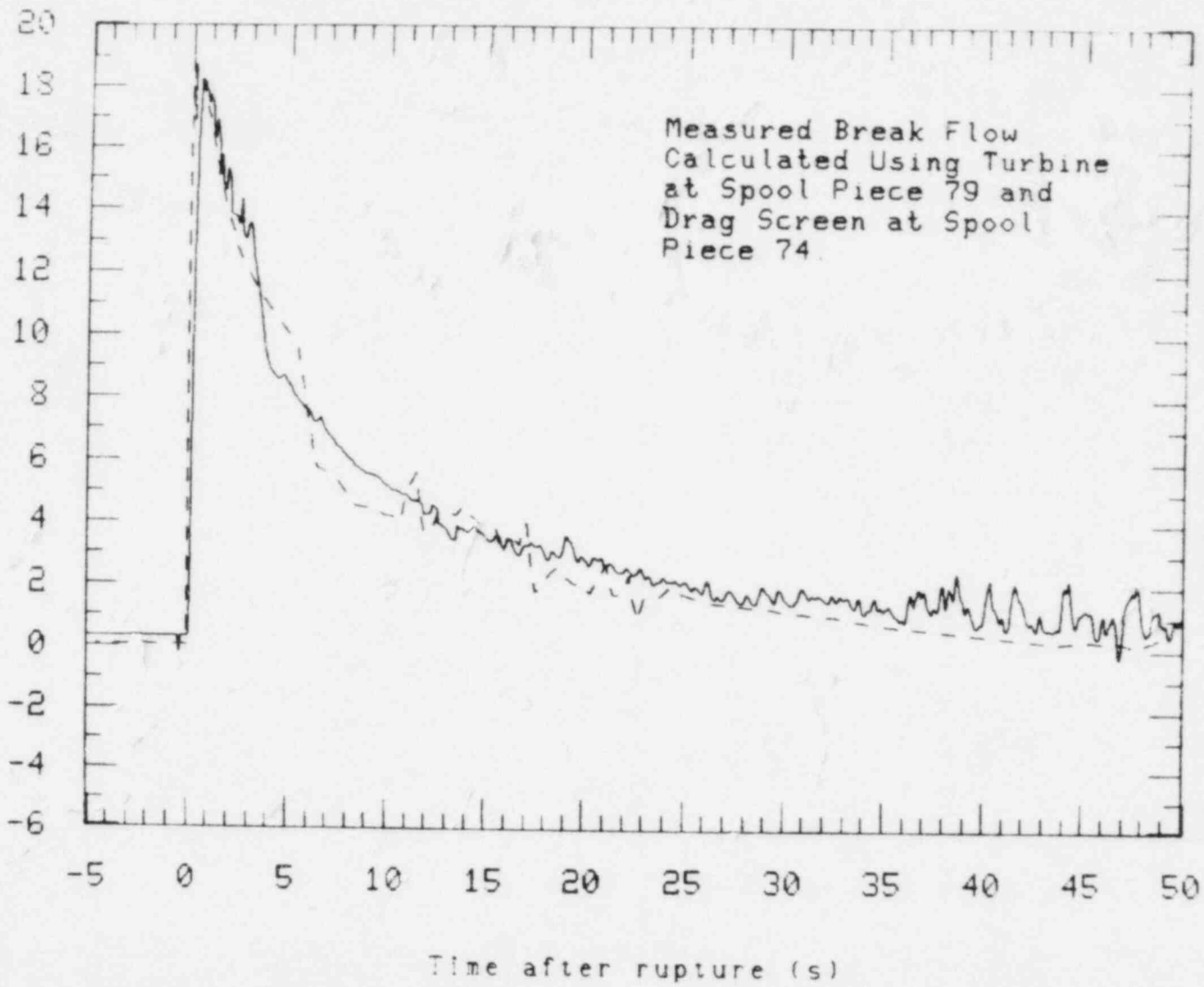
Figure 42. Comparison of measured and calculated upper plenum pressures.

1 BREAK FLOW ———

2 0375000000MFL0WJ - - - -

71

Mass flow (kg/s)



Measured Break Flow  
Calculated Using Turbine  
at Spool Piece 79 and  
Drag Screen at Spool  
Piece 74.

Figure 43. Comparison of measured and calculated break mass flow rates.

flow rate was smaller than that calculated because of differences in the break upstream temperatures. The initial measured Broken loop cold leg temperature of 562 K was 4 K above the initial calculated value. Because there was less subcooling upstream of the break in the test, the break mass flow rate and, therefore, the primary coolant system depressurization rate was less than that calculated.

Figure 44 presents the measured and calculated pressurizer pressures, respectively. Both pressures initially decreased at a slower rate relative to the corresponding upper-plenum depressurization rate (Figure 42). The slower pressurizer depressurization rate was the result of the surge line hydraulic resistance and the immediate flashing of the pressurizer saturated liquid (compared to the more subcooled system liquid). The test data showed that the pressurizer drained in approximately 4.5 s, whereas in the calculation, draining was completed in 16 s. During the initial 5 s of the transient, the measured and calculated pressurizer pressures were in good agreement. Examination of the test data indicated that the initial pressurizer mass was approximately 35% lower than the initial value (13.6 kg) used in the pretest prediction. The smaller measured initial pressurizer mass caused the pressurizer to drain out sooner relative to the calculated drain time.

During the transient the actual and calculated operation of the primary coolant pumps was different. The difference was due to changes in the experiment operating specification (EOS) for Test S-IB-1 after the pretest prediction calculation was completed. However, these differences in pump operation were only important during approximately the first 10 s of the transient. After approximately 10 s, complete pump head degradation occurred as a result of voiding in the loop seal piping.

The pump head degradation induced similar thermal-hydraulic behavior in both the test and calculation. Figure 45 presents the measured and calculated downcomer flows. Both the measured and calculated downcomer mass flows reversed during the subcooled blowdown phase. Following voiding in the core which was measured and calculated to occur at 0.15 s and

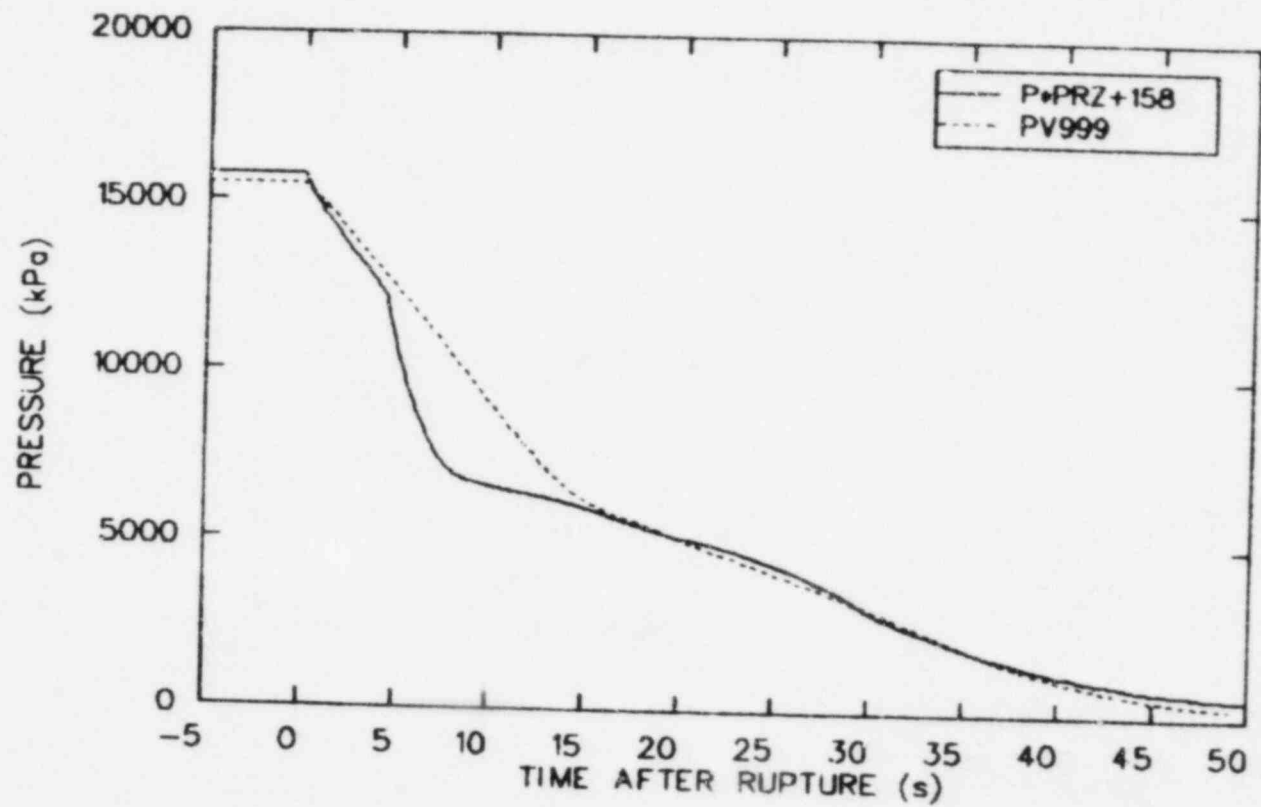


Figure 44. Comparison of measured and calculated pressurizer pressures.

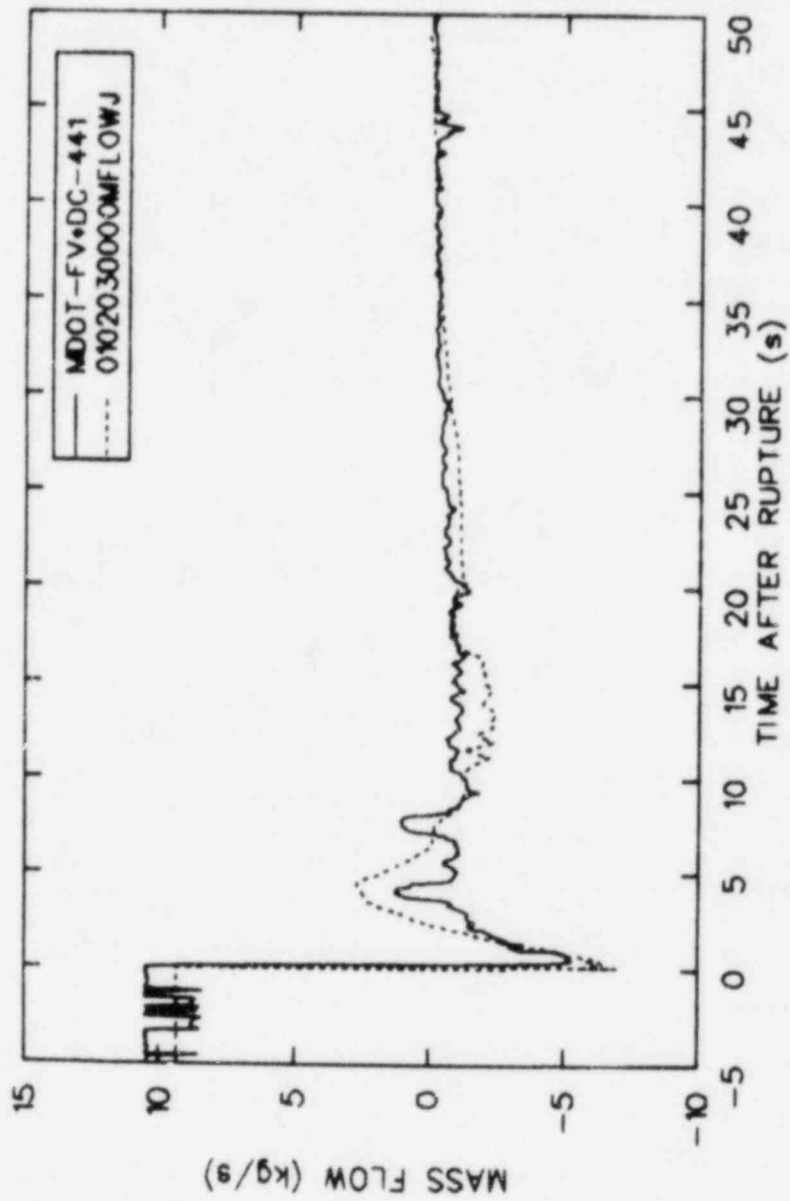


Figure 45. Comparison of measured and calculated downcomer mass flow rates.

0.05 s, respectively, the pumps in both the test and calculation temporarily reestablished positive downcomer flow until the primary coolant pump heads began to significantly degrade.

The measured and calculated heater rod surface temperatures were characterized by rapid temperature increases caused by core voiding (Figure 46).<sup>a</sup> The initial temperature excursions began at 1.1 s and 0.4 s for the measured and calculated heater rod temperatures, respectively. During approximately the first 5 s, core voiding induced rapid heatup followed by some cooling between 5 s and 7 s. During this period the core power was turned off (Figure 47).<sup>b</sup> After approximately 7 s the core power was resumed and both the measured and calculated temperatures began to increase again. It is believed that the slightly different times at which the core power was reactivated (calculated power was resumed sooner) was in part responsible for the calculated temperature increasing at a much faster rate up to 17 s where it peaked at 982 K.

Beginning at 17 s in the calculation, the rods were nearly quenched by fluid draining from the upper head through the guide tube into the core. As discussed in Section 3, the measured upper head drainage did produce significant cooling, but only in the top regions of the core heater rods. Consequently, most heater rod temperatures were measured to undergo extended temperature excursions after 20 s. The calculated rod cooling is attributed to the larger (calculated) upper head liquid drainage. The calculated and measured drainage rates are compared in Figure 48.

The measured and calculated ECC mass flow rates during blowdown were significantly different. However, during this period ECC had not

---

a. The initial difference between the measured and calculated heater rod surface temperatures is because the location of the thermocouple is inside the cladding. However, after the transient is initiated, the measured cladding temperature rapidly equilibrates to the outer surface temperature.

b. The measured and calculated core powers are normalized to 1.9 MW, which is the initial power used in the test prediction calculation.

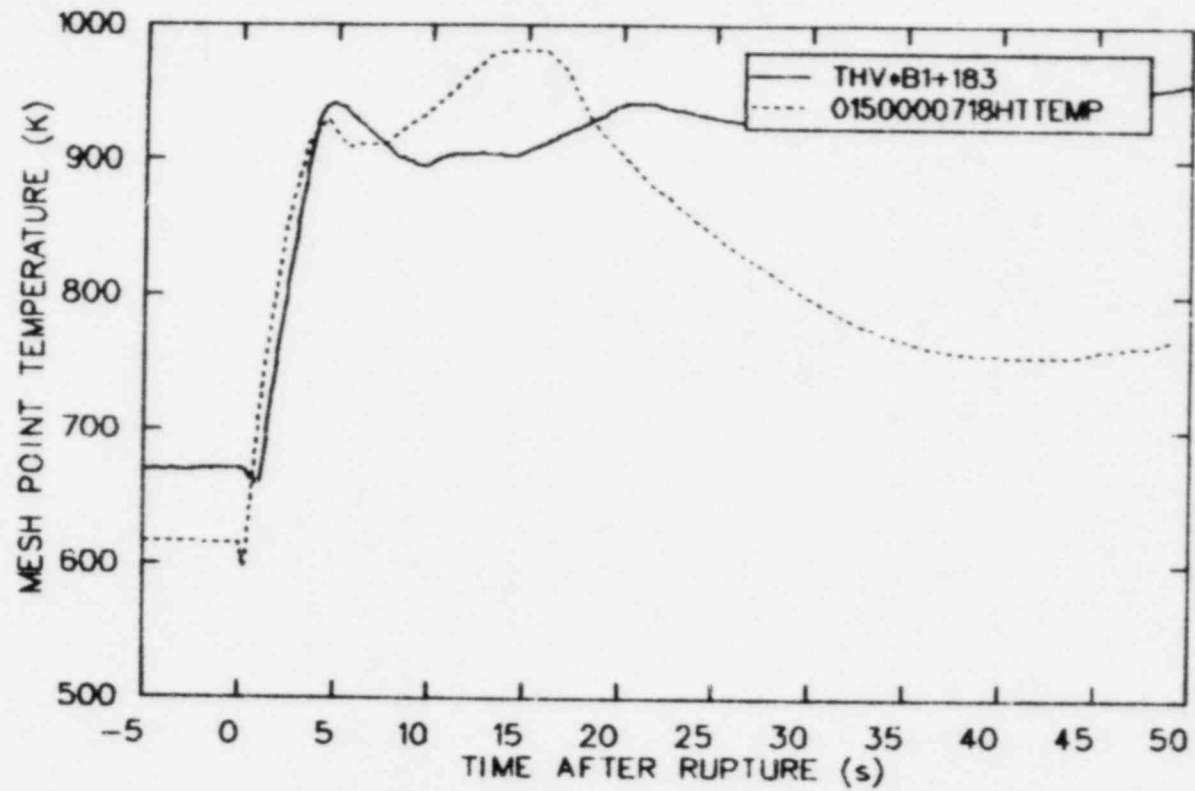


Figure 46. Comparison of measured and calculated midplane heater rod temperatures at elevation 183-214 cm.

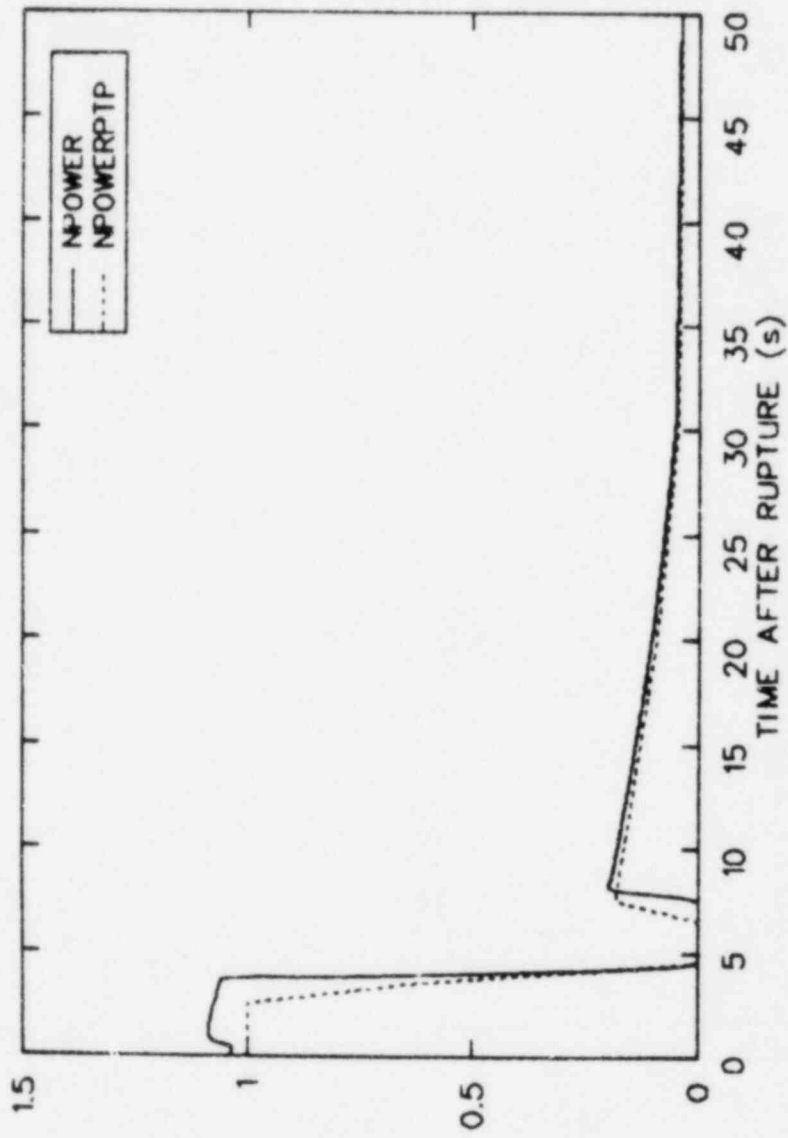


Figure 47. Comparison of measured and calculated core powers.



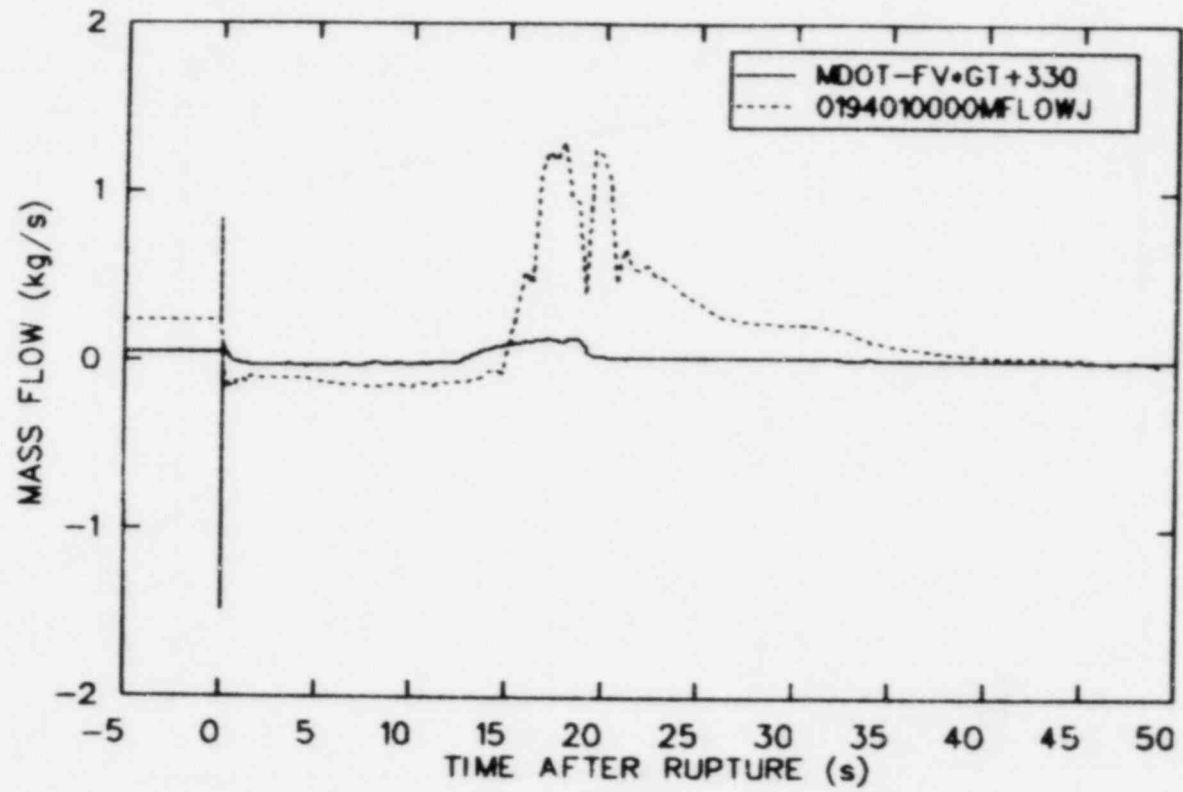


Figure 48. Comparison of measured and calculated guide tube mass flow rates.

penetrated the lower plenum. Consequently, the differences in ECC operation did not significantly affect the core heater rod temperature response nor overall system depressurization. The measured and calculated times for the activation of the Intact loop accumulator were in good agreement. Presented in Figure 49 are the calculated and measured Intact loop accumulator volumetric flow rates. The significantly smaller calculated flow is due to an error in the RELAP5 accumulator model. In addition, Broken loop HPIS and LPIS was employed in the pretest calculation, but was not used in the test. This difference was due to changes to the EOS after the pretest prediction calculation was completed. Moreover, the test results showed that the Intact loop HPIS and LPIS was substantially less than that calculated because the LPIS was not controlled during the test as specified in the EOS.

#### 5. CONCLUSIONS

The following major conclusions are pertinent to Semiscale Test S-IB-1.

1. No new thermal/hydraulic phenomena were detected in this 100% break test, the blowdown was qualitatively similar to a previous 200% break experiment.
2. Heatup begins within 1 second after blowdown and is due to the voiding of the core region.
3. Upper-head-liquid drainage into the core is an important factor in core cooling during blowdown.
4. No oscillations were observed in the reflood (as were in Semiscale Test S-07-6); but no conclusion can be reached from S-IB-1 data concerning the supposed relation of these oscillations to metal-to-water heat transfer in the (interior) insulated downcomer, since the downcomer never filled with accumulator water in this test.

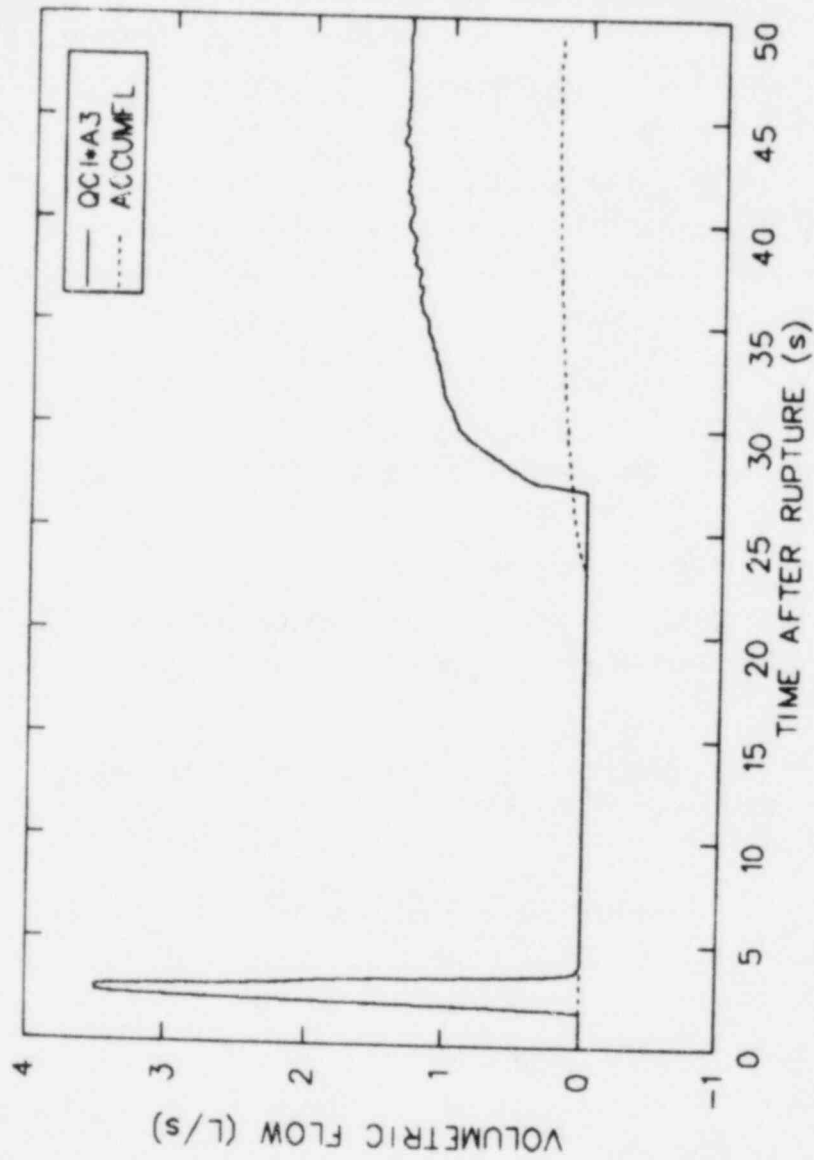


Figure 49. Comparison of measured and calculated accumulator volumetric flow rates.

5. The physical configuration of the downcomer inlet annulus and its modeling should be reviewed with the intent of resolving the best way(s) to address ECC bypass in Semiscale.
6. The experimental data from the test should be useful for checking calculations of a degraded-LPIS induced reflood, but are not useful for comparison against a "normal", i.e., filled-downcomer, reflood.

Generally, the measured and calculated test prediction results were in good agreement. In particular, the calculated system depressurization, core heater rod temperature responses, and primary coolant mass flows agreed reasonably well with the data during blowdown. Discrepancies were noted in the upper head drainage behavior and accumulator flow which are attributable to modeling deficiencies. Differences in predicted and actual ECCS boundary conditions (e.g., HPIS flowrate) rendered the comparison ineffectual beyond the blowdown phase.

## 6. REFERENCES

1. A. G. Stephens, Experiment Operating Specification (EOS) for Semiscale Mod-2A Experiments S-IB-1 and S-IB-2, EG&G Idaho, Inc., Idaho Falls, Idaho, EGG-SEMI-5722, January, 1982.
2. T. K. Larson, J. L. Anderson, and D. L. Shimeck, Scaling Criteria and An Assessment of Semiscale Mod-3 Scaling for Small Break Loss-of-Coolant Transients, EG&G Idaho, Inc., Idaho Falls, Idaho, EGG-SEMI-5121, March, 1980.
3. J. M. Cozzuol, Quick Look Report for Semiscale Mod-3 Test S-07-6 Baseline Test Series, EG&G Idaho, Inc., Idaho Falls, Idaho, WR-S-78-020, October, 1978.
4. V. Esparza, K. E. Sackett, and K. Stanger, Experiment Data Report for Semiscale Mod-3 Integral Blowdown and Reflood Heat Transfer Test S-07-6 (Baseline Test Series), EG&G Idaho, Inc., Idaho Falls, Idaho, NUREG/CR-0467, TREE-126, January, 1979.
5. C. M. Kullberg, J. L. Perryman, and J. L. Steiner, Semiscale Mod-2A Tests S-IB-1 and S-IB-2 Pretest Prediction Report, EG&G Idaho, Inc., Idaho Falls, Idaho, PN-4-82, January, 1982.

APPENDIX

The measurements and initial condition values are listed in the following order. Within each subgroup, e.g., "Downcomer", measurements are listed alphabetically by parameter symbols and by elevation for a given parameter.

1. Reactor Vessel
  - 1.1 Core
  - 1.2 Downcomer
  - 1.3 Upper and Lower Plenum
  - 1.4 Upper Head and Core Bypass
  
2. Intact Loop
  - 2.1 Hot Leg (at Reactor Vessel Outlet)
  - 2.2 Pressurizer
  - 2.3 Steam Generator Inlet and Primary Side
  - 2.4 Steam Generator Secondary
  - 2.5 Steam Generator Outlet (Primary)
  - 2.6 Pump Suction and Pump Parameters
  - 2.7 Pump Discharge
  - 2.8 Cold Leg (at Downcomer Inlet)
  - 2.9 Loop  $\Delta P$ 's
  
3. Broken Loop
  - 3.1 Hot Leg
  - 3.2 Steam Generator Inlet and Primary Side
  - 3.3 Steam Generator Secondary
  - 3.4 Steam Generator Outlet (Primary)
  - 3.5 Pump Suction and Pump Parameters
  - 3.6 Pump Discharge
  - 3.7 Cold Leg
  - 3.8 Loop  $\Delta P$ 's
  
4. ECCS
  - 4.1 Accumulator
  - 4.2 HPIS/LPIS

5. Break Flow and Pressure Suppression

5.1 Break Flow

5.2 Pressure Suppression Tank

6. Miscellaneous

The parameter symbols and units are listed below.

<u>Parameter</u>	<u>Symbol</u>	<u>Units</u>
Differential pressure	D, DP	kPa
Voltage	E	volts
Force	F	Newtons
Current	I	amps
Power	kW	kW
Level	L	cm
Pressure	P	MPa
Volumetric flow	Q	$\ell/s$
Density	R	$kg/in^3$
Fluid temperature	TF	K
Metal temperature	TM	K
Heater rod temperature	TH	K
Angular speed	W	radians/s
Position (valve)	X	volts



# 1. REACTOR VESSEL

## 1.1 Core

<u>System</u>	<u>Measurement ID</u>	<u>Initial Condition</u>
I	EV*HIPWBUS	328.94 Volts
I	EV*LOPWBUS	329.36 Volts
I	IV*HIPWBUS	2295.07 amps
I	IV*LOPWBUS	3830.83 amps
I	KW*HIBUS	754.95 kW
I	KW*LOBUS	1261.74 kW
I	KW*TOTAL	2016.69 kW
II	LV-105-195	-38.03 kPa
II	LV-195-278	-17.2 <sup>a</sup> kPa
II	LV-278-360	-16.69 kPa
II	LV-360-442	-14.12 kPa
II	LV-442-501	-6.55 kPa
I	RV*AB-6	741.22 kg/m <sup>3</sup>
II	RV*23+13	744.20 kg/m <sup>3</sup>
II	RV*23+113	723.96 kg/m <sup>3</sup>
II	RV*AB+173	725.77 kg/m <sup>3</sup>
II	RV*23+183	709.72 kg/m <sup>3</sup>
II	RV*23+253	655.69 kg/m <sup>3</sup>
II	RV*AB+332	F <sup>a</sup>
II	RV*23+342	680.43 kg/m <sup>3</sup>
I	TFV*A4+79	567.11 K
I	TFV*A4+242	596.20 K
I	TFV*A4+283	604.99 K
I	TFV*A4+323	605.28 K
I	TFV*A4+361	595.91 K
I	TFV*B3+45	F <sup>a</sup>
I	TFV*B3+122	571.87 K

1. REACTOR VESSEL (continued)

1.1 Core

<u>System</u>	<u>Measurement ID</u>	<u>Initial Condition</u>
I	TFV*B3+162	580.54 K
I	TFV*B3+242	598.78 K
I	TFV*B3+323	605.87 K
I	TFV*D1+162	581.29 K
I	TFV*D1+200	F <sup>a</sup>
I	TFV*D1+242	F <sup>a</sup>
I	TFV*D1+283	F <sup>a</sup>
I	TFV*D1+323	605.21 K
II	THV*A1+115	564.15 K
I	THV*A2+112	651.53 K
I	THV*A2+182	677.06 K
I	THV*A2+353	606.05 K
II	THV*A3+137	661.92 K
II	THV*A3+208	663.55 K
II	THV*A3+228	674.41 K
II	THV*A3+291	649.09 K
II	THV*A4+115	654.39 K
II	THV*A4+185	689.65 K
II	THV*A4+355	668.70 K
II	THV*A5+185	679.96 K
I	THV*B1+11	578.91 K
I	THV*B1+183	670.20 K
I	THV*B1+253	675.39 K
I	THV*B2+107	F <sup>a</sup>
I	THV*B2+180	686.34 K
I	THV*B2+227	684.91 K
I	THV*B2+353	F <sup>a</sup>

1. REACTOR VESSEL (continued)

1.1 Core

<u>System</u>	<u>Measurement</u> <u>ID</u>	<u>Initial Condition</u>
I	THV*B3+114	661.18 K
I	THV*B3+184	F <sup>a</sup>
I	THV*B3+229	681.79 K
I	THV*B3+354	631.56 K
I	THV*B4-12	557.66 K
II	THV*B4+140	F <sup>a</sup>
II	THV*B4+170	682.38 K
II	THV*B4+256	684.45 K
I	THV*B5+133	668.93 K
I	THV*B5+180	679.59 K
I	THV*B5+252	671.45 K
I	THV*C1+140	670.06 K
I	THV*C1+211	686.85 K
I	THV*C1+232	687.82 K
I	THV*C1+292	662.70 K
II	THV*C2+15	579.31 K
II	THV*C2+137	667.78 K
II	THV*C2+168	669.28 K
II	THV*C2+254	670.91 K
II	THV*C3+140	663.46 K
II	THV*C3+231	684.16 K
II	THV*C3+292	674.78 K
II	THV*C4+20	579.92 K
II	THV*C4+142	670.11 K
II	THV*C4+187	676.01 K
II	THV*C4+257	681.25 K
I	THV*C5+133	665.50 K

I. REACTOR VESSEL (continued)

1.1 Core

<u>System</u>	<u>Measurement ID</u>	<u>Initial Condition</u>
I	THV*C5+207	673.05 K
I	THV*C5+228	675.39 K
I	THV*C5+290	656.21 K
I	THV*D1+131	657.86 K
I	THV*D1+178	674.65 K
I	THC*D1+251	673.22 K
I	THV*D2+16	581.83 K
II	THV*D2+138	672.68 K
II	THV*D2+185	684.93 K
II	THV*D2+254	656.32 K
II	THV*D3+109	645.92 K
II	THV*D3+227	678.67 K
II	THV*D3+354	620.87 K
II	THV*D4+106	F <sup>a</sup>
II	THV*D4+179	679.23 K
II	THV*D4+228	640.19 K
II	THV*D4+352	644.63 K
II	THV*D5+13	580.65 K
II	THV*D5+139	666.04 K
II	THV*D5+184	679.49 K
II	THV*E1+172	677.11 K
II	THV*E2+109	640.90 K
II	THV*E2+181	673.32 K
II	THV*E2+354	615.33 K
II	THV*E3+141	673.49 K
II	THV*E3+211	659.90 K
II	THV*E3+231	683.81 K
II	THV*E3+292	645.47 K

# 1. REACTOR VESSEL (continued)

## 1.1 Core

<u>System</u>	<u>Measurement ID</u>	<u>Initial Condition</u>
II	THV*E4+112	646.07 K
II	THV*E4+183	677.91 K
II	THV*E4+354	606.81 K
II	THV*E5+181	675.06 K

## 1.2 Downcomer

I	LVD+29-170	22.77 kPa
I	LVD-170-435	23.57 kPa
I	LVD-435-578	F <sup>a</sup>
I	LVD+29-578	58.70 kPa
I	PV*DC+29	15.89 MPa <sup>b</sup>
II	RV*DC-72	751.97 kg/m <sup>3</sup>
II	RV*DC-260	748.39 kg/m <sup>3</sup>
I	TFV*DC-84	558.25 K
I	Ti V*DC-270	560.42 K

### 1.2.1 Outlet Flow

I	FV*DC-441	6.31 N
I	PV*DC-435L	9.67 MPa <sup>b,c</sup>
I	QV*DC-423	9.26 t/s
I	RV*DC-456	755.07 kg/m <sup>3</sup>
II	TFV*DC-436	555.53 K

## 1.3 Upper and Lower Plenum

I	FV*UP-9	4.38 N
I	LV-13M-105	-19.27 kPa

## 1. REACTOR VESSEL (continued)

### 1.3 Upper and Lower Plenum

<u>System</u>	<u>Measurement ID</u>	<u>Initial Condition</u>
I	LV-13M-578	-120.20 kPa
I	PV*UP-13	15.98 MPa <sup>b</sup>
I	QV*UP+1	14.52 $\epsilon/s$
I	RV*UP-11	675.42 kg/m <sup>3</sup>
II	TFV*UP-13	594.02 K
I	TFV*UP-63	595.01 K
I	TFV*UP+79	572.12 K
I	TMV*FPD+79	497.70 K
I	LV-501-578	-15.76 kPa
I	PV*LP-578L	9.60 MPa <sup>b,c</sup>
II	TFV*LP-552	557.77 K

### 1.4 Upper Head and Core Bypass

II	DVD+29+421	148.71 kPa
I	FV*GT+330	0.10 N
I	LV+421+160	6.25 kPa
I	LV+160+135	16.40 kPa
I	LV+135-13M	1.52 kPa
I	LV+421-13M	22.70 kPa
I	LV+421-578	-98.58 kPa
I	PV*UH+421	15.73 MPa <sup>b</sup>
I	QV*GT+321	0.13 $\epsilon/s$
I	QV*BYPASS	2.08 $\epsilon/s$
I	RV*UH+173	766.34 kg/m <sup>3</sup>
I	RV*UH+339	746.87 kg/m <sup>3</sup>
II	TFV*BYPASS	556.13 K
I	TFV*GT+304	613.34 K

1. REACTOR VESSEL (continued)

1.4 Upper Head and Core Bypass

<u>System</u>	<u>Measurement ID</u>	<u>Initial Condition</u>
I	TFV+UHQ180	553.75 K
I	TFV+UHQ282	556.46 K
I	TFV*UH+343	567.53 K
I	TFV*UH+402	549.15 K
I	TMV+FPF221	542.54 K
I	TMV+TSQ221	553.49 K

2. INTACT LOOP

2.1 Hot Leg

I	FI*1	2.35 N
I	PI*1	15.77 MPa <sup>b</sup>
I	QI*1	11.49 e/s
I	RI*1B	686.63 kg/m <sup>3</sup>
I	RI*1T	692.28 kg/m <sup>3</sup>
I	TFI*1	592.69 K

2.2 Pressurizer

I	DP*PRZ*13	131.11 kPa
I	LPRZ158+25	9.22 kPa
I	P*PRZ+158	15.78 MPa <sup>b</sup>
I	Q*PRZ-30	0.30 e/s
II	TF*PRZ-73	528.15 K
II	TF*PRZ+132	618.51 K
II	TF*PRZ*13	549.35 K

## 2. INTACT LOOP

### 2.3 Steam Generator Inlet and Primary Side

<u>System</u>	<u>Measurement ID</u>	<u>Initial Condition</u>
I	FI*5	2.97 N
I	QI*6	10.97 g/s
II	RI*5M	680.33 kg/m <sup>3</sup>
II	TFI*5	592.96 K
I	LIP970-55E	-59.73 kPa
I	TFIP+LC211	557.56 K
I	TFIP+LH30	591.86 K
I	TFIP+LH452	578.19 K
I	TFIP+LH922	569.00 K

### 2.4 Steam Generator Secondary Feedwater

I	DPSC*IGFDW	258.07 kPa
I	LSCT488+97	18.86 kPa
I	TFSC+IGFDW	497.08 K
I	TFSC+IGFWL	496.90 K

#### 2.4.1 Riser and Steam Dome

I	LIS1117+50	46.36 kPa
I	PIS+1117	5.53 MPa
I	TFIS+1117	543.75 K
I	TFIS+LC211	541.56 K
I	TFIS+LH30	521.39 K
I	TFIS+LH452	544.79 K
I	TFIS+LH922	544.35 K



## 2. INTACT LOOP (continued)

### 2.4.2 Steam Flow

<u>System</u>	<u>Measurement ID</u>	<u>Initial Condition</u>
I	DPSC*IGSTM	203.29 kPa
I	PSC*IGSTM	5.55 MPa
I	TFSC*IGSTM	543.79 K

### 2.5 Steam Generator Outlet (Primary)

I	DIG-55E55X	162.63 kPa
I	FI*9	F <sup>a</sup>
II	RI*9M	759.49 kg/m <sup>3</sup>
II	TFI*9	556.42 K

### 2.6 Pump Suction and Pump Parameters

I	FI*15	2.25 N
I	PI*14L	9.59 MPa <sup>b,c</sup>
I	QI*15	10.11 l/s
II	TFI*15	556.33 K
I	TFI*17	557.67 K
I	DPI*21*18	1091.08 kPa
II	EI*PUMP	401.80 volts
II	II*PUMP	80.04 amps
I	WI*PUMP	353.93 rad/s

### 2.7 Pump Discharge

I	QI*21	10.32 l/s
I	RI*21B	764.44 kg/m <sup>3</sup>

2. INTACT LOOP (continued)

2.7 Pump Discharge

<u>System</u>	<u>Measurement ID</u>	<u>Initial Condition</u>
I	RI*21T	779.45 kg/m <sup>3</sup>
II	TFI*21	554.99 K

2.8 Cold Leg

I	FI*22	2.41 N
II	PI*22L	3.86 MPa <sup>b,c</sup>
I	QI*22	10.20 t/s
I	RI*22B	733.07 kg/m <sup>3</sup>
I	RI*22T	684.06 kg/m <sup>3</sup>
II	TIF*22	554.03 K

2.9 Loop ΔP's

I	D-V13A*11	13.70 kPa
I	DPI*1*3	8.40 kPa
I	DPI*3*5	4.46 kPa
I	DPI*5*9	199.54 kPa
I	DPI*9*14	641.59 kPa
I	DPI*14*18	F <sup>a</sup>
I	DPI*21*22	1.62 kPa
I	D*I22+VD29	10.97 kPa

3. BROKEN LOOP

3.1 hot Leg

I	FB*50	0.90 N
II	PB*50	15.67 MPa <sup>b</sup>

### 3. BROKEN LOOP

#### 3.1 Hot Leg

<u>System</u>	<u>Measurement ID</u>	<u>Initial Condition</u>
I	QB*50	3.83 $\ell/s$
I	RB*50M	$F^a$
I	RB*50T	701.16 $kg/m^3$
I	TFB*50	585.08 K

#### 3.2 Steam Generator Inlet and Primary Side

I	FB*57	1.03 N
I	QB*57	3.45 $\ell/s$
II	RB*57M	$F^a$
I	TFB*57	594.97 K
I	TFBP+LH211	588.31 K
I	TFBP+LH452	581.57 K
I	TFBP+LH668	577.52 K
I	TFBP+LH922	572.75 K

#### 3.3 Steam Generator Secondary

##### 3.3.1 Feedwater

I	DPSC*BGFDW	188.00 kPa
I	TFSC*BGFDW	496.13 K
I	TFSC*BGFWL	492.08 K

##### 3.3.2 Riser and Steam Dome

I	LBS1117+50	46.41 kPa
I	PBS+1117	$F^a$
I	TFBS+1117	551.60 K

### 3. BROKEN LOOP (continued)

#### 3.3.2 Riser and Steam Dome

<u>System</u>	<u>Measurement ID</u>	<u>Initial Condition</u>
I	TFBS+LH211	549.68 K
I	TFBS+LH452	550.86 K
I	TFBS+LH668	552.89 K
I	TFBS+LH922	550.92 K

#### 3.3.3 Steam Flow

II	DPSC*BGSTM	94.06 kPa
II	PSC*BGSTM	6.15 MPa
I	TFSC*BGSTM	548.49 K

#### 3.4 Steam Generator Outlet (Primary)

I	DBG-55E55X	171.84 kPa
I	FB*62	0.67 N
II	RB*62M	747.25 kg/m <sup>3</sup>
I	TFB*62	564.23 K

#### 3.5 Pump Suction and Pump Parameters

II	PB*65L	F <sup>a</sup>
I	QB*73	3.83 e/s
II	RB*73	811.53 kg/m <sup>3</sup>
I	TFB*73	522.44 K
I	DPB*74*73	443.49 kPa
II	KWB*PUMP	3.24 kW
I	WB*PUMP	1121.67 rad/s

### 3. BROKEN LOOP (continued)

#### 3.6 Pump Discharge

<u>System</u>	<u>Measurement ID</u>	<u>Initial Condition</u>
I	FB*74	0.72 N
I	PB*74L	9.58 MPa <sup>b,c</sup>
I	QB*74	3.42 $\epsilon/s$
II	RB*74M	769.59 $kg/m^3$
II	RB*74T	766.80 $kg/m^3$
I	TFB*74	552.47 K

#### 3.7 Cold Leg

II	DPB*79.25D	2.55 kPa <sup>f</sup>
II	DPB*79.50D	-2.31 kPa <sup>f</sup>
II	DPB*79.75D	-0.58 kPa <sup>f</sup>
I	FB*79	4.85 N
II	PB*79L	9.61 MPa <sup>b,c</sup>
I	QB*79	3.52 $\epsilon/s$
I	RB*79M	743.70 $kg/m^3$
I	RB*79T	750.28 $kg/m^3$
I	TFB*79	561.80 K

#### 3.8 Loop $\Delta P$ 's

I	D-V13A*B50	8.96 kPa
I	DPB*50*55	9.37 kPa
I	DPB*55*57	2.42 kPa
I	DPB*57*62	186.05 kPa
I	DPB*62*65	18.72 kPa

### 3. BROKEN LOOP (continued)

#### 3.8 Loop $\Delta P$ 's

<u>System</u>	<u>Measurement ID</u>	<u>Initial Condition</u>
I	DPB*65*73	4.76 kPa
I	DPB*74*76U	9.81 kPa
I	DPB*76U*79	3.37 kPa
I	D*B79+VD29	0.10 kPa

### 4. ECCS

#### 4.1 Accumulator

I	LCI*A3+277	0.65 kPa
I	PCI*A3+277	4.45 MPa <sup>e</sup>
I	QCI*A3	0.0 $\text{g/s}$ <sup>d</sup>
I	TFCI*A3+76	296.34 K
I	TFCI*I22	496.16 K

#### 4.2 HPIS/LPIS

I	LCI*T7+277	25.51 kPa
---	------------	-----------

### 5. BREAK FLOW AND PRESSURE SUPPRESSION

#### 5.1 Break Flow<sup>d</sup>

II	DPB*76.25D	-2.36 kPa
II	DPB*76.50D	0.17 kPa
I	DB*76F*76D	2.95 kPa
I	FB*76	0.01 N
I	PB*76L	3.53 MPa <sup>h,c</sup>

## 5. BREAK FLOW AND PRESSURE SUPPRESSION

### 5.1 Break Flow<sup>d</sup>

<u>System</u>	<u>Measurement ID</u>	<u>Initial Condition</u>
II	RB*76M	842.93 kg/m <sup>3</sup>
II	RB*76T	845.30 kg/m <sup>3</sup>
I	TFB*76	512.78 K
I	DB*76U*76D	-0.37 kPa <sup>b</sup>
II	PB*76U	15.87 MPa <sup>b</sup>
I	TFB*76U	499.64 K

### 5.2 Pressure Suppression

I	LPS+384+0	18.02 kPa
I	PPS*1T+384	0.25 MPa <sup>b,e</sup>
I	TFPS*1T+43	298.49 K
I	TFPS*1T330	400.90 K

## 6. MISCELLANEOUS

I	PB*RDP	8.05 MPa
I	XSC*IGFDW	2.25 volts
I	XSC*IGSTM	3.59 volts
II	XSC*BGFDW	1.33 volts
II	XSC*BGSTM	2.13 volts
II	THV*AVG	659.52 K

An optical probe was mounted at the upstream side of the break, looking directly across the flow at the (upstream) face of the 100% break orifice. See Figure 6 for configuration. A video tape was produced showing fluid conditions at that position during the entire experiment.

## NOTES

- 
- a. F - failed during warmup or during test.
  - b. These measurements supplied with 50 Hz amplifier filters.
  - c. These are low range transducers. They are saturated at initial conditions, thus this reading is not the true value of the parameter.
  - d. There is no flow in this leg at initial conditions.
  - e. These tanks are isolated from the primary coolant system at initial conditions, but pressurized by their own pressurizing source.
  - f. The pitot tubes point toward the downcomer, and so do not provide readings of the initial condition flow, which is toward the downcomer.
  - g. The above listed 316 entries consist of 313 measurements and three calculated values (power on the high and low power buses and total core power). The 313 measurements coincide with those on the final copy of the log sheet for this test. The other 17 channels on the log sheet consist of six for calibration, ground noise monitoring and sequencer checking; three Westinghouse RVLIS measurements; three experimental temperature measurements in the steam generator downcomers; four spare channels; and one channel (PB\*76U) duplicated on System II for blowdown time determination for that System.
-